Aus der
Medizinischen Klinik und Poliklinik IV
Klinik der Universität München
Direktor: Prof. Dr. med. Martin Reincke

Analysis of Growth Differentiation Factor 15 And Its Role in Acute and Chronic Kidney Injury

Dissertation

zum Erwerb des Doktorgrades der Medizin
an der Medizinischen Fakultät
der Ludwig-Maximilians-Universität zu München

vorgelegt von

Moritz Johannes Krill

aus Gräfelfing

Jahr
2024

Mit Genehmigung der Medizinischen Fakultät
der Universität München

Berichterstatter:	Prof. Dr. Maciej Lech
Mitberichterstatter:	Prof. Dr. André Brändli
	Prof. Dr. Alexander Dietrich
Mitbetreuung durch den promovierten Mitarbeiter:	
Dekan:	Prof. Dr. med. Thomas Gudermann
Tag der mündlichen Prüfung:	16.05.2024

Table of Contents

I List of Abbreviations

(7-)AAD	(7-)Aminoactinomycin D
AKT	Protein Kinase B
ANV	Akutes Nierenversagen
APC	Allophycocyanin
ATP	Adenosine Triphosphate
Bad	Bcl-2 Associated Agonist of Cell Death Protein
Bcl2	B-Cell Lymphoma 2
BMDC	Bone Marrow-Derived Dendritic Cell
BMDM	Bone Marrow-Derived Macrophage
BUN	Blood Urea Nitrogen
BV	Brilliant Violet
CCL2	CC-Motif Chemokine Ligand 2
CD	Cluster of Differentiation
cDNA	Complementary Deoxyribonucleic Acid
cf.	Compare
CKD	Chronic Kidney Disease
CNI	Chronische Niereninsuffizienz
CpG	Unmethylated Cytosine Guanosine Oligodeoxynucleotides
Ctrl	Control
CXCL2	CXC-Motif Chemokine Ligand 2
°C	Degree Celsius
DAMP	Danger-Associated Molecular Pattern
ddH2O	Double Distilled Water
DNA	Deoxyribonucleic Acid
dNTP	Desoxyribonukleosidtriphosphate
DMEM	Dulbecco’s Modified Eagle’s Medium
(D)PBS	(Dulbecco's) Phosphate-Buffered Saline
DTT	Dithiothreitol
ECM	Extracellular Matrix
e.g.	Exempli Gratia/ For Example
ELISA	Enzyme-Linked Immunosorbent Assay
EMT	Epithelial-To-Mesenchymal Transition
ESRD	End-Stage Renal Disease
f	Forward
FACS	Fluorescence Activated Cell Sorting
FBS	Fetal Bovine Serum
FcR	Fc Region
FITC	Fluorescein Isothiocyanate
FSC	Forward Scatter
FSGS	Focal Segmental Glomerulosclerosis
GAPDH	Glycerinaldehyd-3-phosphate Dehydrogenase

GBM	Glomerular Basement Membrane
GDF15	Growth Differentiation Factor 15
Gdf15 -/-	Homozygous *Gdf15* Knockout
GDNF	Glial Cell-derived Neurotrophic Factor
GFR	Glomerular Filtration Rate
GFRAL	GDNF Family Receptor Alpha Like
HBS	Hepes Buffered Saline
HEPES	2-(4-(2-Hydroxyethyl) -1-Piperazinyl) - Ethansulfon Acid
HIF(1)α	Hypoxia-Inducible Factor (1) Alpha
HMGB1	High-Mobility Group Box 1
Hpf	High-power field
HPRT	Hypoxanthine Phosphoribosyltransferase 1
HSP90ab1	Heat Shock Protein 90 Alpha Family Class B Member 1
Ibid.	Ibidem
i.e.	Id est
IgG	Immunglobulin G
IL	Interleukin
IMQ	Imiquimod
iNOS	Inducible Nitric Oxide Synthase
I/R	Ischemia/Reperfusion (deutsch: Ischämie/Reperfusion)
JAK	Janus Kinase
kDA	Kilo Dalton
KDIGO	Kidney Disease: Improving Global Outcomes
KIM1	Kidney Injury Molecule-1
KO	Knockout
LDH	Lactate Dehydrogenase
LPS	Lipopolysaccharide
M1	M1 Type Macrophage
M2	M2 Type Macrophage
MCPIP	Monocyte Chemotactic Protein-Induced Protein
MCSF	Macrophage Colony Stimulating Factor
MHC	Major Histocompatibility Complex
MIC-1	Macrophage Inhibitory Cytokine-1
Mio.	Million
mRNA	Messenger Ribonucleic Acid
MYD88	Myeloid Differentiation Primary Response Gene (88)
NAG-1	Non-Steroidal Anti-Inflammatory Drug-Inducible Gene-1
NGAL	Neutrophil Gelatinase-Associated Lipocalin
NLR	Nucleotide-Binding Oligomerization Domain Receptor
NLRP3	NACHT, LRR and PYD Domains-Containing Protein 3
N-Myc	N-Myc Protooncogene
ns	Not Significant

OSOM	Outer Stripe of the Outer Medulla
PAMP	Pathogen-Associated Molecular Pattern
PAS	Periodic Acid-Schiff
PCR	Polymerase Chain Reaction
PDF	Prostate-Dreived Factor
PE/Cy7	Phycoerythrin/Cyanine Dye 7
PI3K	Phosphoinositid-3-Kinase
PLAB	Placenta Bone Morphogenetic Protein
PLCγ	Phospholipase C Gamma
pO_2	Partial Pressure of Oxygen
PRR	Pattern Recognition Receptor
PS	Penicillin-Streptomycin Solution
pTGFβ	Placental Transforming Growth Factor Beta
PTS	Proximal Tubular Segment/s
r	Reverse
RBC	Red Blood Cell
re	Recombinant
resp.	Respectively
RET	Rearranged during Transfection
RNA	Ribonucleic Acid
rRNA	Ribosomal RNA
ROS	Reactive Oxygen Species
rpm	Rounds per Minute
RPMI	Roswell Park Memorial Institute Medium
RT	Room Temperature
RT-PCR	Reverse Transcription PCR
(q)RT-PCR	Quantitative Real-Time PCR
s.c.	Subcutaneous
SCr	Serum Creatinine
SDS-PAGE	Sodium Dodecyl Sulfate Polyacrylamide Gel Electrophoresis
SEM	Standard Error of the Mean
SN	Supernatant
SSC	Side Scatter
STAT	Signal Transducer and Activator of Transcription Proteins
Taq	Thermus Aquaticus
TEC	Tubular Epithelial Cell
TGFβ	Transforming Growth Factor Beta
TGFβR	Transforming Growth Factor Beta Receptor
TLR	Toll-Like Receptor
TNFα	Tumor Necrosis Factor Alpha
TNFR1/2	Tumor Necrosis Factor Alpha Receptor 1/2
UUO	Unilateral Ureteral Obstruction
VEGF	Vascular Endothelial Growth Factor
VIM	Vimentin

Wnt	Wingless Related Integration Site
WT	Wild Type

II Introduction

1 Acute Kidney Injury

Acute kidney injury (AKI) is a widespread pathologic condition, characterized by an acute deterioration in renal function (Kellum et al., 2021). It has been reported in one out of five hospitalized individuals and almost every second critically ill patient (Luo et al., 2014; Susantitaphong et al., 2013) with its incidence continuously increasing over the past few decades (Bagshaw et al., 2007; Lameire et al., 2006). AKI is currently diagnosed in accordance with the KDIGO criteria by either laboratory evidence of increased serum creatinine levels, clinical evidence of reduced urine output or both (Kellum et al., 2021; Mehta et al., 2007). It can occur due to a wide variety of aetiologies, which are commonly grouped into either pre-, intra-, or postrenal causes (Hoste et al., 2018). Prerenal AKI corresponds to renal hypoperfusion (ischemia) resulting from a reduction in circulating effective arterial blood volume (Moore et al., 2018). At approximately 60%, the majority of all AKI cases can be traced back to a prerenal ischemic genesis (Moore et al., 2018). Intra- (direct damage to the nephrons, e.g., in acute tubular necrosis or glomerulonephritis) or postrenal causes (inadequate urine drainage, e.g., due to ureteral obstruction) are less prevalent (Moore et al., 2018). While AKI itself is resulting in significantly increased length of hospital stay, health care costs and in-hospital mortality, its downstream effects additionally include increased risks of long-term mortality and progression to chronic kidney disease (Chertow et al., 2005; Gameiro et al., 2021). Since AKI is an entity that can be treated successfully, it is clear, that sufficient diagnosis and timely initiation of treatment are crucial to prevent long-term loss of kidney function and the development of end-stage renal disease with the inevitable necessity of renal replacement therapy.

1.1 Ischemia/Reperfusion Injury-Induced AKI

Renal ischemia/reperfusion (I/R) injury is one of the most frequent causes of AKI, commonly resulting from prerenal pathologies (Ronco et al., 2019; Sharfuddin et al., 2011). It is characterized by a sudden, transient impairment of blood-, and thereby, oxygen supply of the renal tissue, followed by reperfusion and reoxygenation (Chatauret et al., 2014). The mismatch between renal oxygen and nutrient supply versus demand leads to a local accumulation of metabolic waste products (Bonventre et al., 2011). This imbalance conditions cellular injury, ultimately resulting in an impairment of renal function and disturbances in electrolyte and water homeostasis (Bonventre et al., 2011).

Generalized or localized renal ischemia can be the result of a wide variety of underlying pathologies (Sharfuddin et al., 2011). Generalized renal ischemia, resulting from a reduced effective arterial volume, can be caused by a myriad of systemic pathologies. However, the

mechanisms conditioning a reduction in effective arterial volume differ. Gastrointestinal fluid losses, such as in diarrhea or vomiting, renal fluid losses, such as in diabetes insipidus, nephrotic syndrome, or diuretic use, as well as liver cirrhosis are culminating in intravascular volume depletion and thus reduced effective arterial volume (Ronco et al., 2019; Sharfuddin et al., 2011). Anaphylaxis as well as sepsis translate to reduced effective arterial volume via systemic vasodilation and imbalanced distribution of intravascular volume, thereby facilitating ischemic AKI (Nakano, 2020; Sharfuddin et al., 2011). Furthermore, low-cardiac-output syndrome, as seen in chronic heart failure, valvular disease, cardiac arrhythmia, or cardiogenic shock, can lead to generalized renal ischemia (Sharfuddin et al., 2011).

Isolated or localized renal ischaemia may occur due to mechanical obstructions of the afferent renal blood flow, such as renal artery thrombosis or renal artery stenosis (Bonventre et al., 2011). On top of that, localized renal ischemia may be the consequence of diseases, primarily affecting small intrarenal vessels. Examples include small vessel vasculitis, haemolytic uremic syndrome, and thrombotic thrombocytopenic purpura (Bonventre et al., 2011).

In addition, long-term use of certain drugs can contribute to the development of renal ischemia. By impairing renal autoregulatory mechanisms, they reduce the ability of the kidney to compensate for a reduction in effective arterial blood volume to maintain sufficient glomerular perfusion (Joannidis et al., 2018; Nelson et al., 2019). Non-steroidal anti-inflammatory drugs decrease the production of vasodilatory prostaglandins by inhibiting the enzyme cyclooxygenase (Drożdżal et al., 2021; Nelson et al., 2019). The resulting relative reduction in renal perfusion predisposes to the development of AKI (Nelson et al., 2019). In case of low effective arterial blood volume with renal hypoperfusion, the renin-angiotensin-aldosterone system is activated and aids in maintaining sufficient glomerular perfusion (Mansour, 2023). Vasoconstriction of the efferent arteriole is a central mechanism in preserving glomerular filtration pressure (Mansour, 2023). It is mediated by angiotensin 2. Angiotensin-converting-enzyme inhibitors decrease the production of angiotensin 2, affecting the delicate balance between the vascular tone of the afferent and efferent arteriole of the glomerulus (Mansour, 2023). Especially in patients with preexisting low renal perfusion (e.g., bilateral renal artery stenosis, chronic heart failure, volume deficiency), the use of angiotensin-converting-enzyme inhibitors increases the risk of AKI (Joannidis et al., 2018; Mansour, 2023).

Moreover, transient renal ischemia inevitably occurs during specific surgical interventions such as aortic cross-clamping, partial nephrectomy, and kidney transplantation, eventually leading to post-operative AKI. In kidney transplantation, this increases the risk of not only delayed graft function but also acute transplant rejection and long-term graft loss (Palmisano et al., 2021).

1.2 Pathophysiological Aspects of I/R-Induced AKI

Ischemia-Induced Acute Tubular Injury

Renal perfusion takes up about 25% of the cardiac output and is in relation to organ weight the highest in the body (Brezis et al., 1995). However, distinct regions of the kidney, are highly susceptible to hypoxic damage due to their delicate balance of oxygen supply and demand. To stabilize glomerular filtration and thereby maintain its excretory function, renal blood flow is mainly channelled to the cortex of the kidney (Brezis et al., 1995). On the opposite, blood supply to the renal medulla is low. Albeit the resulting cortico-medullary gradient in partial pressure of oxygen (pO_2) being imperative for efficient urine concentration, it is inevitably accompanied by a high susceptibility of the medullary nephron segments for hypoxia (Schiffer et al., 2018). Particularly, the S3 segment of the proximal tubule within the outer stripe of the outer medulla, where oxygen levels are even under normal conditions critically low, is challenged by a further decrease in oxygen (Scholz et al., 2021). Cells of the proximal tubule reabsorb the majority of the primary glomerular filtrate and, hence, display a high energy demand (Scholz et al., 2021). While proximal tubular cells generate the gross of their ATP through aerobic glycolysis and oxidative phosphorylation, they have a comparably limited anaerobic capacity (Lyu et al., 2018; Scholz et al., 2021). The combination of their localization within the critically low oxygenated outer stripe of the outer medulla, their high ATP demand and their low anaerobic reserve make tubular epithelial cells (TECs) of the S3 segment most prone to ischemic kidney injury (Brezis et al., 1984; Scholz et al., 2021). Acute tubular injury is a hallmark of AKI. It is defined by characteristic histomorphological changes of the tubular structure. This includes tubular necrosis, loss of brush boarder, tubular cast formation and dilation of tubular lumina (Gaut et al., 2021). Ischemia-induced ATP-depletion of the tubular cells within the corticomedullary junction causes cellular injury leading to apoptosis and secondary necrosis (Kers et al., 2016). At the same time, AKI results in a loss of epithelial polarity and cytoskeletal integrity (Molitoris et al., 1996). It is associated with mislocalization of membrane adhesion molecules such as β-integrins, with disruption of the actin membrane cytoskeleton and with dislocation of Na^+K^+-ATPase molecules. All three mechanisms promote both loss of apical brush border and detachment of tubular cells from the basement membrane (Gailit et al., 1993; Molitoris et al., 1992; Zuk et al., 1998). In combination with distinct proteins such as fibronectin, the desquamated cells, or their debris, tend to accumulate as tubular casts (Zuk et al., 2001). The resulting tubular obstruction conditions an increased intratubular pressure and thus tubular dilation. Furthermore, AKI causes altered gene expression in proximal tubular cells (Villanueva et al., 2006). Upregulation of specific genes such as *KIM1* and *NGAL* in TECs have been described to correlate with the severity of proximal tubular injury (Hanindita et al., 2016; Ichimura et al., 1998; Mishra et al., 2003; Staender et al., 1997; Vaidya

et al., 2008) and can therefore be helpful to assess the extent of tubular damage *in-vivo* and *in-vitro*.

Immune Cell Infiltration and Inflammation

Influx of various immune cells, due to upregulation of endothelial adhesion molecules such as selectins and integrins in the postischemic kidney, represents a major pathomechanism of AKI (Jang et al., 2009; Jang et al., 2009). In context of the immune response, neutrophils, macrophages/monocytes, dendritic cells, and T cells are involved in mediating not only acute tissue injury but also consecutive regeneration of renal parenchyma (Sharfuddin et al., 2011). Thereby, neutrophils are the first leucocytes recruited into the postischemic kidney (Miyazawa et al., 2002; Ysebaert et al., 2000). They are involved in the initiation of renal injury by producing and secreting reactive oxygen species (ROS), proteases and cytokines (Radi, 2018). In combination with a leucocytic microvascular obstruction, this facilitates increased vascular permeability, and hence, immune cell infiltration (Radi, 2018). In addition, increased cytokine and chemokine levels following AKI result in enhanced recruitment of monocytes, or macrophages (Anders et al., 2003; Lech et al., 2013). These phagocytotic cells can exhibit different functional phenotypes depending on their surrounding microenvironment (Han et al., 2019; Lech et al., 2012; Saeed et al., 2018). Within the first 3 days after AKI a pro-inflammatory macrophage response by recruitment of classically activated M1-macrophages can be observed (Han et al., 2019; Lee et al., 2011). These cells are activated by ligating DAMPs, released by injured TECs, with their membrane bound pattern recognition receptors (Zhang et al., 2012). M1-macrophages thereupon secrete inflammatory cytokines, such as IL1β, IL12, IL18, IL23 and tumor necrosis factor alpha (TNFα), conditioning the inflammatory microenvironment necessary for tissue damage clearance (Novak et al., 2013). The increasing secretion of anti-inflammatory cytokines such as IL4, IL10, IL13, and transforming growth factor beta (TGFβ) by various immune cells between day 3 and 7 after ischemic kidney injury induces a switch of macrophage polarization towards an anti-inflammatory M2-dominant macrophage response (Mosser et al., 2008). Due to their secretion of resolvins, TGFβ, and chemokine-cleaving proteases, M2-macrophages possess anti-inflammatory and pro-regenerative properties, mandatory for the resolution of inflammation and structural tubular regeneration (Han et al., 2019; Saeed et al., 2018). Multiple studies have shown that prolonged pro-inflammatory M1-macrophage activation delays the resolution of injury and contributes to further tissue damage by aggravating inflammation (Huen et al., 2015; Lee et al., 2011). A sequential and precisely orchestrated participation of the depicted phenotypes is essential for structural and functional renal recovery (Han et al., 2019; Lech et al., 2014).

Innate Immune Signaling and Inflammation

Inflammatory processes and immune cell recruitment play a pivotal role in the pathophysiology of acute kidney injury. While there is always a delicate interplay between the innate and the adaptive immune system, the early stages of acute kidney injury are predominantly characterized by signaling mechanisms of the innate immunity (Jang et al., 2009). In this context, pattern recognition receptors (PPRs), including Toll-like receptors (TLRs) and nucleotide-binding oligomerization domain receptors (NLRs), together with the NLRP3 inflammasome play a central role in orchestrating the innate immune response and maintaining renal homeostasis (Kezi et al., 2017; Leemans et al., 2014). PPRs comprise evolutionary highly conserved families of transmembrane and intracellular receptors, that are localized both on circulating myeloid and lymphatic immune cells and on resident renal parenchymal cells (Leemans et al., 2014). They are capable of recognizing and responding not only to distinct pathogen motifs during infectious conditions but also to endogenous compounds released by injured cells in the context of sterile inflammation (Kezi et al., 2017; Leemans et al., 2014).
In particular, danger signaling via Toll-like receptors (TLRs) has emerged as a central concept of the innate immune response during AKI (Gluba et al., 2010). These receptors are located either on the cell surface (TLR1/2/4/5/6) or in intracellular endosomes (TLR3/7/8/9) of numerous immune cells and partly also tubular epithelial cells (Tammaro et al., 2020). Early findings showed the prominent role of TLRs in infectious pathogen control by recognition of so-called pathogen-associated molecular patterns (PAMPs). However, in the last decades, TLRs have been shown to be also involved in the recognition of non-pathogenic molecules, so-called damage-associated molecular patterns (DAMPs), which are released in the context of numerous non-pathogenic diseases as a consequence of unspecific tissue damage (Roh et al., 2018). These DAMPs are released by necrotic cells and can independently trigger a local inflammatory response via TLR activation (Roh et al., 2018). A variety of DAMPs and their corresponding TLRs have been described (see table 1).

Tab. 1: DAMPs and corresponding TLRs

Damage-Associated Molecular Pattern	Toll-Like Receptor	
Biglycan	TLR2, TLR4	(Schaefer et al., 2005)
CpG DNA (hypomethylated)	TLR9	(Papadimitraki et al., 2009)
Defensins	TLR4	(Biragyn et al., 2002)
Fibrinogen	TLR4	(Smiley et al., 2022)
Heat shock proteins	TLR2, TLR4	(Asea et al., 2002)
Heparan sulphate	TLR4	(Johnson et al., 2002)
HMGB1	TLR2, TLR4	(Magna et al., 2014)
Hyaluronates	TLR2, TLR4	(Termeer et al., 2002)

Single stranded RNA	TLR7	(Patra et al., 2020)
S100A8/S100A9	TLR4	(Wang et al., 2018)

CpG, cytosine guanosine oligodeoxynucleotides; HMGB1, high-mobility group box 1

These innate immune receptors play a key role in danger signaling during ischemic kidney injury (Gluba et al., 2010). *In-vivo* observations depicted, that in addition to antigen-presenting immune cells also TECs express specific TLRs on their surface membrane, indicating their importance for the initial innate immune response upon kidney injury (Leemans et al., 2005). Consistent mRNA expression of both *Tlr2* and *Tlr4* on TECs with significant upregulation following I/R injury could be detected by several groups (Leemans et al., 2005; Vries et al., 2002). *Tlr2*-deficiency in mice was associated with a reduction in renal injury alongside with reduced amounts of cytokines, chemokines and local leucocyte infiltration after ischemic injury compared with WT controls (Leemans et al., 2005). Moreover, *Tlr2*-antisenese treatment of mice mitigated renal dysfunction and tubular atrophy in the context of renal ischemia, supporting the hypothesis, renal resident TLR2 being a major driver of excessive and detrimental inflammation following I/R injury. Interestingly, both MyD88-dependent and MyD88-independent pathways could be demonstrated for TLR2-signaling (Shigeoka et al., 2007). Other studies pointed out, that mice deficient for *Tlr4* were also protected from I/R injury, displaying reduced kidney dysfunction and histopathological damage compared to WT controls (Pulskens et al., 2008). TLR4 activation might be another key mechanism in the initiation of an exaggerated proinflammatory immune response, given that absence of *Tlr4* in mice was associated with lower levels of chemokines and lower influx of immune cells following I/R injury (Pulskens et al., 2008). Remarkably, *Tlr4* expression on renal resident cells appears to have a greater impact on renal injury than *Tlr4* expression on leukocytes, considering that *Tlr4* knockout mice transplanted with WT hematopoietic cells displayed markedly lower renal dysfunction and less tubular damage after ischemic injury than WT mice reconstituted with *Tlr4* knockout bone marrow cells (Wu et al., 2007). Huang et al. suggested a proinflammatory role for TLR7 signaling in ischemic AKI in the setting of preexisting diabetes as they found that human renal tubular epithelial cells subjected to hypoxia-reoxygenation, after being precultured in varying glucose concentrations, showed a significant increase in the expression of *TLR7* and its associated proteins (Huang et al., 2019). Interestingly, not only increase in *TLR7* expression, but also cell damage, apoptosis, and proinflammatory response were found to be significantly greater in the high glucose group (Huang et al., 2019). As another cytosolic receptor of the innate immune system, TLR9 appears to participate in mediating ischemic AKI (Han et al., 2019). Han et al. proposed that activation of renal proximal tubular TLR9 aggravates ischemic AKI, as they were able to demonstrate that mice, lacking *Tlr9* in renal proximal tubules, were protected against I/R-induced renal injury (Han et al., 2019). Activation of TLRs by binding DAMPs is a prerequisite for the conversion of a local tissue damage into

an orchestrated immune response, which in theory provides the basis for successful repair of injured tubules and renal regeneration (Anders, 2010). However, reactive intrarenal inflammation cannot control or eliminate the cause of renal injury if that cause originates outside the renal system and does not resolve by itself (Anders, 2010). Hence, sustained or excessive activation of TLRs in the context of non-pathogen renal inflammation can be understood as a maladaptive pathogenic mechanism, resulting in perpetuated and aggravated renal damage (Anders, 2010).

In addition to TLR-mediated signaling, TNFα appears to function as a key driver in the innate immune response during AKI (Al-lamki et al., 2014). TNFα is a pleiotropic cytokine that is involved in multiple biological processes, including the induction of apoptosis and inflammation (Al-lamki et al., 2014). In parallel with infiltrating immune cells, local renal cells, such as tubular epithelial cells, mesangial cells, and podocytes, are also known to produce TNFα (Al-lamki et al., 2014). Its effects are mediated by binding and activation of 2 distinct transmembrane cell surface receptors, TNFR1 and TNFR2 (Al-lamki et al., 2014). While TNFR1 is constantly expressed under physiological conditions (primarily in glomeruli and peritubular endothelial cells), TNFR2 is almost absent (Al-lamki et al., 2014). However, expression of the latter has been found to be significantly induced in various renal cells after injury, depending on the primary site of the lesion (Al-lamki et al., 2014). A pivotal role for TNFα in inducing tubular atrophy during ischemic AKI was proposed by Adachi et al. as they demonstrated that blockade of TNFα by administration of neutralizing antibodies resulted in significantly decreased tubular apoptosis in mice, previously exposed to I/R injury (Adachi et al., 2014). Moreover, Choi et al. demonstrated that pretreatment of rats with a TNFα blocker, the soluble TNFR2 fusion protein etanercept, protected them from I/R-induced renal injury by neutralizing TNFα (Choi et al., 2009).

2 Chronic Kidney Disease

Chronic kidney disease (CKD) is defined as persistent structural or functional abnormality of the kidney due to various causes with an impact on the health of the affected individual (Levey et al., 2020). While renal cysts, tumours, and vesicoureteral reflux represent structural abnormalities, renal dysfunction can manifest as oedema, hypertension, or reduced urine output (Romagnani et al., 2017). In addition to diabetic and hypertensive nephropathy, the most common causes of CKD include glomerulonephritis, recurrent pyelonephritis, polycystic kidney disease, and post-AKI CKD (Kalantar-zadeh et al., 2021; Kellum et al., 2021). The impact of CKD on global health is immense. Currently, CKD affects about 10% of the world's adult population (with significant regional variation) and is associated with approximately 1.2 million deaths per year (Hill et al., 2016). The Kidney Disease Improving Global Outcomes (KDIGO) Initiative classifies CKD into different stages based on the reduction in renal function

(Levey et al., 2020). The severity of excretory renal dysfunction is determined by either estimated or measured glomerular filtration rate (GFR; Kalantar-zadeh et al., 2021; Romagnani et al., 2017). Albuminuria is used to assess renal filtration barrier dysfunction (Romagnani et al., 2017). According to the KDIGO classification, individuals with CKD have a stage-dependent risk of developing renal failure, and end-stage renal disease (ESRD; Romagnani et al., 2017). Regardless of causation, it is associated with progressive uraemia, acid-base disturbances, anaemia, bone metabolism disorders, and severe electrolyte imbalances (Romagnani et al., 2017; Zoccali et al., 2017). Therapeutic options of ESRD are usually limited to renal replacement therapy in form of chronic dialysis, and occasionally kidney transplantation (Kalantar-zadeh et al., 2021).

2.1 AKI-to-CKD Transition

Severe AKI is often associated with maladaptive repair mechanisms within the tubular, vascular and interstitial segment, leading to incomplete recovery of renal function, and predisposing to the development of CKD (Venkatachalam et al., 2015). This process is commonly referred to as AKI-to-CKD transition (Basile et al., 2016; Venkatachalam et al., 2015). In addition to the increased likelihood of CKD development after AKI in initially healthy individuals, the term also encompasses the accelerated progression of pre-existing CKD to ESRD caused by AKI (Venkatachalam et al., 2015). Endogenous risk factors for a poor outcome after and transition of AKI to CKD include advanced age, existing comorbidities such as diabetes mellitus, hypertension, preexisting CKD and heart failure, as well as laboratory evidence of low serum albumin (Chawla et al., 2011; Chawla et al., 2012; Guzzi et al., 2019). In addition, the severity, duration, and number of episodes of AKI have been shown to correlate with the likelihood of developing CKD (Ishani, 2011; Mehta et al., 2018; Thakar et al., 2011). These findings suggest that for some patients, a single episode of AKI – in relation to endogenous risk factors and AKI modalities - may have pathophysiological sequelae far beyond the duration of the initial event by predisposing to the development of CKD.

There is a large body of evidence that many different pathological mechanisms participate in AKO-to-CKD transition, including incomplete regeneration of proximal tubular epithelial cells with G2/M phase cell cycle arrest and consecutively increased proinflammatory as well as profibrotic signaling, endothelial dysfunction with microvascular rarefication and subsequential hypoxia, and prolonged maladaptive low-grade inflammation (Fiorentino, 2018; Sato et al., 2023). Remarkably, over the past decade evidence has accumulated that isolated acute tubular injury may be sufficient to cause the development of the typical CKD pathologies outlined below (Venkatachalam et al., 2015).

Renal I/R models provide an important tool to uncover the underlying mechanisms of AKI-to-CKD transition and to identify novel therapeutic targets for its prevention (Polichnowski et al., 2020). As the extent of AKI-to-CKD pathology depends on the severity of the initial ischemic

insult, unilateral I/R models allow effective imitation of the pathological process, by enabling particularly long ischemia times (Dong et al., 2019; Polichnowski et al., 2020).

2.2 Pathophysiological Aspects of CKD

Regardless of the underlying aetiology, progression of CKD towards ESRD presents as a consistent pathophysiological syndrome with mutually reinforcing components resulting in renal dysfunction and scarring.

Tubulointerstitial Inflammation and Fibrosis

Tubulointerstitial inflammation involves chronic immune cell infiltrates (Schnaper, 2017). The release of chemotactic proinflammatory mediators such as CCL2 from injured tubules, glomeruli, and capillaries promotes the influx of T-lymphocytes and macrophages into the tubulointerstitial space (Schnaper, 2017). After activation, macrophages in turn secrete proinflammatory cytokines and mediators such as TNFα, ROS and TGFβ, thereby perpetuating chronic inflammation (Schnaper, 2017). Persistent low-grade renal inflammation causes progressive tubulointerstitial fibrosis, which along with glomerulosclerosis is a hallmark of CKD (Agarwal et al., 2020). It is defined as the replacement of physiological renal parenchyma by non-functional scar tissue (Agarwal et al., 2020). The central pathological mechanism is the excessive and aberrant deposition of extracellular matrix (ECM) components (Agarwal et al., 2020). Several studies have identified activated myofibroblasts as the primary cellular source of increased ECM production in renal scar tissue formation (Agarwal et al., 2020). These cells comprise a phenotypically very heterogeneous group, whose common feature is the synthesis and deposition of interstitial collagens I, III, and IV as well as other matrix components such as fibronectin (Agarwal et al., 2020). Recent studies suggest that myofibroblasts may arise from a variety of different sources. Besides renal resident interstitial cells (Hutchison et al., 2013), bone marrow derived cells (Jang et al., 2013), endothelial cells (Li et al., 2009) and tubular epithelial cells (Iwano et al., 2002) have been suggested as possible cellular origins. A hypothesis widely promoted and intensively investigated in the past is the phenomenon known as epithelial-to-mesenchymal transition (EMT), describing the injury-induced phenotypic metamorphosis of TECs through the acquisition of mesenchymal characteristics into a fibroblast-like cell type (Kriz et al., 2011). Although numerous *in-vitro* studies have suggested EMT as a feasible cause of renal fibrosis, solid data confirming EMT as a tangible *in-vivo* mechanism are still lacking (Kriz et al., 2011), leaving the hypothesis highly debatable. Ultimately, an *in-vivo* study from 2013, using fate-mapping in transgenic mice, was able to identify local fibroblasts as main source of the intrarenal myofibroblast population (Lebleu et al., 2013). Accordingly, approximately 50% of all renal myofibroblasts arise via proliferation from renal resident fibroblasts, whereas non-proliferating myofibroblasts are primarily derived from bone marrow cells, and to a minor extent from tubular epithelial and

endothelial cells (Lebleu et al., 2013). Considering that many other cell types besides myofibroblasts are participating in renal fibrogenesis, renal scar formation must be viewed as the result of a complex interplay of multiple players linked by multidirectional cellular crosstalk (Gewin et al., 2017).

The activation of various signaling pathways, such as TGFβ, JNK/STAT, Hedgehog, Wnt/β-catenin, have been documented in relation to renal fibrogenesis (Edeling et al., 2016; Meng et al., 2016). However, multiple studies have pinpointed TGFβ as the key driver of fibrosis in CKD (Meng et al., 2016).

Nephron Loss and Adaptive Glomerulosclerosis

Functionally, severe renal injury translates into loss of nephrons (Romagnani et al., 2017). The remnant nephrons can temporarily increase their filtration capacity without undergoing structural changes, serving as a renal reserve, to compensate for the relatively increased filtration load per single nephron (Agati, 2017; Hostetter et al., 1981). However, if a persistent increase in single-nephron-GFR exceeds the threshold of the renal reserve for a prolonged period, hypertrophy of the remaining nephrons occurs (Hostetter et al., 1981; Zamami, 2021). Albeit compensatory glomerular hypertrophy effectively reduces glomerular hypertension by increasing the overall filtration surface area, it simultaneously exposes podocytes to increased shear forces and mechanical diameter distension (Agati, 2017; Vriese et al., 2018). The consequence is focal detachment of podocytic foot processes from the glomerular basement membrane (GBM) and hence progressive podocyte loss, ultimately resulting in structural deterioration of the glomeruli and the histopathological picture of adaptive focal segmental glomerulosclerosis (FSGS; Zamami, 2021). Since adaptive FSGS itself conditions nephron loss, leading to a further increase in single-nephron-GFR of remnant nephrons, a vicious circle is enclosed (Kriz et al., 2015; Romagnani et al., 2017). In summary, adaptive FSGS ensuing from the pathological triad of glomerular hypertension, glomerular hyperfiltration, and podocyte loss constitutes a central mechanism of CKD progression (Kriz et al., 2015).

3 Growth Differentiation Factor 15

Growth differentiation factor 15 (GDF15) is a divergent member of the TGFβ superfamily (Böttner et al., 1999). It was first described in 1997 by Bootcov and colleagues as macrophage inhibitory cytokine (MIC)-1 (Bootcov et al., 1997). Due to its involvment in various pathophysiological processes, it is also known as non-steroidal anti-inflammatory drug-inducible gene (NAG)-1, prostate-derived factor (PDF), placental bone morphogenetic protein (PLAB) and placental transforming growth factor beta (pTGFβ; Wischhusen et al., 2020). Since GDF15 comprises seven cysteine residues, constituting the characteristic cysteine knot as the defining common group feature, it is officially designated as TGFβ

superfamily member (Bootcov et al., 1997). Nevertheless, it is a rather distant relative, as it shares only about 30% amino acid sequence homology with other family members such as TGFβ1 regarding the otherwise highly conserved seven-cysteine domain (Bootcov et al., 1997; Böttner et al., 1999). GDF15 is synthesized as a monomeric pro-peptide and dimerized in the endoplasmic reticulum through a disulfide bond (Bootcov et al., 1997). A small fraction is activated immediately by intracellular proteolytic cleavage and thereupon secreted as ~25 kDa active homodimer (Bauskin et al., 2000). Yet interestingly, the vast majority of GDF15 is released as unprocessed pro-GDF15 dimer (Wischhusen et al., 2020). Unlike the mature GDF15, the immature precursor protein remains anchored within the ECM via its pro-domain after secretion, resulting in the formation of large extracellular cytokine reservoirs (Bauskin et al., 2010). It has been shown, that proteolytic cleavage of the extracellularly stored immature molecules by pro-protein convertases of the subtilisin/kexin type can lead to rapid release of large amounts of active GDF15 (Li et al., 2018). Based on these findings, a distinct local mechanism of action has been hypothesized for GDF15 (Bauskin et al., 2010). Apart from the placenta and prostate, most tissues, including kidney, liver, heart, lung, pancreas and gastrointestinal tract, display low to absent *Gdf15* expression under physiological conditions (Assadi et al., 2020). However, since GDF15 is known to be a stress-inducible cytokine, GDF15 levels are upregulated in many pathological conditions (Tsai et al., 2018). There is a broad body of literature on the pleiotropic functions of GDF15. Diverse roles in relation to energy metabolism, inflammation, tissue injury, cardiovascular diseases, cancer and immune tolerance have been depicted (Assadi et al., 2020; Tsai et al., 2018).

3.1 The GDF15-GFRAL axis in energy metabolism

Among the numerous proposed mechanisms of action for GDF15, its involvement in body weight control and apetite regulation has received particular attention in recent years. Its anorexigenic effect first came to light in 2007, when GDF15 appeared to be responsible for aptetite and consecutive weight loss in transgenic mice xenografted with a human prostate cancer cell line overexpressing GDF15 (Johnen et al., 2007). The observed effect could be reversed by administration of neutralizing GDF15 antibodies and replicated by administration of recombinant GDF15 (Johnen et al., 2007). Likewise, GDF15 overexpressing mice, whether fed a regular chow diet or an obsogenic diet, displayed a dramatic loss of body weight and fat mass, which was primarily due to a reduction in food intake (Macia et al., 2012). Studies in humans revealed that in both advanced prostate cancer and chronic renal failure, elevated GDF15 serum levels correlated with a reduction in body weight measured by body mass index, supporting the role of GDF15 as mediator of chronic disease-induced cachexia (Breit et al., 2012; Johnen et al., 2007). In addition, recent studies showed that administration of metformin, a widely prescribed anti-diabetic drug, led to increased GDF15 serum concentrations in both mice and human and that its anorexigenic effect was attributable to those elevated GDF15

serum levels (Coll et al., 2020; Day et al., 2019; Gerstein et al., 2017). In 2017, four independent research groups were finally able to identify glial-derived neurotrophic factor family receptor α-like protein (GFRAL), an orphan receptor of the glial-derived neurotrophic factor (GDNF) receptor family, as binding site of GDF15 and the receptor possibly mediating its anorexigenic effects (Emmerson et al., 2017; Hsu et al., 2017; Mullican et al., 2017; Yang et al., 2017). Remarkably, in both mice and humans, GFRAL appears to be localized almost exclusively in closely defined areas of the central nervous system, the area postrema and the nucleus of the solitary tract (Yang et al., 2017). Binding of GDF15 to GFRAL initiates the recruitment and activation of the tyrosine kinase co-receptor RET (Emmerson et al., 2017; Hsu et al., 2017; Mullican et al., 2017; Yang et al., 2017). Furthermore, one of the research groups that first discovered GFRAL demonstrated that in engineered cell lines binding of GDF15 to GFRAL resulted in phosphorylation of RET, leading to activation of intracellular downstream singal cascades such as AKT and PLC-γ (Mullican et al., 2017). As anticipated, germline knockout of *Gfral* in mice completely abolished the anti-obesity effect of GDF15, as treatment with recombinant GDF15 in obese mice lacking *Gfral* did not result in a decrease in food intake or body weight (Yang et al., 2017).

However, considering the almost ubiquitous stress-inducible expression of *Gdf15* and its pleiotropic functions, the highly confined distribution of GFRAL strongly implies other, yet undiscovered, receptor systems to be involved in GDF15 signaling.

3.2 GDF15 in Tissue Injury and Inflammation

As mentioned previously, GDF15 is secreted under resting conditions at low levels by presumably most tissues (Assadi et al., 2020). Its abundance commonly increases in reaction to a disruption of tissue homeostasis due to either cellular and mitochondrial stress or tissue injury (Breit et al., 2021; Wischhusen et al., 2020).

After induction of acute liver injury in mice either by chemical treatments, such as administration of carbon tetrachloride, or by surgical procedures, such as partial hepatectomy, significantly increased *Gdf15* transcript levels could be observed examining the remnant hepatic tissues (Chung et al., 2017; Hsiao et al., 2000). *In-vivo* mouse models of lung injury caused by bleomycin administration or hyperoxic exposure of murine neonates likewise resulted in a significant induction of *Gdf15* expression (Zimmers et al., 2005). Furthermore, a significant increase in *Gdf15* expression in the kidney after both surgical 5/6 nephrectomy and I/R injury has been described (Zimmers et al., 2005). A protective effect of GDF15 has been reported regarding cardiac tissue (Kempf et al., 2006; Xu et al., 2006). A study, using transgenic mice with a cardiac-specific overexpression of GDF15, observed that GDF15 secreted by the myocardium served as a protective and antihypertrophic factor in mice, exposed to transient pressure overload (Xu et al., 2006). Moreover, studies have demonstrated that endogenous GDF15 ameliorates myocardial ischemic injury *in-vivo* (Kempf et al., 2006).

When subjected to myocardial I/R, *Gdf15*-deficient mice developed greater infarct sizes and evidenced more cardiomyocyte apoptosis within the infarcted border zone compared to their WT controls (Kempf et al., 2006). The same research group later demonstrated that induction of GDF15 in mice is crucial for suppressing augmented leucocyte infiltration into the insulted myocardium and thus for preventing cardiac rupture after myocardial infarction (Kempf et al., 2011). Vice versa, influx of leucocytes into the infarcted tissue after myocardial I/R was attenuated by administration of recombinant GDF15 (Kempf et al., 2011). The observed anti-inflammatory effect of GDF15 could be attributed to the suppression of chemokine-induced activation of β_2 integrins by GDF15 (Kempf et al., 2011). The protective, anti-inflammatory function of GDF15 was also highlighted by a study investigating septic AKI and myocardial injury using a murine LPS-induced sepsis model (Abulizi et al., 2017). While *Gdf15* deficiency was associated with augmented inflammation, aggravation of renal and cardiac injury, and increased mortality after LPS-induced sepsis, *Gdf15* overexpression resulted in diminished endotoxin-mediated organdysfunction in both kidney and heart (Abulizi et al., 2017). Another murine *in-vivo* study analyzed the influence of GDF15 treatment on the development of LPS-induced liver injury (Li et al., 2018). Mice treated with recombinant GDF15 displayed significantly less hepatic leukocyte influx as well as attenuated increases in serum and hepatic IL6, TNFα and IL1ß levels after LPS-induced liver injury compared to their untreated controls, emphasizing the anti-inflammatory properties of GDF15 (Li et al., 2018).

3.3 GDF15 in Kidney Disease

Clinical studies have illuminated the potential of GDF15 as valuable risk stratification tool in renal disease by revealing the strong correlation between elevated GDF15 serum levels in humans and the increased likelihood of developing chronic renal failure (Ho et al., 2013). At the same time, however, increased GDF15 levels are well known to be associated not only with the development but also the progression of pre-existing CKD towards ESRD and an overall increased mortality (Breit et al., 2012; Nair et al., 2017; Tuegel et al., 2018; You et al., 2017). A study, investigating the prognostic value of GDF15 in children either with CKD or after renal transplantation revealed that circulating GDF15 levels were strongly correlated with excretory renal dysfunction, as measured by GFR, in both conditions (Thorsteinsdottir et al., 2020). In addition, several studies identified GDF15 as independent predictor of postoperative AKI in patients undergoing elective cardiac surgery (Guenancia et al., 2015; Heringlake et al., 2016). The authors of one of these studies pointed out the particular benefit of GDF15 in risk stratification in patients with normal creatinine (Heringlake et al., 2016). Elevated GDF15 serum levels seem to be also associated with disease progression and worse outcomes in numerous other renal pathologies, such as diabetic nephropathy or renal involvement in the context of systemic light chain amyloidosis (Bidadkosh et al., 2017; Kastritis et al., 2018; Lajer et al., 2010).

Despite the growing number of clinical studies highlighting the value of GDF15 as a prognostic biomarker regarding various renal diseases, there is still little firm knowledge about the functional role of GDF15 within the kidney. Surprisingly, considering the clinical findings, in both type 1 and type 2 models of diabetes GDF15 was found to protect mice from the development of diabetic kidney injury (Mazagova et al., 2013). Mice deficient for *Gdf15* exhibited augmented tubular and interstitial damage as well as increased glucosuria and polyuria relative to their diabetic WT controls (Mazagova et al., 2013). Interestingly, the protective effect of GDF15 appeared to be confined to the renal interstitium and tubular compartment, as no difference in glomerular damage was observed between the respective diabetic and corresponding control group (Mazagova et al., 2013). Furthermore, it has been reported that GDF15 is responsible for the adaptive proliferation and regeneration of collecting duct cells in experimental models of metabolic renal acidosis, indicating its importance for tissue homeostasis (Cheval et al., 2021; Paul et al., 2008). Examination of a murine anti-GBM nephritis model also revealed protective effects for GDF15, as *Gdf15*-deficient mice displayed increased proteinuria together with aggravated crescent formation and mesangial expansion compared to their WT controls (Moschovaki-Filippidou et al., 2020). A pivotal regulatory role for GDF15 has been proposed in the onset of CKD, since treatment with recombinant GDF15 reduced renal fibroblast activation and significantly attenuated renal fibrosis in mice subjected to unilateral ureteral obstruction (UUO), potentially due to blockade of TGFβ and *N*-Myc signaling (Kim et al., 2018). Yet, the association between elevated GDF15 levels in patients and the progression of renal diseases on one side and the reported protective effects *in-vivo* on the other side remain contradictory and thus imply the need for further investigations.

4 Objective

Despite the clear link between GDF15 biology and functional renal integrity, it is still unsettled, whether its activity either promotes further progression of renal disease or mediates protective effects. Hence, the aim of this thesis is to analyse the role of GDF15 and its effect on inflammation and innate immunity in both acute kidney injury (AKI) and chronic kidney disease (CKD). Therefore, a two-step approach is to be applied:

In the first step, ischemia/reperfusion (I/R) injury-based models of AKI and CKD with *Gdf15 -/-* and control C57BL/6 WT mice should be evaluated using gene expression analysis and histological studies to assess

1) the impact of *Gdf15* deficiency on the development of AKI, or CKD *in-vivo.*

In the second step, primary renal cells are to be isolated from *Gdf15 -/-* and control C57BL/6 WT mice to elucidate the *in-vivo* observations by

2) determining the main source of renal GDF15 and
3) shedding light on the innate immune responses, affected by GDF15 activity in the kidney.

III Material

1 Sets and Kits

Tab. 2: Sets and kits

Description	Manufacturer	Cat-Nr.
Blood Urea Nitrogen FS Kit	DiaSys Diagnostic Systems	131019910026
Creatinine FS Kit	DiaSys Diagnostic Systems	117119910026
DuoSet Elisa Mouse GDF15	R&D Systems	DY6385
Total RNA Purification Kit	Norgen Biotek	17250
PureLink™ RNA Mini Kit	Ambion	12183025
QS Bradford Protein Assay Kit 1	Bio-Rad Laboratories	5000201EDU

2 Substances

Tab. 3: Substances

Description	Manufacturer	Cat-Nr.
5x First Strand Buffer	Invitrogen	18064014
Absolute Ethanol	Merck	65-17-5
Acrylamide	Ambion	AM9520
Aqua	Braun	388 0079
BSA Fraction V	Roche	107350860001
Chrome Pure Sheep IgG 128948	Jackson Immuno Research	013-000-003
Collagenase D	Merck	11088858001
CpG B ODN 1668	InvivoGen	tlrl-1668
DMEM	Gibco	21885-025
dNTPs	Thermo Scientific	R0186
DPBS	PAN BioTec	P04-361000
DPBS (10x)	PAN BioTec	P04-53500
DTT	Invitrogen	18064014
FBS	Merck	S0115
Gelatin	Sigma	G1393-100ml
HEPES Dry Powder	Sigma Aldrich	90909C
Hexanucleotide Mix	Roche	11277081001
Imiquimod	InvivoGen	tlrl-imqs
LPS	InvivoGen	tlrl-pb5lps
Pam3CSK4	InvivoGen	tlrl-pms

Penicillin-Streptomycin Solution	Pan BioTec	P06-07100
Percoll® Solution	Merck	P1644-25ML
Re-GDF15	R&D Systems	8944-GD-025
Re-MCSF	Immunotools	12343115
Re-TNFα	Merck	T7539-10UG
RNAlator™ Stabilization Solution	Ambion	AM7023
RNAsin	Promega	N2515
RPMI	Gibco	61870-010
Substrate Solution	R&D Systems	DY994
Sulfuric Acid (2 N)	Roth	X873.1
Superscript	Invitrogen	18064014
SybrGreen	Fluka Sigma Aldrich	Discontinued
Taq DNA Polymerase	BioLabs	M0267X
Thiazolyl Blue Tetrazolium Bromide	Sigma Aldrich	M5655
Tween 20 SLBT4396	Sigma	9005-64-5

3 Buffers and Modified Media

Tab. 4: Buffers and modified media

Description	Composition
FACS buffer	1% BSA 0.1% NaN_3 PBS
HEPES buffer	1 M HEPES (pH = 7.55) ddH_2O
Hormone mixture	PEG1 (c_{FINAL} = 31.25 pg/ml) T3 (c_{FINAL} = 3.4 pg/ml) Hydrocortisone (c_{FINAL} = 18 ng/ml) HBSS
K1 medium	10% FBS 2.5% HEPES Buffer 1% PS 1% Hormone Mix ITSS (c_{FINAL} = 9.56 µg/ml) EGF (c_{FINAL} = 20 ng/ml)

Modified RPMI	10% FBS 1% PS reMCSF (c_{FINAL} = 100 ng/ml) RPMI
RBC lysis buffer	0.155M NH_4CL PBS

4 Consumables

Tab. 5: Consumables

Description	Manufacturer	Cat-Nr.
23 G Needle	Becton Dickinson	300700
70 µm Strainer	Sigma	Z742103 SIGMA
96 Well Light Cycler Plate	Sarstedt	72.1982.202
Capillary Tubes	Fisherbrand	15625677
Cell Scraper	TPP	99003
Eppendorf Tubes 1.5 ml	Eppendorf	0030125150
Eppendorf PCR tubes 0.5 ml	Eppendorf	0030124537
Falcon Tubes 15 ml	Greiner Bio-One	188271
Falcon Tubes 50 ml	Greiner Bio-One	227261
Feather Disposable Scalpel No. 10	Andwin Scientific	NC9999403
Nunc Maxisorp 96 Well Elisa Plate	Thermo Scientific	439454
Nunc Maxisorp 96 Well Microtiter Plate	Thermo Scientific	269620
Sealing Tape	Sarstedt	95.1994
Syringe 5 ml	Braun	4606051V
Syringe 20 ml	Braun	4606205V
Tissue Culture Dish 100 mm^2	TPP	93100
Tissue Culture Dish 150 mm^2	TPP	93150
Tissue Culture Flasks 75 cm^2	TPP	90075
Tissue Culture Flasks 150 cm^2	TPP	90150
Tissue Culture Plates 6 Well	TPP	92006
Tissue Culture Plates 12 Well	TPP	920012
Tissue Culture Plates 96 Well	TPP	92696
Total RNA Purification Kit 35700	Norgen	37500-NB
Vacuum Filtration “rapid” Filtermax 0.2 µm	TPP	99155

5 Technical Equipment

Tab. 6: Technical equipment

Description	Manufacturer
Biofuge Pico	Hereaus Instruments
Centrifuge 5402	Eppendorf
Combimag RCO	IKA
FACSCanto II Flowcytometer	Becton Dickinson
Heating Pad / Kleintier-OP-Tisch	Medax
LEICA DMR Upright Light Microscope	LEICA
Light Cycler 480	Roche
Microaneurysm Clamp	Medicon
Micro Tweezers	Medicon
Nanodrop 1000 Spectrophometer	PEQLAB Biotechnologie
Neubauer Improved Hemocytometer	Optik Labor
Opsys Microplate Reader	Dynex Technologies
Precision Balance	Scaltec
Thermomixer Comfort	Eppendorf
Vortex Genie 2	Scientific Industries
Wound Spreader	Medicon
Galaxy 48R CO2 Incubator	Eppendorf

6 Primer

The qRT-PCR primers used are detailed in the following table. Their specificity was validated using Blast software (https://blast.ncbi.nlm.nih.gov/).

Tab. 7: Primer sequences for qRT-PCR

Gene		Sequence [5‘ → 3‘]
18s	s	GCAATTATTCCCCATGAACG
	as	AGGGCCTCACTAAACCATCC
Ccl2	s	GCTACAAGAGGATCACCAGCA
	as	GTCTGGACCCATTCCTTCTTG
Cxcl2	s	CGGTCAAAAAGTTTGCCTTG
	as	TCCAGGTCAGTTAGCCTTGC
E-cadherin	s	GGTCATCAGTGTGCTCACCT
	as	GCTGGTGTGCTCAAGCCTTC
Gapdh	s	CGTCCCGTAGACAAAATGGT

	as	TTGATGGCAACAATCTCCAC
Gdf15	s	AGCCGAGAGGACTCGAACTC
	as	GGTTGACGCGGAGTAGCAGC
Hif1α	s	CCTGCACTGAATCAAGAGGTTGC
	as	CCATCAGAAGGACTTGCTGGCT
Hprt	s	CTGGTGAAAAGGACCTCTCGAAG
	as	CCAGTTTCACTAATGACACAAACG
Il4	s	ATGGATGTGCCAAACGTCCT
	as	AGCTTATCGATGAATCCAGGCA
Il6	s	CCGGAGAGGAGACTTCACAG
	as	GGAAATTGGGGTAGGAAGGA
Il10	s	ACAGCCGGGAAGACAATAACT
	as	CCTGCATTAAGGAGTCGGTTA
Il13	s	CACACAAGACCAGACTCCCC
	as	TCTGGGTCCTGTAGATGGCA
Kim1	s	TGGTTGCCTTCCGTGTCTCT
	as	TCAGCTCGGGAATGCACAA
Mcpip	s	CCTGTGGTCATCGACGGAAG
	as	GAAGGATGTGCTGGTCTGTGATA
Ngal	s	AATGTCACCTCCATCCTGGT
	as	ATTTCCCAGAGTGAACTGGC
Tgfß1	s	GGAGAGCCCTGGATACCAAC
	as	CAACCCAGGTCCTTCCTAAA
Tnfα	s	GATCGGTCCCCAAAGGGATG
	as	GGTGGTTTGCTACGACGTG
Vegf	s	CTGCTGTAACGATGAAGCCCTG
	as	GCTGTAGGAAGCTCATCTCTC
Vimentin	s	AGAGAGAGGAAGCCGAAAGC
	as	TCCACTTTCCGTTCAAGGTC

s, sense; as, antisense.

IV Methods

1 Animal Breeding and Housing

Gdf15 knockout mice were obtained from Se-Jin Lee (University of Connecticut & The Jackson Laboratory, Connecticut, USA). C57BL/6 mice (Charles River Laboratories, Sulzfeld,

Germany) were used both for backcrossing and as wildtype controls. In the knockout model, the *Gdf15* gene was disrupted by replacement of exon 2 with a neomycin resistance cassette via homologous recombination. More specific information on the *Gdf15* knockout is freely accessible in the mouse genome index under the identifier GDF15^{tm1Sjl}.

All mice were kept in a pathogen-free facility. They were housed in groups of five in a top filter polypropylene cage in a standard humidity- and temperature-controlled environment under a 12 h light/dark cycle with unlimited access to water and food. Cages, nestlets, food and water were sterilized by autoclaving before use.

All experimental procedures, i.e., animal handling, were performed in accordance with the European law regarding protection of animal welfare and with approval by the local government authorities, ROB and IILKE (55.2-1-54- 2532-63-12, 55.2-1-54- 2532-70-2016 and 112/2020). This study was carried out in accordance with the principles of the directive 2010/63/EU on the protection of animals used for scientific purpose.

2 Ischemia/Reperfusion Injury Model

Paired Groups (n = 6 – 13) of 6 – 8-week-old C57BL6/6 WT and *Gdf15* knockout mice were anesthetized with a compound mixture of 0.5 mg/kg medetomidine, 5 mg/kg midazolam and 0.05 mg/kg fentanyl prior to surgical treatment. After complete onset of anaesthesia mice were placed with their back on a 37 °C heating pad in order to maintain physiologically normal body temperature throughout the whole procedure, while constantly being monitored with a rectal probe. The abdominal cavity was opened with a flank incision, 1 - 1.5 cm of length and kept open using a wound spreader. After exposing the kidney, perihilar adipose tissue was gently removed with micro tweezers to guarantee best possible conditions for successful pedicle clamping. Subsequently, paired groups of mice (n = 6 – 13) underwent either sham surgery or renal pedicle clamping with a nontraumatic micro aneurysm clamp. In the setup of acute kidney injury bilateral clamping was conducted to evaluate renal function while unilateral clamping was utilized for gene expression and histopathological analysis. To induce chronic kidney disease mice were clamped unilaterally. In both setups applied ischemia time was 30 minutes, followed by reperfusion. Successful renal pedicle clamping was verified by gradual color change from normal to ischemic (pale). Vis versa successful initial reperfusion after clamp removal was assessed by color change from ischemic (pale) back to normal. Immediately after the kidney was placed back inside the retroperitoneal abdomen, 1 ml saline was injected subcutaneously to compensate for losses of fluid. Wounds were enclosed by suturing muscular and cutaneous layers with biologically resorbable sutures. Anaesthesia was terminated by antagonizing it with 2.5 mg/kg atipamezole, 0.5 mg/kg flumazenil and 1.2 mg/kg naloxone. 0.05 mg/kg buprenorphine was injected subcutaneously for pain control. Sham operated mice were handled in the exact same manner, except for renal pedicle clamping. In this study mice

were sacrificed 1, 5, 10 and 35 days after surgery by cervical dislocation. Both post-ischemic and contralateral kidneys, serving as intraindividual controls, were collected, decapsulated and divided into three parts with the middle part, including the renal hilus, being stored in 4% formalin buffer for advanced histomorphological examination and both other parts being snap frozen in RNAlator for subsequent gene expression profiling.

3 Assessment of Proteinuria, Blood Urea Nitrogen and Serum Creatinine

In the setup of AKI, blood samples were collected from the posterior-orbital venous plexus 1 day after the surgery, right before sacrificing the mice. Therefore, the head of the mice was restrained, and a capillary tube was inserted into the medial canthus of the eye. Blood flow was generated by capillary action. Kidney function was assessed by measuring blood urea nitrogen via enzymatic testing (DiaSys, Diagnostic Systems GmbH, Holzheim, DE) and serum creatinine levels using the Jaffe method (DiaSys Diagnostic Systems GmbH, Holzheim, DE) in accordance with the manufacturer's protocols. To assess proteinuria in the setup of AKI, urine samples were taken 1 day after the surgery. The mice belly was gently stroked, and the urine was collected in 1.5 ml Eppendorf tubes. Proteinuria was spectrophometrically determined via the Bradford method in accordance with the manufacturer's protocol (Bio-Rad Laboratories GmbH, Feldkirchen, DE).

4 Measurement of Kidney Weight

After unilateral pedicle clamping followed by 35 days of reperfusion kidney weight was assessed to evaluate the severity of CKD in both *Gdf15* deficient and C57BL/6 wildtype mice. Therefore, following cervical dislocation, kidneys were immediately collected, decapsulated and weighed on a Scaltec microbalance, sensitive to 0.001 g.

5 Total Kidney RNA Preparation and Quantitative Real-Time PCR from Renal Tissues

In order to obtain high quality, total RNA from renal tissues was stored in RNAlator and Ambion's PureLink™ RNA Mini Kit was used in accordance with the manufacturer's protocol. After concentration and purity was assessed with a NanoDrop 1000 spectrophotometer, cDNA was synthesized from 2 µg of total renal RNA of each individual sample by reverse transcription and polymerase chain reaction, using the following chemical components: 5x first-strand buffer, acrylamide, dNTPs, DTT, hexanucleotides and thermostable RNAsin inhibitor. Using an Eppendorf Thermomixer Comfort, initial cycling for 10 min at 65 °C was followed by 90 min at 42 °C and finally 5 min at 90 °C. After cooling down on ice, the obtained cDNA samples were kept at -20 °C until further processing. Subsequent quantitative real-time PCR was

performed using 10 µl SYBRGreen Mastermix, 0.12 µl Taq DNA polymerase, 0.45 µl of both reverse and forward, target gene-specific primers (Tab. 6), 6.98 µl ddH2O and 2 µl of 1:10 diluted cDNA on a total scale of 20 µl per reaction. *18s* rRNA was used as reference transcript for relative quantification, hence all qRT-PCR data for genes of interest were normalized to *18s*. Additional controls with ddH2O were negative for reference and target genes. All target gene primers were designed to be cDNA specific. Melting point curves were analysed in order to detect existing primer dimers or unspecific products. qRT-PCR was performed using a Roche Light Cycler 480. In total, 40 cycles were conducted with each cycle comprising an initiation phase at 95 °C, annealing phase at 60 °C and amplification phase at 72 °C. Relative expression of target genes was evaluated by ΔCt analysis.

6 Histological Evaluation

Both WT and *Gdf15* KO mice were sacrificed 1, 5, 10 and 35 days after I/R injury, or sham surgery. Kidneys were collected, fixed in 4% neutral-buffered formalin, dehydrated in graded alcohols, embedded in paraffin and cut into serial sections of 2 µm thickness for comprehensive histopathological examination. These sections were stained with periodic acid-Schiff (PAS), Lotus lectin and Picro-Sirius red using standard procedures. Immunostaining was performed as described below. Each section was examined under a LEICA DMR upright light microscope at a magnification of x100 or x200.

6.1 Acute Tubular Injury Score

The corticomedullary junction, also known as the “outer stripe of the outer medulla” (OSOM), is, due to its high oxygen consumption, the renal area, most susceptible to ischemic damage (Schiffer et al., 2018; Scholz et al., 2021). Therefore, this area was chosen for histopathological analysis of renal damage induced by ischemia/reperfusion and a semi-quantitative analysis of PAS-stained renal sections was conducted. Post ischemic tubular injury was scored by assessing the percentage of tubules in the corticomedullary junction, displaying tubular cell necrosis, tubular dilation and cast formation. 5 – 10 representative, nonoverlapping high-power fields per kidney within the outer stripe of the outer medulla were analysed at a magnification of x100. Tubular cell necrosis, tubular dilation and cast formation were separately scored as percentage of the high-power field. To guarantee precise and repeatable scoring, each high-power field got subdivided into areas equating 10% of the high-power field, by superposing a grid using Fiji software (Schindelin et al., 2012). Tubular injury score for each high-power field was calculated by taking the combined mean value of all three scored parameters. In turn, the scores of all high-power fields from one kidney were averaged. Total tubular injury score resulted by taking the mean of all kidneys from the same group of treatment and phenotype.

6.2 Immune Cell Infiltration

The collected kidneys were fixed and serially cut as described before. For immunostaining the following primary antibodies were used: rat anti-mouse lymphocyte antigen Ly-6B.2 (Serotec, Oxford, UK) for detection of neutrophils and rat anti-mouse F4/80 (Serotec, Oxford, UK) for detection of macrophages. Immune cell infiltration was scored by digitally quantifying the percentage of immune cells per high power field using ImageJ software (Schindelin et al., 2015). 5 – 10 representative, nonoverlapping high-power fields per kidney, taken within the corticomedullary junction, were analysed at a magnification of x100.

6.3 Renal Fibrosis and Glomerular Density

Renal fibrosis and differences in glomerular density were visualized by Picro-Sirius red staining. At least 5 representative, nonoverlapping pictures of the corticomedullary junction per kidney were captured and examined at a magnification of x200. Chronic, post ischemic renal fibrosis was scored by assessing the percentage of Picro-Sirius red positive area per high-power field in a semi-quantitative manner as follows: 0, none; 1, ≤ 10%; 2, 11% - 25%; 3, 26% - 49%; 4, 50% - 75%; 5, ≥ 76%. Glomerular density was assessed by counting the number of entire glomeruli per high-power field at a magnification of x200.

6.4 Tubular Atrophy

In order to score loss of tubular compartments, formalin-fixed tissue sections were stained with L. tetragonolobus lectin (Lotus lectin). 5 – 10 representative, nonoverlapping pictures per kidney within the outer stripe of the outer medulla were taken at a magnification of x100. Loss of intact tubuli was detected by digitally quantifying the percentage of integral tubular compartments, visualized as the Lotus lectin positive area per high power field using ImageJ software (Schindelin et al., 2015).

6.5 Chronic Loss of Structural Renal Integrity

Chronic loss of structural renal integrity after I/R-induced CKD was visualized by periodic acid-Schiff staining. The proportional amount of both histomorphological integral tubuli and infiltrative substance was assessed in a semi-quantitative manner. Taking the process of chronic kidney shrinkage after I/R injury into account, as many representatives, nonoverlapping high-power fields per kidney within the corticomedullary junction as possible were analysed at a magnification of x200. To guarantee precise and repeatable scoring, each high-power field got subdivided into areas equating 10% of the high-power field, by superposing a grid using Fiji software (Schindelin et al., 2012).

7 Isolation and Cultivation of Renal Tubular Epithelial Cells

After sacrificing the mouse by cervical dislocation, the mouse was placed on its back and fixated on both its hind and rear legs with needle tips. All surgical instruments as well as the mouse front sides were disinfected using 100% Ethanol. The abdominal cavity was opened with a midline incision, about 1.5 - 2.5 cm of length. After exposing the renal hilus, the kidneys were gently removed by cutting through the renal vessels and the ureter. Subsequently, the remaining adipose tissue was removed using micro tweezers and the renal capsules were peeled off. After finely mincing the kidneys with the back of a syringe, renal tissue was digested with 1 ml Collagenase D (1.5 mg/ml) for 30 min at 37 °C in a cell culture incubator. All following steps were performed under a sterile cell culture hood. The digested kidneys were sieved through a 70 µm filter and centrifuged at 1500 rpm and 4 °C for 5 min with break. The obtained pellet was resuspended in 2 ml PBS and carefully pipetted in a 15 ml falcon onto 10 ml of 31% Percoll® solution in order to separate cell types. After centrifuging at 3000 rpm and 4 °C for 10 min, a pellet was obtained, mainly consisting of PTS. The PTS pellet was washed twice by alternately resuspending with 1 ml PBS and centrifuging at 1500 rpm and 4 °C for 5 min with break. The final pellet was cultured with K1 medium (as described in Tab. 2) in a 150 mm^2 Petri dish. After keeping it for 2 days at 37 °C in the incubator, K1 medium was changed for the first time. The successful growth of the TECs out of the PTS was monitored daily via light microscope. After 10 – 14 days, TECs had fully grown out of the PTS, and could be used for experiments. Meanwhile medium was changed every 3 – 5 days and cells were incubated at 37 °C and 5% CO_2.

8 Extraction of Bone Marrow Cells

In order to cultivate and differentiate them into bone marrow-derived macrophages or bone marrow-derived dendritic cells, bone marrow cells were extracted in the following manner: In preparation a 23 G needle was pushed through the bottom of a 0.5 ml Eppendorf tube and put into a 1.5 ml Eppendorf tube. After sacrificing the mouse, both hind legs were isolated, and the surrounding muscle tissue was removed using micro tweezers and a pair of micro scissors. Femur and tibia were kept, and the bone marrow cavity was opened by cutting off both ends of every bone. About 4 bones together were put in the 0.5 ml Eppendorf tube (within the 1.5 ml Eppendorf tube) and centrifuged at 8800 rpm and 4 °C for 15 sec. to extract bone marrow and collect it into the 1.5 ml Eppendorf tube. The obtained pellet was carefully resuspended in 1 ml of RBC lysis buffer, and transferred into a 15 ml falcon, where another 2 ml RBC lysis buffer were added. After keeping it at RT for 1 min, the reaction was stopped by diluting the lysis buffer with 10 - 20 ml modified RPMI medium. The solution was centrifuged at 1500 rpm and 4 °C for 2 min with break. This step was once repeated with fresh medium to wash out the lysis buffer. The finally obtained pellet was resuspended in 1 ml medium and the live cells were

counted using a hemocytometer. The cells were immediately seeded for experiments in a 6 or 12 well plate, with 3 mio. and 1.5 mio. cells respectively. 1.5 ml modified RPMI medium, containing reMCSF, or reGM-CSF to differentiate the cells into BMDMs, or BMDCs respectively, were added to each 6 well, respectively 1 ml to each 12 well, for initial cultivation.

9 Cultivation of Bone Marrow Derived Cells

On day 2 after isolation, the same amount of modified RPMI medium, as used for initial cultivation, was added to each well. On day 5 the medium was completely replaced by fresh modified RPMI. Cells were cultivated at 37 °C and 5% CO_2 and cell viability and differentiation were monitored daily via light microscope. Between day 7 and day 10 BMDMs or BMDCs were completely differentiated and could be used for experiments.

10 Isolation and Cultivation of Renal Fibroblasts

Prior to tissue explanting, 100 mm^2 Petri dishes were coated with 1% gelatin solution in order to allow the minced tissue to be adequately secured to the Petri. Therefore, 2% gelatin solution was 1:1 diluted with 0.01 M PBS and filter sterilized into a falcon tube using a syringe and a 0.2 µm pore filter unit. The entire surface of the petri dishes was coated with 1% gelatin solution and incubated at 37 °C for 30 min. Right before starting cell isolation, excess gelatin solution was removed, and the petri dishes were washed twice with PBS.

Mice were sacrificed, fixated and the kidneys were isolated exactly as described for the TECs. Remaining adipose tissue was removed and the renal capsules were peeled off. Each kidney was divided into two parts by a longitudinal incision using a scalpel in order to have clear sight on the anatomical division between medulla and cortex. Subsequently only very small sections of the renal cortex were cut off to avoid yielding an unnecessarily mixed cell population. The explanted cortical sections were minced finely with the back of a syringe. After sieving this cortical mass through a 70 µm filter, it was centrifuged at 1500 rpm and RT for 5 min with break. The obtained pellet was resuspended in 1 – 2 ml PBS. Both sieving and resuspending were repeated twice. Subsequently, the minced and filtered tissue was transferred into the gelatin coated petri dishes and 2 ml of enriched DMEM medium (20% FBS, 1% PS) was added. On day 1 another 2 ml of medium were added. Cells were cultivated at 37 °C and 5% CO_2. After 3 – 5 days of incubation initial population of renal fibroblasts were established. Cells could be used for experiments 7 – 10 days after isolation.

11 Cell Harvesting and RNA Isolation

Before harvesting the cells, the supernatant was collected and stored immediately at -20 °C until quantification of its GDF15 concentration using ELISA. Subsequently, 350 µl of Buffer RL of Norgen´s Total RNA Purification Kit were added directly to each well of the cell culture plate.

After enhancing cell lysis by gentle scraping of each well, cells were incubated with the lysis buffer for 5 min at RT. The lysate was then transferred into a 1.5 ml Eppendorf tube and 200 µl of absolute alcohol were added. After thoroughly vortexing the tube for 10 sec., all following steps were performed using Norgen's Total RNA Purification Kit in accordance with the manufacturer's instructions. Just within the last step, the amount of added Elution Solution A was adjusted from previously 50 µl to now 30 µl. The purified RNA sample was stored immediately at -20 °C until further processing.

12 RNA Measurement

RNA concentration in was measured using a NanoDrop 1000 Spectrophometer. Sample purity was monitored by both the E260/E280 and the E260/230 ratio.

13 cDNA-Conversion and Quantitative Real-Time PCR

cDNA was synthesized from total RNA by RT-PCR using Eppendorf Thermomixer Comfort. The amount of total RNA used was normalized for all samples in each experiment to at least 500 ng, if possible 1 µg or 2 µg of total RNA. ddH_2O was added to the individual amount of RNA on a total scale of 15 µl. For each reaction 15 µl RNA/ddH_2O were mixed with 7.45 µl of master mix on a total scale of 22.45 µl per reaction. The composition of the master mix is indicated in table 7. Reverse transcription was performed for 90 min at 42 °C and subsequently ended by enzyme inactivation for 5 min at 90 °C. Afterwards the obtained cDNA samples were cooled down, diluted 1:10 with ddH_2O and stored at -20 °C.

Tab. 8: Master mix for reverse transcription

Component	Stock Concentration	Amount per Sample [µl]
5x First Strand Buffer		4.5
DTT	0.1 M	1
dNTPs	25 mM	0.45
RNAsin	40 U/µl	0.5
Acrylamide	15 µ/ml	0.25
Hexanucleotide Mix	10x conc.	0.25
Superscript	200 U/µl	0.5

Quantitative Real-time PCR (qRT PCR) from cDNA was performed with 2 µl of 1:10 diluted cDNA and 18 µl of PCR master mix (Tab. 8) per well on a total scale of 20 µl per reaction. Both *18s* rRNA and *Gapdh* mRNA were used as reference genes for relative quantification. Additional controls with ddH2O were negative for reference and target genes. All target gene primers (Tab. 6) were designed to be cDNA specific. Melting point curves were analysed in

order to detect existing primer dimers or unspecific products. qRT-PCR was performed using a Roche Light Cycler 480 following a touchdown PCR program. In total, 40 cycles were conducted with each cycle comprising an initiation phase at 95 °C, annealing phase at 60 °C and amplification phase at 72 °C. Relative expression of target genes was evaluated by ΔCt analysis.

Tab. 9: Master mix for qRT PCR

Component	Stock Concentration	Amount per Sample [µl]
Forward Primer	10 µM	0.45
Reverse Primer	10 µM	0.45
SybrGreen	2x	10
Taq DNA Polymerase	5 U/ml	0.12
ddH_2O		6.98

14 GDF15 ELISA

In order to quantify GDF15 protein levels from cell culture supernatants, both the DuoSet ELISA Development System Kit and the reagent diluent were purchased from R&D Systems and used in accordance with the manufacturer's protocol. Optimal sample concentration was determined making use of a standard curve ranging from 500 pg/ml to 7.81 pg/ml employing a two-fold serial dilution. Absorbance was measured at 450 nm while wavelength correction was set to 570 nm, using a Dynex Opsys 96-well microplate reader.

15 Fluorescence Activated Cell Sorting (FACS)

Fluorescence activated cell sorting (FACS) was used to immunophenotype by analysing protein expression on the cell surface. In this technique, single cells are stimulated by a laser beam while passing through a capillary. The result is a cell-specific scattering of light, which is primarily expressed as both forward scatter (FSC) and side scatter (SSC). While FSC intensity correlates with the size of the cells and is especially helpful to distinguish between different immune cells, SSC intensity provides information about the internal complexity of the cells. In addition, dyes, such as fluorophore labelled antibodies, can be used to immunophenotype specific subsets of cells.

FACS was used to analyse M1/M2 differentiation of BMDMs under various culture conditions. Cells were collected, washed with FACS buffer and FcR-blocked with anti-mouse CD16/32 for 5 min at 4 °C. After blocking, cells were stained with surface antibodies V450 anti-mouse CD11b, APC anti-mouse F4/80, FITC anti-mouse CD206, PE anti-mouse CD80, PE/Cy7 anti-mouse CD11c and BV510 anti-mouse MHC II for 25 min at 4 °C in the dark (All Antibodies

were obtained from BD Biosciences, Heidelberg, DE). 7-AAD (BD Biosciences, Heidelberg, DE) was added to each reaction, followed by incubation for 10 min at 4 °C in the dark. Cells were washed twice and resuspended in FACS buffer.

Flow cytometry was performed with a BD FACS Canto II, and all data were analysed using FlowJo v8.7 (Tree Star Inc., Ashland, OR, USA) software, displaying the measured data in a scatter plot or a histogram.

16 Statistical Analysis

As far as only two groups were compared unpaired two-tailed Student´s t test or Mann-Whitney U test was used. Unpaired two-tailed Student's t test was used when normal distribution of data could be assumed. Mann-Whitney U test was used for direct comparisons between single groups when non-parametric distribution of data was assumed. For multiple comparisons of normally distributed or non-parametric data one-way ANOVA, respectively Kruskal-Wallis test - subsequently followed by post-hoc Bonferroni´s test - was used. Data are shown as mean ± SEM. Statistical significance was assumed at a p-value of <0.05 (shown as n.s. = not significant, * $p < 0.05$, ** $p < 0.01$ and *** $p < 0.001$). Data evaluation and statistical analysis were performed using GraphPad Prism 6.0 software (GraphPad Software Inc., San Diego, CA, USA).

V Results

In the first step, ischemia/reperfusion (I/R) injury-based models of AKI and CKD with *Gdf15 -/-* and control C57BL/6 WT mice were evaluated using gene expression analysis and histological studies to assess

1) the impact of *Gdf15* deficiency on the development of AKI, or CKD *in-vivo.*

In the second step, primary renal cells were isolated from *Gdf15 -/-* and control C57BL/6 WT mice to elucidate the *in-vivo* observations by

2) determining the main source of renal GDF15 and
3) shedding light on the innate immune responses, affected by GDF15 activity in the kidney.

1 Impact of *Gdf15* Deficiency on the Development of AKI and CKD *in-vivo*

1.1 Implementation of Ischemia/Reperfusion Injury

In both the acute and the chronic setup, paired groups of *Gdf15 -/-* and C57BL/6 WT mice underwent either renal pedicle clamping or sham surgery at 8 weeks of age. To induce AKI groups of mice (n = 6 – 10) were subjected to 30 min of renal pedicle clamping followed by reperfusion. For the evaluation of AKI, mice were sacrificed 1 and 5 days after surgery. To induce CKD, groups of mice (n = 6 – 13) underwent 30 min of unilateral renal pedicle clamping

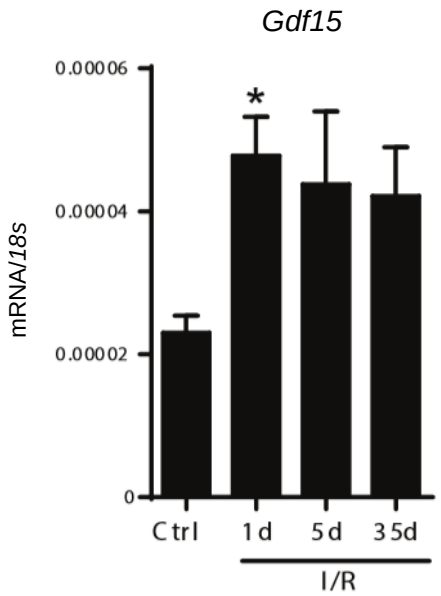

Fig. 1. Renal *Gdf15* mRNA expression 1, 5 and 35 days after unilateral I/R. Paired groups of 8-week-old *Gdf15 -/-* and control C57BL/6 WT mice underwent either 30 min of unilateral renal pedicle clamping or sham surgery. Mice were sacrificed 1, 5 and 35 days after the procedure. The induction of *Gdf15* mRNA expression was analysed by qRT-PCR from whole kidney lysates of C57BL/6 WT mice. Data are shown as mean ± SEM.

followed by reperfusion (Fig. 1, A and B). To assess chronic kidney disease, mice were

sacrificed 35 days after the procedure. Before conducting further analysis, *Gdf15* mRNA transcript levels from renal tissues of WT mice, subjected to I/R, were evaluated. Therefore, mRNA was isolated from renal tissues of WT mice after either I/R or sham surgery, using Ambion's PureLink™ RNA Mini Kit. After generating cDNA via reverse transcription, gene expression of *Gdf15* was quantified by qRT-PCR. Figure 1C indicates the relative expression of *Gdf15* in renal tissues from WT mice after sham surgery (Ctrl) or at day 1, 5 and 35 after I/R. *18s* was used as housekeeping gene. Throughout all evaluated timepoints *Gdf15* mRNA expression in post-ischemic renal tissues of C57BL/6 WT mice was elevated in comparison to the sham control (Fig. 1C). The observed induction of renal *Gdf15* mRNA expression met statistical significance only on day 1 after I/R (Fig. 1C).

1.2 Comparison of AKI in *Gdf15* KO and WT Mice

1.2.1 Assessment of Kidney Function

Since ischemic kidney injury fundamentally results in loss of functional tubuli, and hence, in decreased tubular reabsorption of protein, measurement of proteinuria can serve as important risk-assessment tool in the period after AKI (Hsu et al., 2020). As well, elevated blood urea

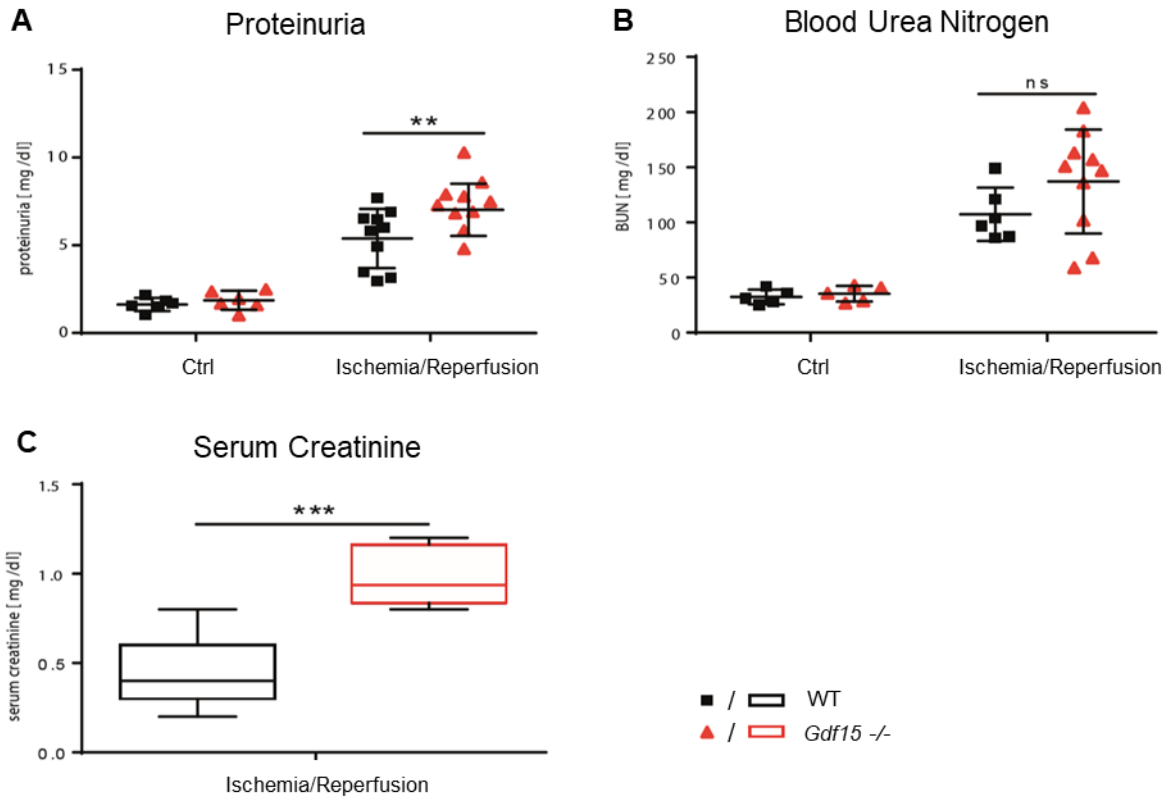

Fig. 2. Assessment of kidney function in I/R-induced AKI. Blood and urine samples were collected from *Gdf15 -/-* and WT mice at day 1 after bilateral I/R, or sham surgery. Functional renal injury was assessed by measurement of proteinuria (A), blood urea nitrogen (B) and serum creatinine (C). All data are represented as means ± SEM.

nitrogen (BUN) and serum creatinine (SCr) levels are widely appreciated as indicators of impaired renal function since both are excreted exclusively by the kidneys (Akcay et al., 2010;

Levey et al., 2020; Luo et al., 2014). Hence, proteinuria, BUN, and SCr levels were quantified, to investigate the impact of *Gdf15* deficiency on kidney function after I/R-induced AKI. Therefore, blood and urine samples were collected from *Gdf15 -/-* and WT mice on day 1 after bilateral I/R, or sham surgery. Subsequently, proteinuria, BUN, and SCr levels were quantified, as illustrated by Figure 2. Proteinuria levels of *Gdf15 -/-* mice, subjected to I/R, were found to be significantly higher than the levels of their corresponding I/R WT controls (Fig. 2A). At the same time *Gdf15* deficiency was found to correlate with increased post-ischemic BUN levels as compared to the corresponding WT control group (Fig. 2B). Yet, this trend was not statistically significant. Moreover, *Gdf15 -/-* mice displayed significantly increased SCr levels at day 1 after I/R in comparison with their WT littermates (Fig. 2C). Together these findings suggest a strong renoprotective role for GDF15 in I/R-induced AKI.

1.2.2 Gene Expression Analysis

Next, the question was addressed, whether the observed differences in post-ischemic kidney function between WT and *Gdf15 -/-* mice would be associated with altered post-ischemic renal expression of pro-inflammatory or injury-associated genes. Therefore, mRNA was isolated from renal tissues of *Gdf15 -/-* and WT mice after unilateral I/R, using Ambion's PureLink™ RNA Mini Kit. After generating cDNA via reverse transcription, gene expression of *Tnfα* and *Kim1* was quantified by qRT-PCR. Figure 3 indicates the relative expression of *Tnfα* and *Kim1* in renal tissues from *Gdf15 -/-* and WT mice at day 1 and 5 after I/R-induced AKI. *18s* was

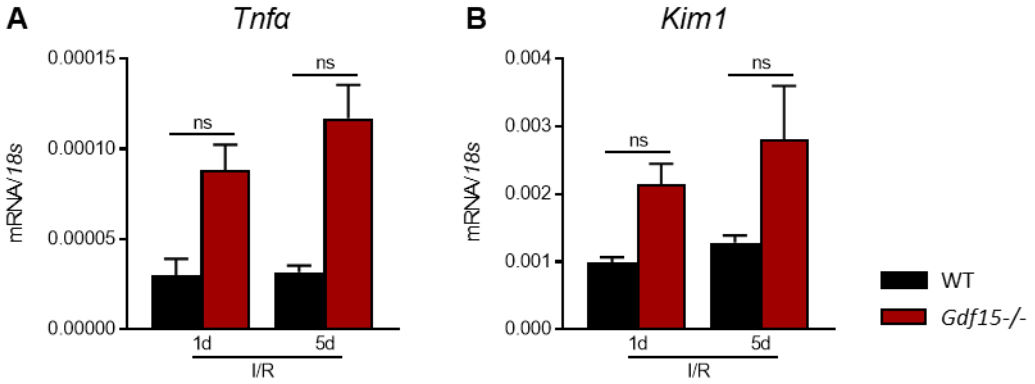

Fig. 3. Renal expression of *TNFα* and *Kim1* in I/R-induced AKI. Renal mRNA was isolated from whole renal tissues of *Gdf15* -/- and C57BL/6 WT mice 1 and 5 days after unilateral I/R, transcribed into cDNA and quantified by qRT-PCR. Renal mRNA expression of *Tnfα* (A) and *Kim1* (B). Data are expressed as mean of the ratio of target gene mRNA expression versus the respective *18s* rRNA level ± SEM.

used as housekeeping gene. *Gdf15* deficiency in mice was associated with mildly increased renal mRNA expression of *Tnfα* and *Kim1* both 1 and 5 days after I/R-induced AKI as compared to the corresponding WT control (Fig. 3, A and B). These findings might indicate that GDF15 could reduce post-ischemic expression of pro-inflammatory or injury-associated genes in the kidney. However, these trends were not statistically significant.

1.2.3 Histological Evaluation

1.2.3.1 Tubular Injury Score

Next, the morphological extent of I/R-induced AKI was assessed by histological evaluation of renal tissue sections from both C57BL/6 WT and *Gdf15 -/-* mice. The outer stripe of the outer medulla (OSOM) within the corticomedullary junction of the kidney is the renal area, most susceptible to ischemic damage. As it predominantly comprises tubular segments, acute tubular injury represents a hallmark of AKI. To assess the influence of *Gdf15* deficiency on the development of tubular injury during I/R-induced AKI, a tubular injury score was quantified from

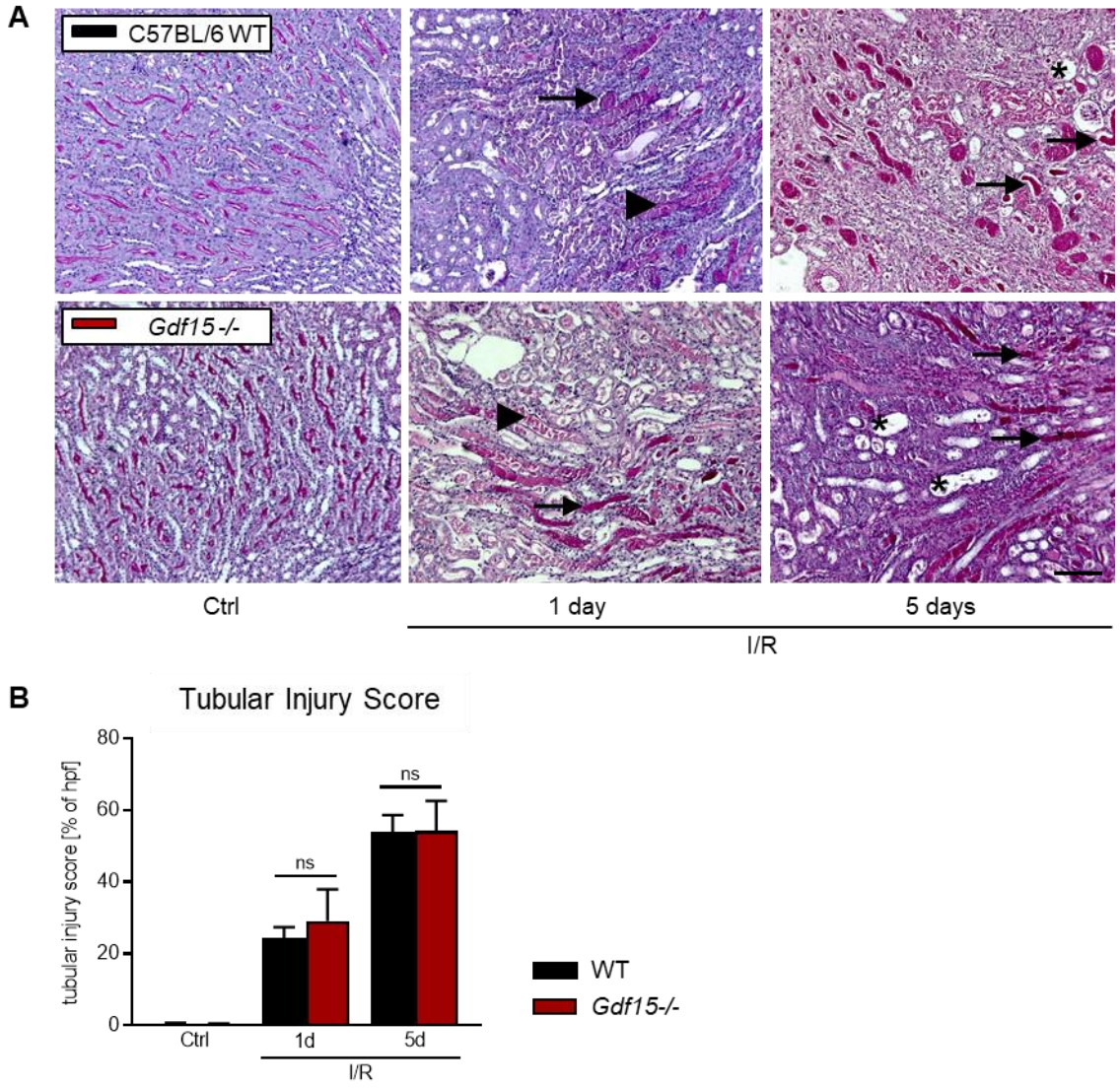

Fig. 4. Tubular injury score in I/R-induced AKI. The outer stripe of the outer medulla (OSOM) was examined in PAS-stained slides from both *Gdf15 -/-* and C57BL/6 WT mice, subjected to unilateral I/R, or sham surgery, followed by 1 or 5 days of reperfusion. Representative PAS-stained pictures of post-ischemic or sham-control kidneys from *Gdf15 -/-* and WT mice are shown in 100-fold magnification (A); scale bar is 20 µm. Tubular injury score (B) was assessed by combining 3 separately scored parameters: Tubular necrosis (arrowheads), tubular cast formation (arrows) and tubular dilation (asterisk). Tubular injury score [% of hpf] is presented as mean ± SEM.

PAS-stained renal tissue sections of WT and *Gdf15 -/-* mice at day 1 and 5 after I/R, or after

sham surgery. Thereby, tubular injury score was evaluated in a semiquantitative manner, by combining three individually scored parameters – tubular necrosis, tubular cast formation and tubular dilation – into an overall injury score. Figure 4 indicates the overall tubular injury score

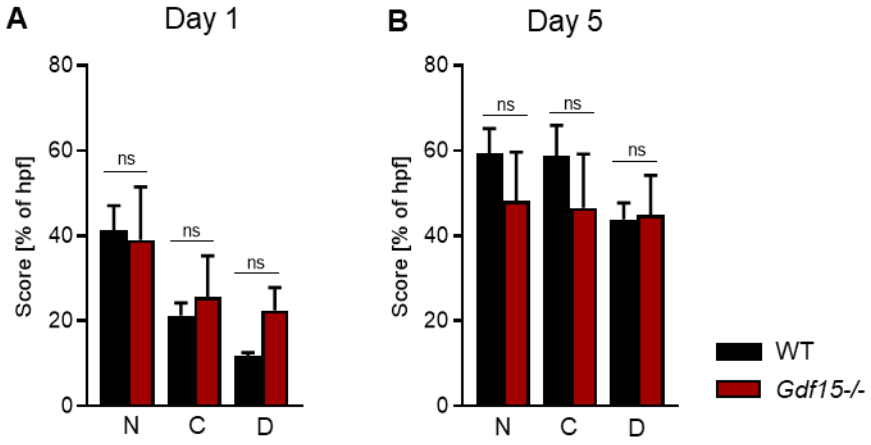

Fig. 5. Tubular necrosis, cast formation and dilation in I/R-induced AKI. The outer stripe of the outer medulla (OSOM) was examined in PAS-stained slides from both *Gdf15* -/- and C57BL/6 WT mice, subjected to unilateral I/R, followed by 1 (A) or 5 days (B) of reperfusion. Tubular injury was assessed by scoring tubular necrosis (N), tubular cast formation (C) and tubular dilation (D). Data are shown as means ± SEM.

of *Gdf15* -/- and WT mice at day 1 and 5 after I/R, or after sham surgery. Figure 5 illustrates the specific injury scores for each individual parameter - tubular necrosis, tubular cast formation and tubular dilation - on day 1 and 5 after I/R. While both *Gdf15* -/- and WT group displayed elevated tubular injury scores 1 and 5 days after I/R as compared to their respective sham controls, no significant differences between the *Gdf15* -/- and WT group regarding the extent of tubular injury 1 or 5 days after I/R could be observed (Fig. 4, A and B). Similarly, analysis of the specific subcategories revealed no significant differences between the *Gdf15* -/- and WT group - neither on day 1 (Fig. 5A), nor on day 5 (Fig. 5B) after I/R.

1.2.3.2 Neutrophil Infiltration

Rapid influx of neutrophils into the tubulointerstitial space of the kidney is a crucial part of the innate immune response upon I/R injury (Jang et al., 2009; Sharfuddin et al., 2011). To evaluate the impact of *Gdf15* deficiency on neutrophil influx during I/R-induced AKI, kidney sections from *Gdf15* -/- and WT mice, subjected to either I/R or sham surgery, were immunostained using a rat anti-mouse lymphocyte antigen Ly6B.2 antibody. Subsequently, neutrophil infiltration was digitally quantified using ImageJ software. As shown in Figure 6, immunostaining for Ly6B.2+ neutrophils revealed no significant differences in neutrophil influx between I/R kidneys from *Gdf15*-deficient and WT mice 1 day after ischemic injury. Of note,

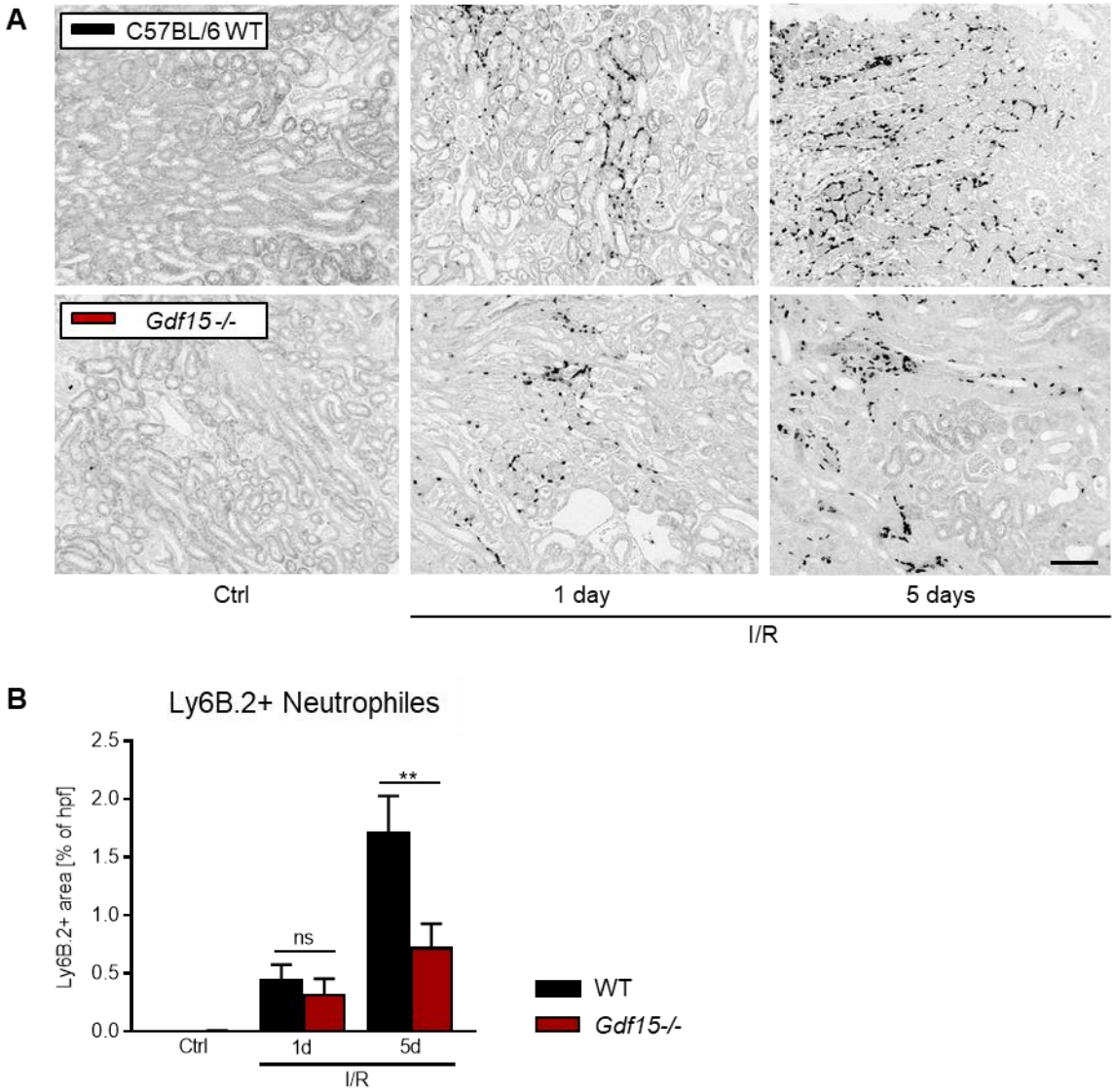

Fig. 6. Influx of Ly6B.2+ neutrophils in I/R-induced AKI. Ly6B.2+ neutrophil infiltration was evaluated from both *Gdf15* -/- and C57BL/6 WT mice 1, and 5 days after I/R injury or sham surgery. Renal sections were immunostained using rat anti-mouse lymphocyte antigen Ly6B.2 antibody and neutrophil influx was digitally quantified using ImageJ software. Representative pictures of post-ischemic or sham-control kidneys from *Gdf15* -/- and WT mice are shown in 100-fold magnification (A); scale bar is 20 µm. Ly6B.2+ area in the corticomedullary junction of post-ischemic and control kidneys (B). Data are presented as means ± SEM.

Gdf15 deficiency was associated with significantly decreased numbers of interstitial neutrophils at day 5 after I/R (Fig. 6, A and B).

1.3 Comparison of CKD in *Gdf15* KO and WT Mice

1.3.1 Assessment of Kidney Weight

Since renal atrophy is a common consequence of advanced CKD (Agarwal et al., 2020; Moghazi et al., 2005), reduction in kidney weight can serve as easily measurable parameter to estimate its severity. To assess the impact of *Gdf15* deficiency on CKD-associated renal atrophy, kidneys from post-ischemic or sham-operated *Gdf15* -/- and WT mice were collected, decapsulated and weighed on a Scaltec microbalance.

As illustrated in Figure 7, both *Gdf15*-deficient and WT mice displayed a reduction in kidney weight 35 days after unilateral I/R as compared to their respective sham controls (Fig. 7A).

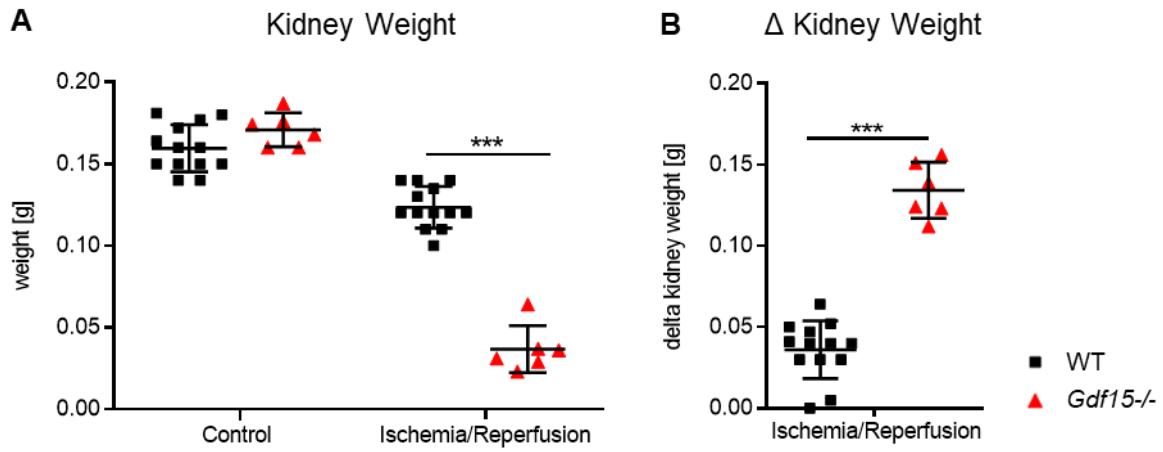

Fig. 7. Assessment of kidney weight in I/R-induced CKD. Kidneys from both *Gdf15* -/- and C57BL/6 WT mice were collected 35 days after unilateral I/R, or sham surgery, decapsulated and weighed on a Scaltec microbalance. Absolut kidney weights presented as dot plot (A), subsequently delta kidney weight shown as dot plot (B). Data are presented as means ± SEM.

Meanwhile, post-ischemic kidneys from mice deficient for *Gdf15*, weighed significantly less than those from their WT littermates (Fig. 7A). In conclusion, *Gdf15 -/-* mice displayed a significantly larger reduction in kidney weight than their WT controls 35 days after unilateral I/R (Fig. 7B). This finding indicates a renoprotektive function of GDF15 in I/R-induced CKD.

1.3.2 Histological Evaluation

1.3.2.1 Disruption of Tubular Architecture

Since *Gdf15* deficiency correlated with significantly aggravated post-ischemic renal atrophy, as shown in Figure 7, its influence on chronic post-ischemic disruption of tubular architecture was analysed. Therefore, kidneys from *Gdf15 -/-* and WT mice were collected 35 days after either I/R or sham surgery. After PAS-staining, the percentage of intact tubuli or of infiltrative mass was quantified using Fiji software. As shown in Figure 8, mice deficient for *Gdf15* displayed significantly less histomorphological intact tubuli on day 35 after I/R as compared to their WT littermates (Fig. 8, A and B). At the same time, renal sections from *Gdf15 -/-* mice revealed more unspecifiable, infiltrative material on day 35 after I/R than those from WT mice (Fig. 8, A and C). However, this trend was not statistically significant.

1.3.2.2 Tubular Atrophy

Tubular atrophy is a hallmark of CKD (Agarwal et al., 2020). It is one of the main histopathological reasons for both long term kidney shrinkage and altered tubular morphology after ischemic injury (Agarwal et al., 2020). Since lack of *Gdf15* was shown to correlate with both increased renal atrophy (c.f. Fig. 7) and aggravated disruption of tubular architecture (c.f.

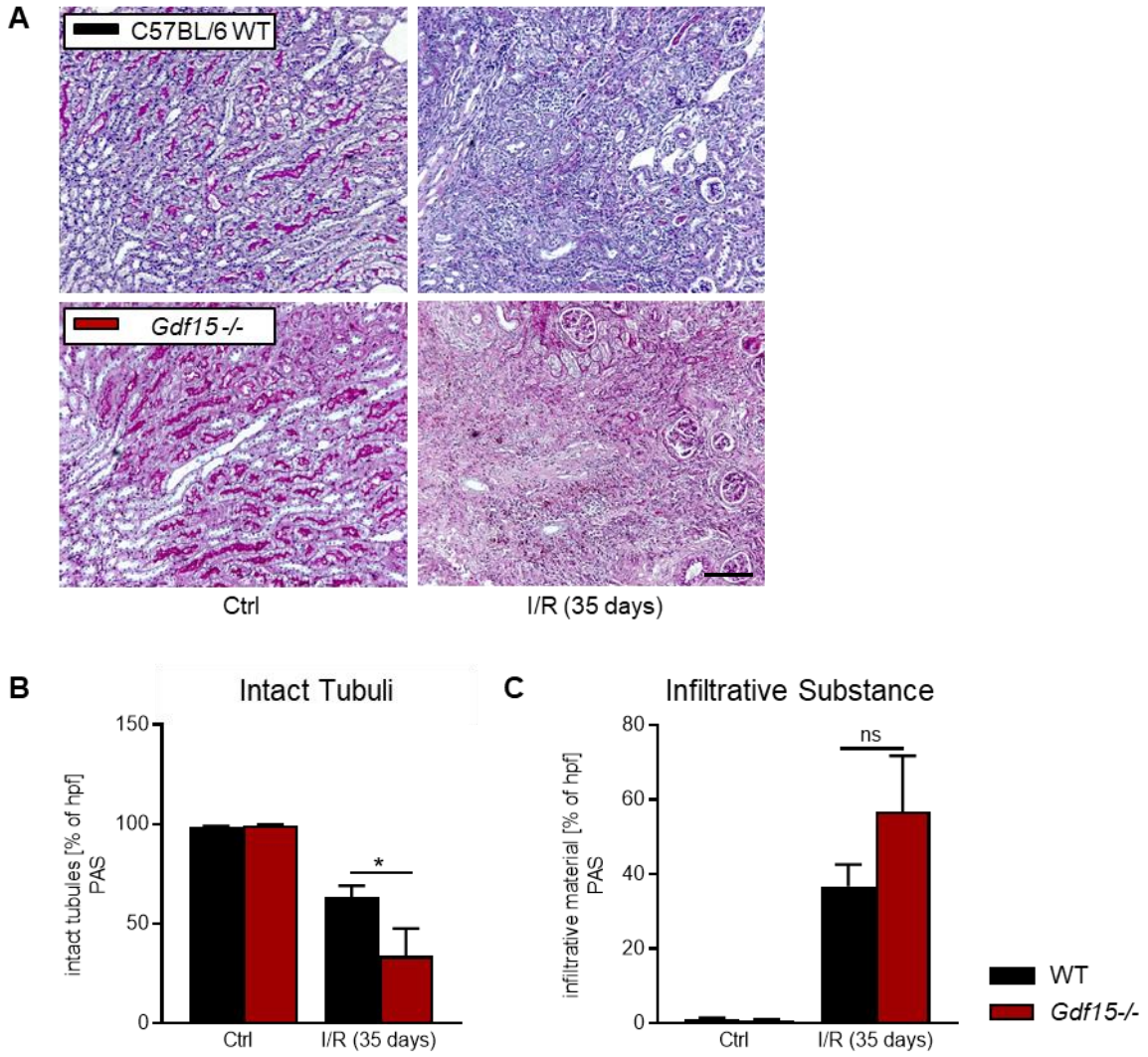

Fig. 8. Disruption of tubular architecture in I/R-induced CKD. Chronic loss of structural renal integrity was analysed in PAS-stained renal sections from *Gdf15 -/-* and WT mice 35 days after unilateral I/R or sham surgery. The proportional amount of histomorphological intact tubuli and infiltrative substance in the corticomedullary junction was assessed in a semi-quantitative manner assisted by Fiji software. Representative PAS-stained pictures of sham-operated and ischemic kidney sections are shown in 200-fold magnification (A); scale bar is 40 µm. Proportional amount of histomorphological intact tubuli (B) and infiltrative substance (C) are shown as bar graphs. Data are presented as means ± SEM.

Fig. 8), it might also be expected that *Gdf15 -/-* mice would exhibit more severe tubular atrophy on day 35 after I/R than WT mice. To address this hypothesis, kidneys from *Gdf15 -/-* and WT mice were collected 35 days after either I/R or sham surgery. After Lotus Lectin immunostaining, the percentage of Lotus Lectin positive tubular structures was digitally quantified using ImageJ software. As illustrated in Figure 9, both *Gdf15 -/-* and WT mice revealed a decrease in Lotus Lectin positive tubular structures 35 days after unilateral I/R. Yet, post-ischemic kidneys from mice deficient for *Gdf15* displayed less Lotus Lectin positive tubular structures than those from their corresponding WT controls, indicating increased tubular atrophy (Fig. 9, A and B). Still, this trend was not statistically significant.

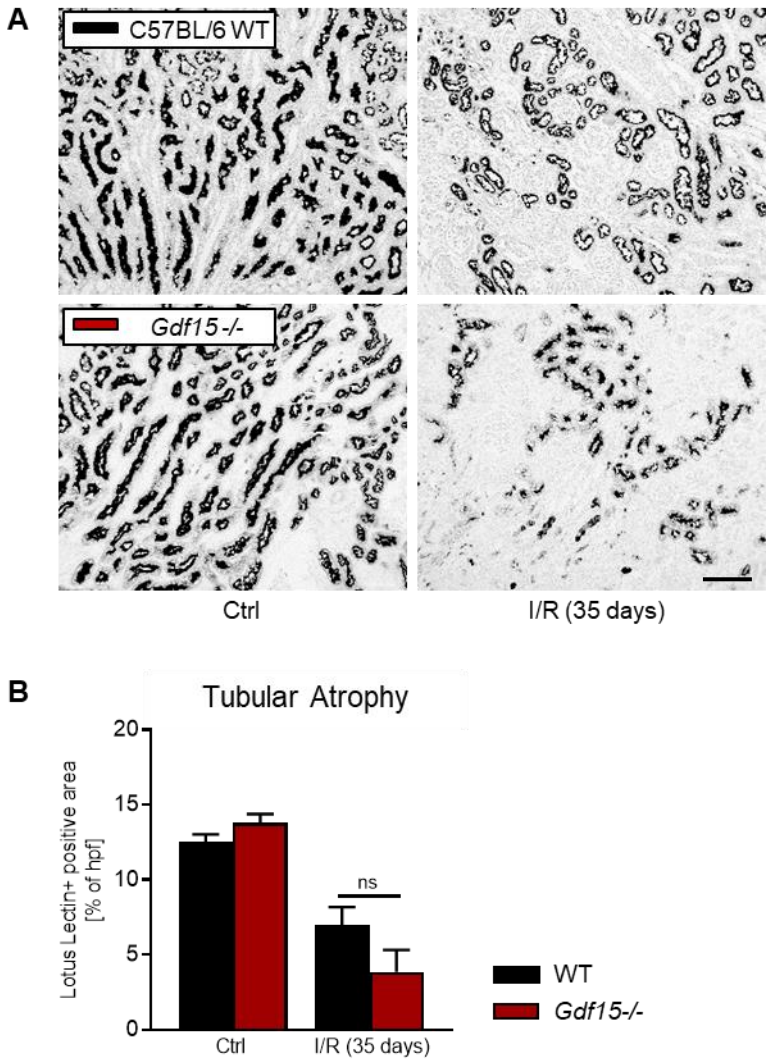

Fig.9. Tubular atrophy in I/R-induced CKD. Tubular atrophy was analysed in Lotus lectin-stained renal sections from *Gdf15 -/-* and WT mice 35 days after unilateral I/R or sham surgery. Loss of intact tubuli was detected by digitally quantifying the percentage of integral tubular compartments, visualized as Lotus lectin positive area per hpf using ImageJ software. Representative Lotus lectin-stained pictures of sham-operated and ischemic kidney sections are shown in 100-fold magnification (A); scale bar is 20 µm. Tubular atrophy (B) is shown as bar graph. Data are presented as means ± SEM.

1.3.2.3 Renal Fibrosis and Glomerular Density

Another crucial pathophysiological process, associated with the development of CKD, is the renal production and deposition of ECM components within the tubulointerstitial space, commonly referred to as fibrosis (Agarwal et al., 2020). To evaluate the impact of *Gdf15* deficiency on the development of I/R-induced renal fibrosis, post-ischemic fibrotic restructuring was quantified by immunostaining for collagen I and III using Picro-Sirius red stain. As illustrated in Figure 10, kidney sections from *Gdf15 -/-* mice, subjected to I/R, showed significantly aggravated renal fibrosis than those from the corresponding WT group (Fig. 10, A and B). Since the tubular compartments are the areas of the kidney most prone to ischemic injury, I/R-induced CKD is predominantly resulting in loss of functional tubuli but not glomeruli. This architectural change results in chronic renal shrinkage. However, the number of glomeruli remains almost unchanged. Consequently, the number of glomeruli per

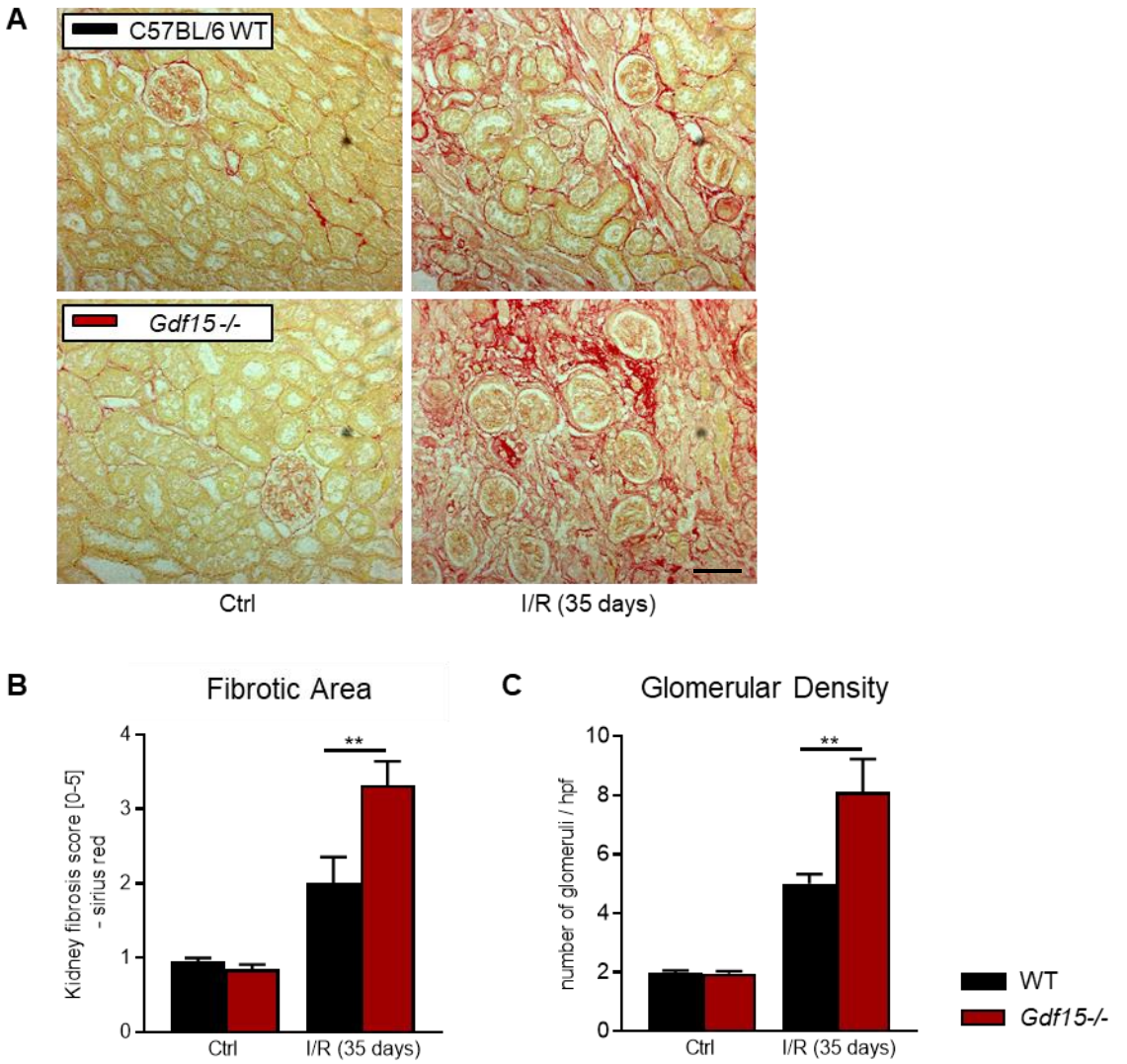

Fig. 10. Renal fibrosis in I/R-induced CKD. Renal fibrosis and glomerular density were analysed in Picro-Sirius red--stained renal sections from *Gdf15 -/-* and WT mice 35 days after unilateral I/R or sham surgery. Representative Picro-Sirius red--stained pictures of sham-operated and ischemic kidney sections are shown in 200-fold magnification (A); scale bar is 40 µm. Fibrotic area (B) and glomerular density (C) are shown as bar graphs. Data are presented as means ± SEM.

high-power field can serve as indirect parameter to stratify the severity of advanced CKD. Evaluating glomerular density, sections of post-ischemic kidneys from *Gdf15*-deficient mice revealed significantly higher numbers of glomeruli per high-power field than those from WT mice (Fig. 10, A and C), indicating more advanced CKD in *Gdf15*-deficient animals. Together, these findings suggest a protective, potent anti-fibrotic role for GDF15 in I/R-induced CKD.

1.3.2.4 Macrophage Infiltration

While interstitial recruitment of macrophages during early stages of ischemic kidney injury is crucial for orchestration of post-ischemic inflammation and thereby dissolvement of tissue damage, prolonged accumulation of macrophages in the tubulointerstitial space can correlate with the development and progression of CKD (Agarwal et al., 2020; Schnaper, 2017). To evaluate the impact of *Gdf15* deficiency on macrophage infiltration in I/R-induced CKD, kidney

sections from *Gdf15 -/-* and WT mice, subjected to either unilateral I/R or sham surgery, were immunostained using a rat anti-mouse F4/80 antibody. Subsequently, macrophage infiltration

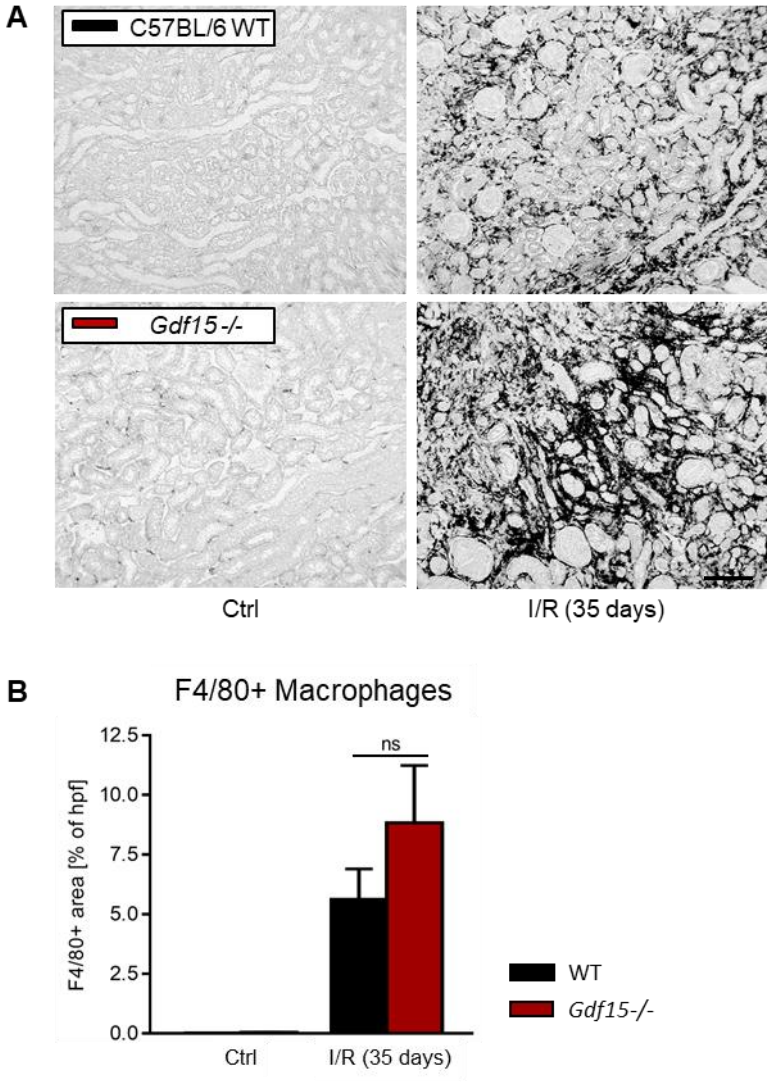

Fig. 11. Influx of F4/80+ macrophages in I/R-induced CKD. F4/80+ macrophage infiltration was evaluated in renal sections from *Gdf15 -/-* and WT mice 35 days after unilateral I/R or sham surgery. Renal sections were immunostained using rat anti-mouse F4/80 antibody and macrophage influx was digitally quantified using ImageJ software. Representative pictures of post-ischemic or sham-control kidneys from *Gdf15 -/-* and WT mice are shown in 100-fold magnification (A); scale bar is 20 µm. F4/80+ area in the corticomedullary junction of post-ischemic and control kidneys (B). Data are presented as means ± SEM.

was digitally quantified using ImageJ software. As shown in Figure 11, immunostaining for cell surface marker F4/80 revealed slightly increased numbers of macrophages in the renal interstitium in *Gdf15*-deficient mice on day 35 after renal pedicel clamping compared to WT mice. However, this trend was statistically not significant (Fig. 11, A and B).

1.3.3 Gene Expression Analysis

As *Gdf15* deficiency was found to aggravate the histomorphological phenotype of I/R-induced CKD, differences in gene expression patterns between post-ischemic kidneys from *Gdf15*-deficient and WT mice were expected. In view of the increased tubular damage (c.f. Fig. 8 and 9), aggravated renal fibrosis (c.f. Fig. 10), and enhanced macrophage infiltration (c.f. Fig. 11) in *Gdf15 -/-* mice, the influence of *Gdf15* deficiency on post-ischemic expression of inflammation-, fibrosis-, and apoptosis-associated genes was to be investigated. Therefore, mRNA was isolated from renal tissues of *Gdf15 -/-* and WT mice after I/R, using Ambion's PureLinkTM RNA Mini Kit. After generating cDNA via reverse transcription, gene expression of target genes was quantified by qRT-PCR. Figure 12 indicates relative expression of inflammation-associated genes (Fig. 12A), fibrosis-associated genes (Fig. 12B) and apoptosis-associated genes (Fig. 12C) in renal tissues from *Gdf15 -/-* and WT mice at day 35

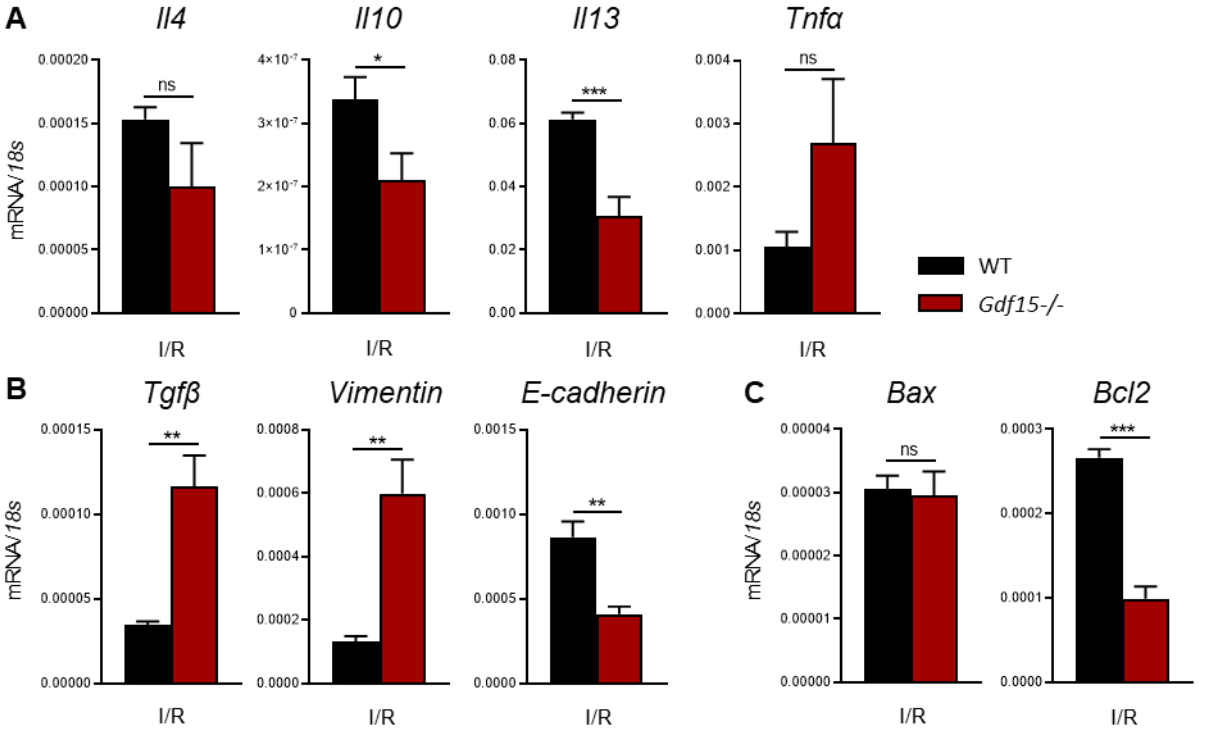

Fig. 12. Renal expression of inflammation-, fibrosis- and apoptosis-associated genes in I/R-induced CKD. Renal mRNA was isolated from whole renal tissues of *Gdf15* -/- and C57BL/6 WT mice 35 days after unilateral I/R, transcribed into cDNA and quantified by qRT-PCR. Renal mRNA expression of inflammation-associated (A), fibrosis-associated (B) and apoptosis-regulating genes (C). Data are expressed as mean of the ratio of specific target gene mRNA expression versus the respective *18s* rRNA level ± SEM.

after unilateral I/R. *18s* was used as reference gene. Lack of *Gdf15* was associated with significantly lower transcript levels of anti-inflammatory cytokines *Il10* and *Il13* as compared to the corresponding WT control (Fig. 12A). The expression of anti-inflammatory cytokine *Il4* showed the same trend but did not reach statistical significance (Fig. 12A). At the same time, post-ischemic kidneys from *Gdf15 -/-* mice revealed higher transcript levels of pro-inflammatory cytokine *Tnfα* as compared to the corresponding WT control (Fig. 12A). Yet,

this trend was statistically not significant. Together, these findings indicate that GDF15 promotes the establishment of an anti-inflammatory milieu in the kidney during I/R-induced CKD. In addition, kidney lysates from *Gdf15 -/-* mice displayed significantly higher transcript levels of *Tgfβ* and *Vimentin*, two key markers of fibrotic tissue remodeling, compared to those from WT mice (Fig. 12B). At the same time, expression of *e-cadherin*, a gene required by renal epithelial cells to maintain epithelial organization, was shown to be significantly lower in post-ischemic renal tissues from *Gdf15 -/-* mice than in those from WT mice (Fig. 12B). Together with the histologically observed aggravated fibrosis in *Gdf15*-deficient mice, these findings advocate an anti-fibrotic role for GDF15 in I/R-induced CKD. Moreover, post-ischemic kidneys from *Gdf15 -/-* mice displayed significantly lower transcript levels of anti-apoptotic *Bcl2* as compared to those from the corresponding WT mice (Fig. 12C). Transcript levels of pro-apoptotic *Bax* did not alter between post-ischemic renal tissues from *Gdf15 -/-* and WT mice (Fig. 12C). Along with the augmented disruption of tubular architecture in *Gdf15*-deficient mice, this finding might suggest that GDF15 potentially shifts the precisely balanced expression of apoptosis regulating genes in favor of a more anti-apoptotic state in the post-ischemic kidney.

2 Determining the Main Source of Renal GDF15

2.1 Basal *Gdf15* Expression and GDF15 Secretion in Renal Cells

To determine the primary source of GDF15 in the kidney, a pilot *in-vitro* experiment assessing basal mRNA expression of *Gdf15* in various renal cell types was performed. Therefore, both immortalized murine cell lines and primary murine cells were studied. An immortalized murine

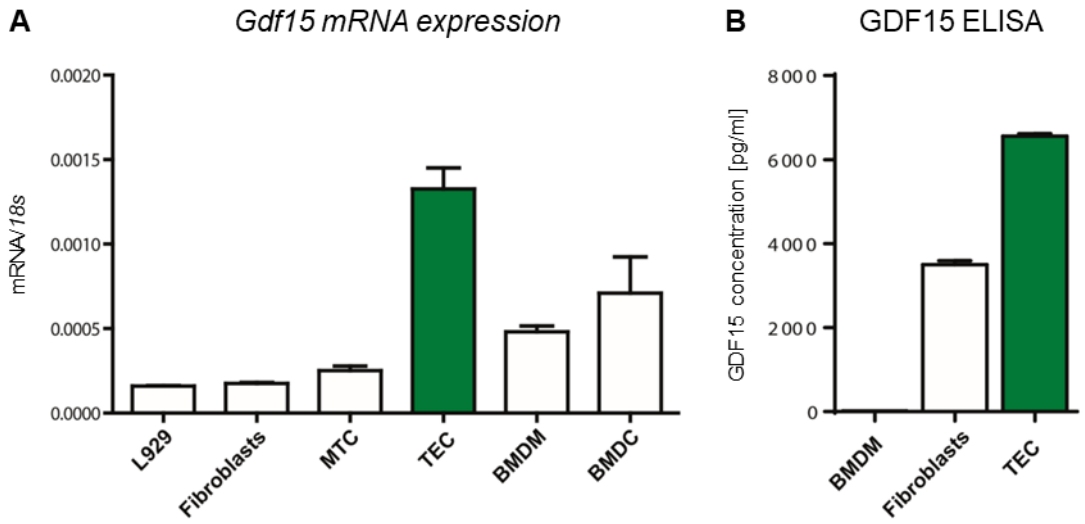

Fig. 13. Cell type specific basal *Gdf15* mRNA expression and GDF15 protein secretion. L929 - immortalized murine fibroblast cell line, MTC – immortalized murine tubular cell line, TEC - primary tubular epithelial cells, primary fibroblasts, BMDM - bone marrow derived macrophages, BMDC - bone marrow derived dendritic cells. All primary cells were isolated from C57BL/6 WT mice. Basal *Gdf15* mRNA expression of renal cells was evaluated by qRT-PCR (A). Basal GDF15 protein concentration in supernatants of primary renal cells from C57BL/6 WT mice was assessed by GDF15 ELISA (B). Data are expressed as mean ± SEM.

fibroblast cell line (L929) and an immortalized murine tubular cell line (MTC) were purchased and cultivated in accordance with the trader's protocol. At the same time, various primary renal cell types, including primary tubular epithelial cells (TECs), primary fibroblasts, bone marrow derived macrophages (BMDMs) and bone marrow derived dendritic cells (BMDCs) were isolated from 4-week-old C57BL/6 WT mice and cultivated as described previously. All cells were cultivated without any stimulation in 150 mm2 petri dishes and kept until a confluency rate of about 80 % to 90 % was achieved. After mRNA isolation and reverse transcription, basal *Gdf15* mRNA expression was evaluated by qRT-PCR. *18s* was used as reference gene. As illustrated in Figure 13A, basal *Gdf15* mRNA expression appeared, out of all groups, to be the highest in primary tubular epithelial cells (TECs; Fig. 13A), indicating TECs to be the primary source of renal GDF15. Interestingly, the corresponding immortalized tubular cell line (MTC) displayed much lower basal *Gdf15* mRNA expression as compared to the respective primary cells (TECs; Fig. 13A). Next, to address the question whether the observed high *Gdf15* mRNA expression in TECs would also be accompanied by an extended release of the translated protein into the local environment, supernatants from primary cells were analysed. Therefore, primary BMDMs, renal fibroblasts and TECs were cultivated without any stimulation in 150 mm2 petri dishes and kept until a confluency rate of about 80 % to 90 %. Supernatants were collected and analysed for GDF15 protein concentration via ELISA. As shown in Figure 13B, highest GDF15 protein concentration was to be found in supernatant from TECs with a mean concentration of 6557 pg/ml compared to only 3567 pg/ml in supernatant from fibroblasts and 10 pg/ml in that from BMDMs (Fig. 13B).

2.2 Effect of LPS Stimulation on *Gdf15* Expression Patterns in Renal Cells

It is well known that Toll-Like receptor 4 (TLR4) activation is a key mechanism in mediating ischemic kidney injury (Leemans et al., 2005; Pulskens et al., 2008; Vries et al., 2002). In order to evaluate cell type specific *Gdf15* expression patterns upon TLR4 activation, BMDMs, renal fibroblasts and TECs were isolated from 4-week-old C57BL/6 WT mice, cultivated, and stimulated with TLR4 ligand Lipopolysaccharide (LPS). In this experiment all cell types were exposed to LPS for varying amounts of time ranging from 3 h to 12 h in order to observe changes in *Gdf15* expression over time. In this process, the stimulation was staged in intervals, with all cells being harvested at the same time point, meaning that the stimulation for the 12 h group was started 12 h prior to harvesting. Respectively, this was done for all other indicated time points. Additionally, *Tnfα* mRNA expression was evaluated to validate the effect of LPS. Confirming the previous finding, unstimulated TECs expressed more *Gdf15* mRNA compared to unstimulated BMDMs or fibroblasts with the relative expression being almost 3 times as high as the expression in BMDMs and fibroblasts (Fig. 14). In LPS-treated BMDMs *Gdf15* expression appeared to slightly decrease over time down to a minimal expression after 12 h,

66.3 % below basal level (Fig. 14A). However, *Gdf15* expression in BMDMs upon time point

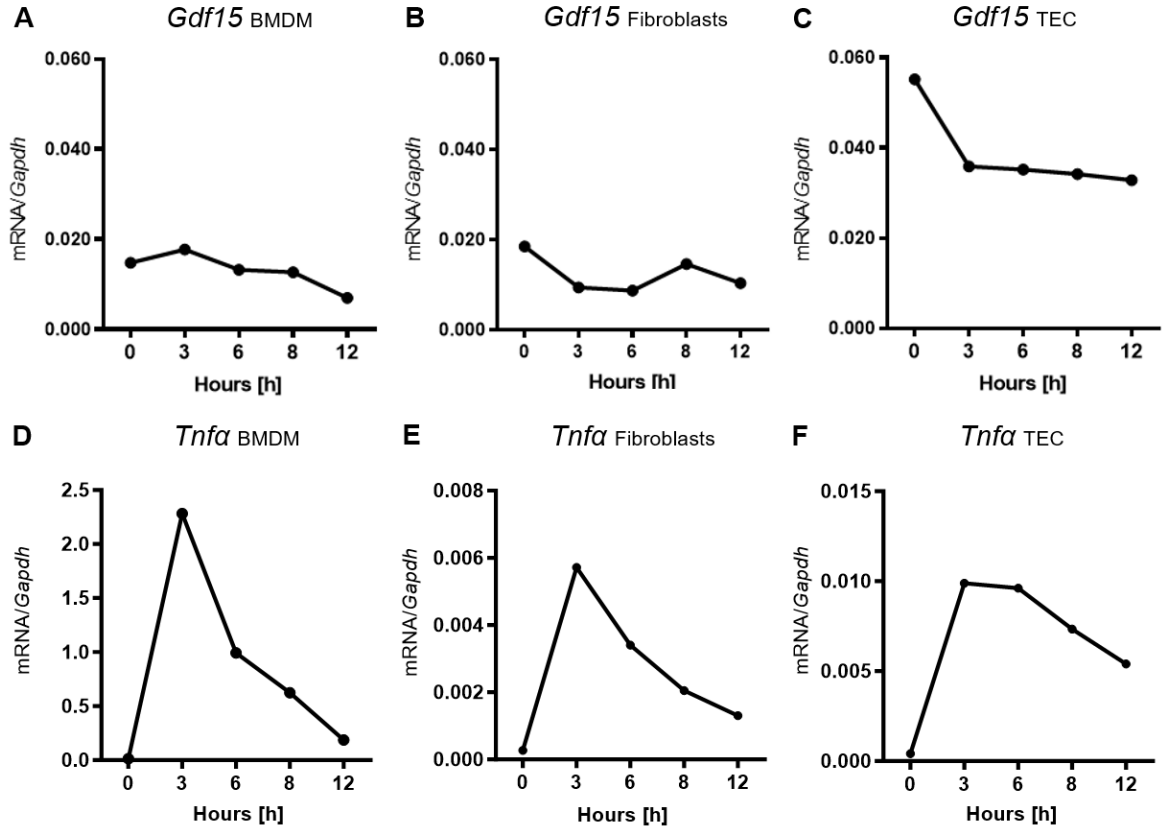

Fig. 14. Cell type specific *Gdf15* and *Tnfα* mRNA expression upon time dependent LPS stimulation. Primary bone marrow derived macrophages (BMDM), renal fibroblasts and tubular epithelial cells (TEC) were isolated from 4-week-old C57BL/6 WT mice, cultivated as described previously and stimulated with 100 ng/ml of TLR4 ligand LPS for 0 h, 3 h, 6 h, 8 h and 12 h. After mRNA isolation and reverse transcription, *Gdf15* and *Tnfα* mRNA expression levels of BMDMs (A and D), primary fibroblasts (B and E) and TECs (C and F) were assessed by qRT-PCR. Data are expressed as mean of the ratio of target gene mRNA expression versus the respective *Gapdh* mRNA level.

dependent LPS stimulation did not correspond with a regulated expression pattern. In fibroblasts, a decrease of *Gdf15* expression after 3 h of stimulation down to 49.3 % below basal level was followed by a slight increase after 8 h of stimulation to 21.0 % below basal level. All the same, a regulated expression pattern of *Gdf15* in fibroblasts upon LPS stimulation was not certainly discernible (Fig. 14B). In contrast, *Gdf15* mRNA expression in TECs was found to be 34.9% below basal level 3h after LPS-stimulation and remained consistently low throughout all observed time points with a minimal expression level after 12 h of LPS stimulation, 38.0 % below basal level (Fig. 14C). All cell types showed an increase in *Tnfα* mRNA expression with a regulated expression pattern after stimulation with LPS (Fig. 14D, E and F). All in all, TECs displayed high basal *Gdf15* transcript levels together with a regulated expression pattern and a slight but stable decrease in *Gdf15* expression after stimulation with TLR4 agonist LPS.

3 Determining Innate Immune Responses Affected by GDF15 Activity in the Kidney

3.1 Intracellular Effects of *Gdf15* Deficiency in TECs

3.1.1 Impact of *Gdf15* Deficiency on Hypoxic Regulation

It is well known that TECs within the corticomedullary junction of the kidney are the cells most prone to hypoxic damage caused by I/R (Brezis et al., 1995; Scholz et al., 2021). At the same time, TECs were found to be the primary source of renal GDF15 (cf. Fig. 13). To answer the question whether *Gdf15* deficiency impacts tubular gene expression after hypoxic exposure,

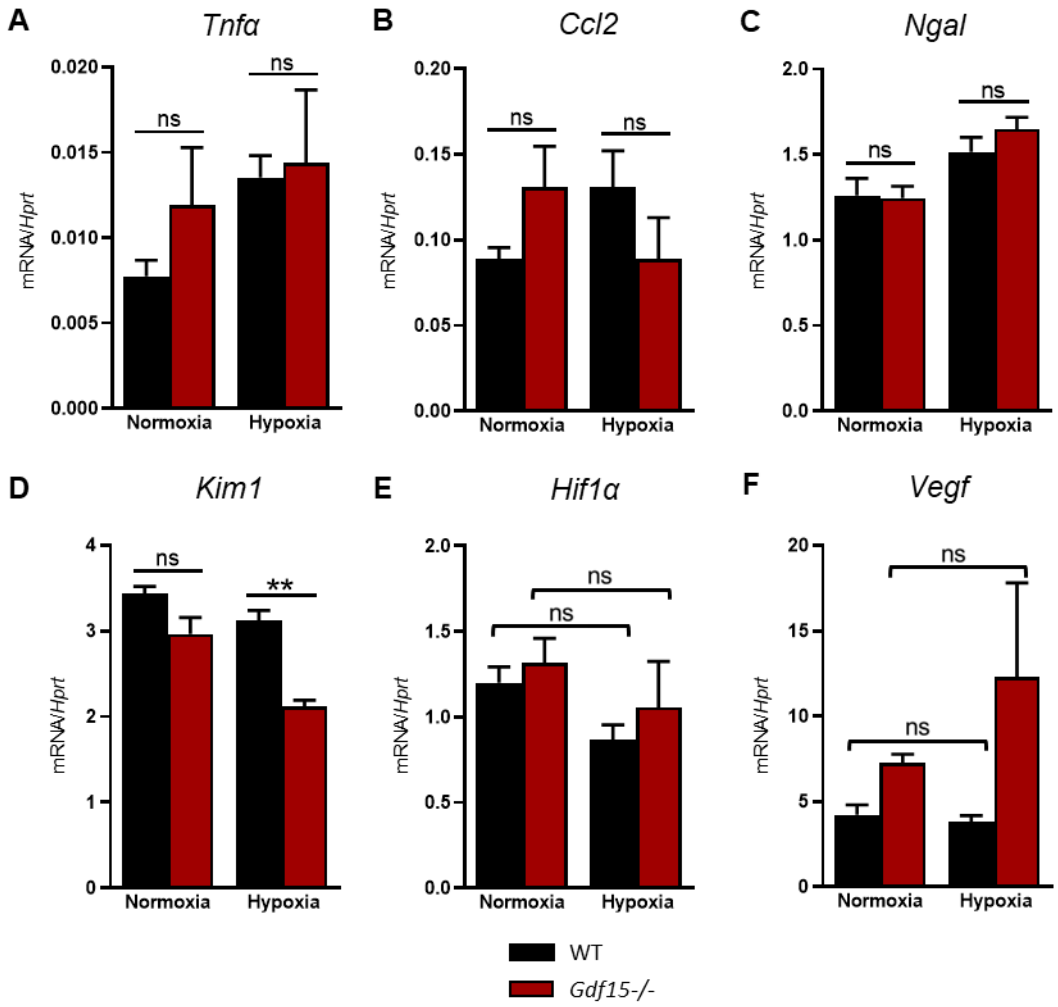

Fig. 15. Impact of *Gdf15* deficiency on hypoxic [$c_{(O2)}$ ~ 5 %] gene expression in TECs. Primary TECs were isolated from 4-week-old C57BL/6 WT and *Gdf15 -/-* mice, maintained under previously described conditions and cultured for 24 h in a regular cell culture incubator providing 20 % oxygen (Normoxia) or a hypoxic incubator (Eppendorf Galaxy 48R CO2 Incubator) providing 5 % oxygen (Hypoxia). Relative mRNA expression of *Tnfα* (A), *Ccl2* (B), *Ngal* (C), *Kim1* (D), *Hif1α* (E) and *Vegf* (F) was assessed by qRT-PCR. Data are expressed as mean of the ratio of specific mRNA expression versus the respective *Hprt* mRNA level ± SEM.

TECs were isolated from 4-week-old WT and *Gdf15 -/-* mice and cultivated as described previously. Next, they were kept for 24 h in either a hypoxic incubation chamber, providing merely 5 % oxygen, or a standard cell culture incubator, providing 20 % oxygen. After mRNA

isolation and reverse transcription, transcript levels of target genes were quantified by qRT-PCR. *Hprt* was used as housekeeping gene. After being exposed to hypoxia, TECs from WT and *Gdf15 -/-* mice revealed no differences in expression of *Tnfα*, *Ccl2* and *Ngal* (Fig. 15, A, B and C). TECs from *Gdf15 -/-* mice showed significantly lower expression of tubular injury marker *Kim1* after hypoxic incubation compared to those from WT mice (Fig. 15D). Yet, both WT and *Gdf15 -/-* TECs subjected to hypoxia displayed no differences in expression of *Hif1α* and its downstream target *Vegf* as compared to their respective normoxia control (Fig. 15, E and F). Since both *Hif1α* and *Vegf* should be regulated upon hypoxic exposure, their unaltered expression might implicate insufficient hypoxic stimulation. Thus, the experiment was repeated as described above with the oxygen concentration being reduced to 1 % during hypoxic exposure. A significant decrease in *Hif1α* expression after hypoxia was detectable in both WT and *Gdf15 -/-* TECs compared to the respective normoxia

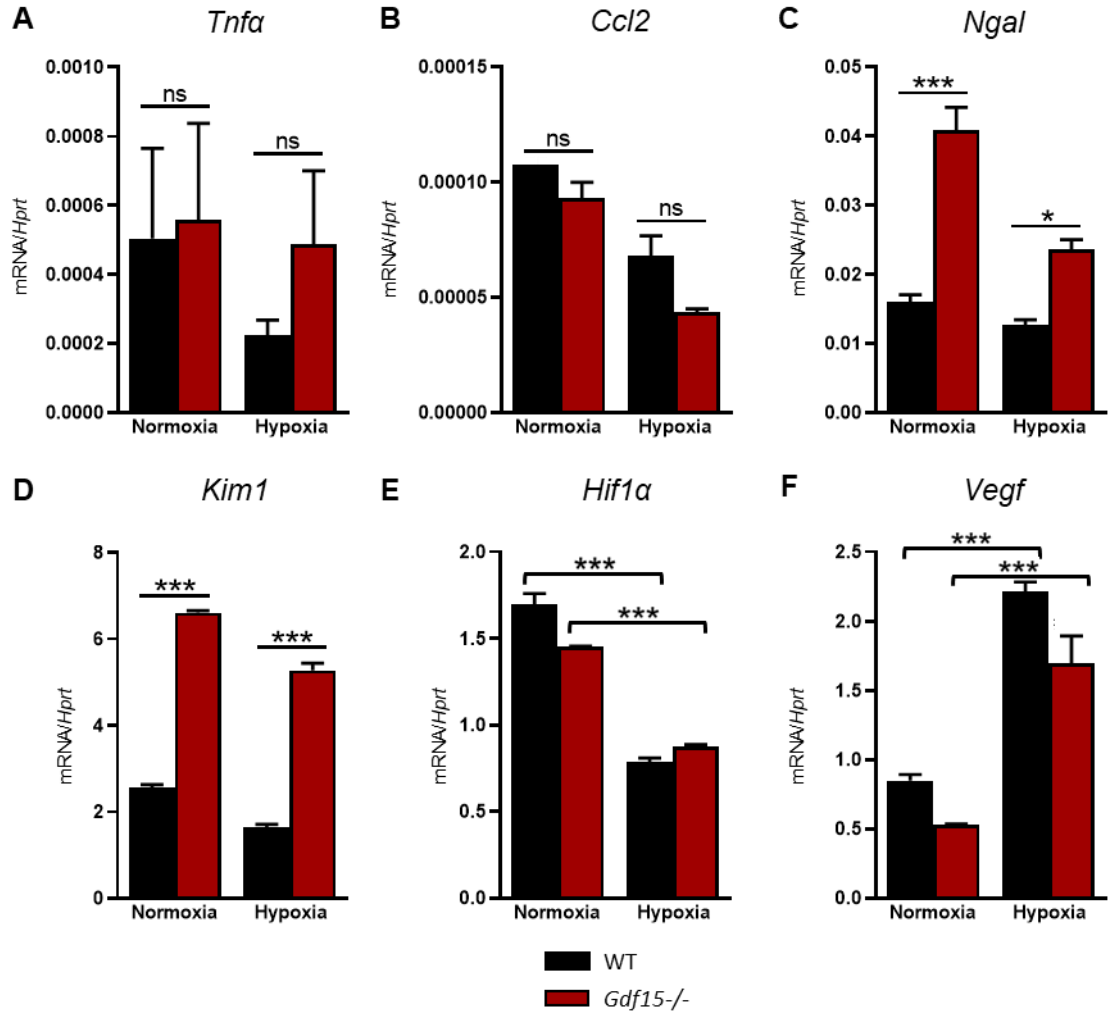

Fig. 16. Impact of *Gdf15* deficiency on hypoxic [$c_{(O2)}$ ~ 1 %] gene expression in TECs. Primary TECs were isolated from 4-week-old C57BL/6 WT and *Gdf15 -/-* mice, maintained under previously described conditions and cultured for 24 h in a regular cell culture incubator providing 20 % oxygen (Normoxia) or a hypoxic incubator (Eppendorf Galaxy 48R CO2 Incubator) providing 1 % oxygen (Hypoxia). Relative mRNA expression of *Tnfα* (A), *Ccl2* (B), *Ngal* (C), *Kim1* (D), *Hif1α* (E) and *Vegf* (F) was assessed by qRT-PCR. Data are expressed as mean of the ratio of specific mRNA expression versus the respective *Hprt* mRNA level ± SEM.

control (Fig. 16E). Simultaneously, *Vegf* appeared to be significantly upregulated after hypoxic incubation in both WT and *Gdf15 -/-* TECs compared to their corresponding normoxia ontrol (Fig. 16F). While cellular hypoxia is well known to induce HIF1α at the protein level, it simultaneously results in decreased *Hif1α* expression at the mRNA level (Chamboredon et al., 2011), presumably due to accelerated mRNA translation. Hence, the observed reduction of *Hif1α* expression after hypoxic exposure together with hypoxia-induced increase in *Vegf* expression proves successful induction of hypoxia. Still, no significant differences in *Tnfα* and *Ccl2* expression between *Gdf15 -/-* TECs, exposed to hypoxia, and their respective WT control could be observed (Fig. 16, A and B). Of note, TECs lacking *Gdf15* revealed, regardless of the surrounding oxygen concentration, significantly increased expression of tubular injury markers *Ngal* and *Kim1 as* compared to their respective WT control (Fig. 16, C and D). Yet, overall, hypoxia-induced gene expression in TECs remained independent of *Gdf15* deficiency.

3.1.2 Impact of *Gdf15* Deficiency on Innate Inflammatory Responses

It is widely appreciated that not only immune cells but also TECs participate in the early innate immune response during renal injury (Anders, 2010; Leemans et al., 2005; Tammaro et al., 2020). TECs are known to play a crucial role in conveying both TLR-mediated danger signaling and pro-inflammatory signaling during ischemic kidney injury by binding and recognizing released DAMPs, respectively TNFα (Al-lamki et al., 2014; Habib, 2021). To evaluate whether *Gdf15* deficiency influences TLR-dependent signaling in TECs and if so, to specify via which distinct receptor, TECs were isolated from 4-week-old *Gdf15 -/-* and C57BL/6 WT mice, cultivated as previously described and incubated for 24 h with the following TLR agonists, or medium control. TLR2 agonist – Pam3Cys (P3C), TLR4 agonist – Lipopolysaccharide (LPS), TLR7 agonist – Imiquimod (IMQ) and TLR9 agonist – oligodeoxyribonucleotides containing CpG motifs (CpG). The characteristics of these synthetic ligands correspond to those of various TLR ligands observed during I/R (cf. Tab. 1). As TNFα is well appreciated as another central mediator in ischemia-induced kidney injury (Habib, 2021), the stimulation panel was extended by TNFα. After mRNA isolation and reverse transcription, transcript levels of target genes were quantified by qRT-PCR. *Gapdh* was used as reference gene. Figure 17 illustrates the relative mRNA expression of *Tnfα*, *Il6*, *Ccl2* and *Cxcl2* in *Gdf15 -/-* or WT TECs after stimulation with the before listed TLR ligands. Comparison of gene expression in *Gdf15 -/-* and WT TECs revealed no differences after stimulation with TLR2 ligand Pam3Cys or TLR9 ligand CpG (Fig. 17, A to D). After stimulation with TLR7 ligand imiquimod, *Gdf15 -/-* TECs displayed a slightly increased *Il6* mRNA expression as compared to WT TECs (Fig. 17B). Furthermore, TECs isolated from *Gdf15*-deficient mice showed significantly higher *Il6* and *Ccl2* expression after stimulation with TNFα than TECs from WT mice (Fig. 17, B and C). Yet, the most remarkable finding were the significant differences in the expression of all target genes between *Gdf15 -/-* and WT TECs after stimulation with TLR4 ligand LPS.

Gdf15-deficient TECs showed significantly higher transcript levels for pro-inflammatory genes *TNFα*, *Il6*, *Ccl2*, and *Cxcl2* after stimulation with LPS as compared to WT TECs (Fig. 17, A to D). This finding indicates that GDF15 might mitigate TLR4-mediated pro-inflammatory

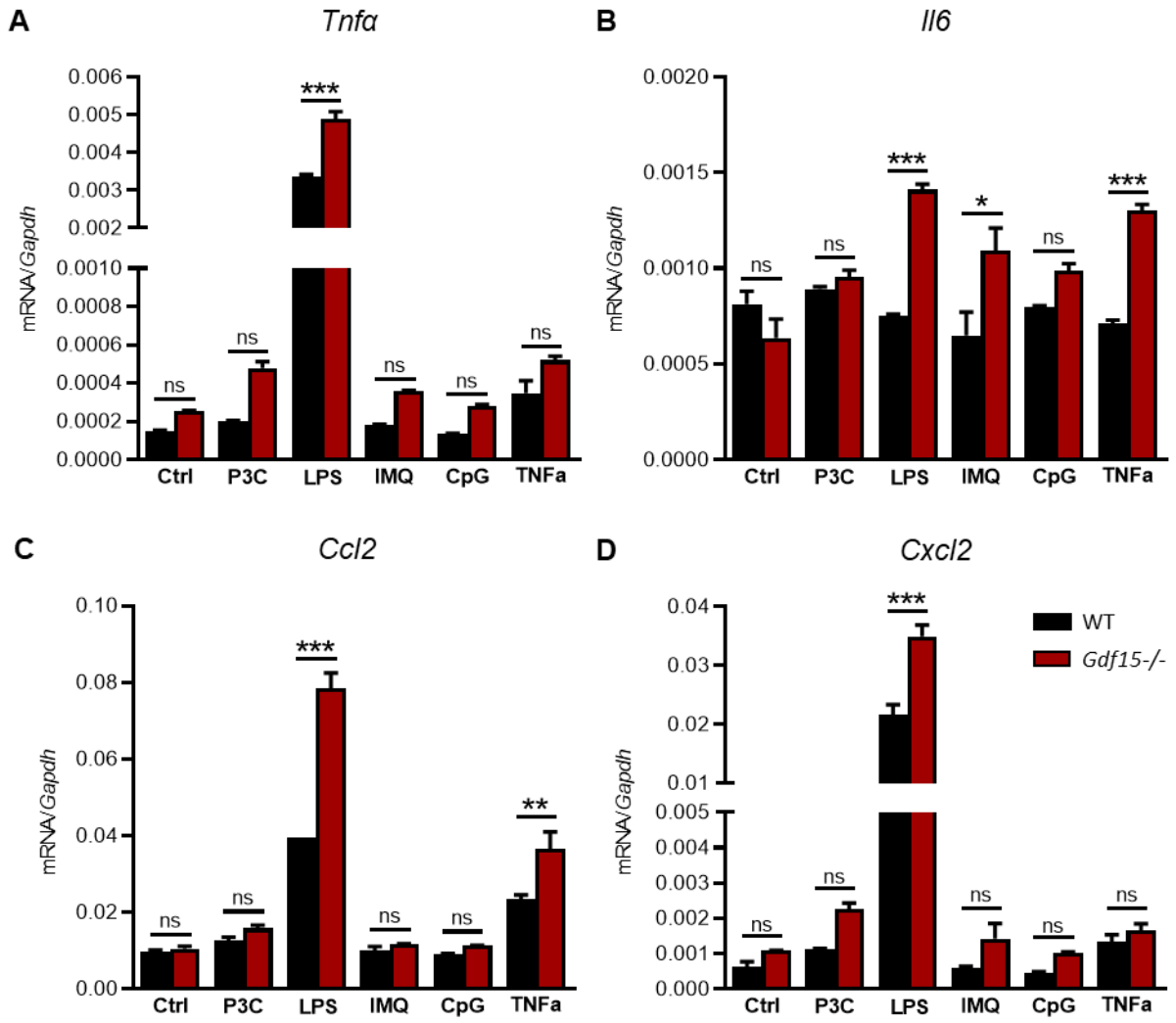

Fig. 17. Impact of *Gdf15* deficiency on gene expression in TECs exposed to ischemia-related, inflammatory stimuli. TECs were isolated from 4-week-old C57BL/6 WT and *Gdf15 -/-* mice, cultivated under previously described cell culture conditions and stimulated for 6 h with either medium (Ctrl), 100 ng/ml of TLR2 ligand Pam3Cys (P3C), 100 ng/ml of TLR4 ligand Lipopolysaccharide (LPS), 1 µg/ml of TLR7 ligand Imiquimod (IMQ), 100 ng/ml of TLR9 ligand unmethylated CpG oligodeoxynucleotides (CpG) or 100 ng/ml Tumor necrosis factor alpha (TNFα). Relative mRNA expression of *Tnfα* (A), *Il6* (B), *Ccl2* (C) and *Cxcl2* (D) was assessed by qRT-PCR. Data are expressed as mean of the ratio of specific mRNA expression versus the respective *Gapdh* mRNA level ± SEM.

signaling in TECs.

3.2 Intercellular Effects of GDF15

3.2.1 Effect of recombinant GDF15 on Innate Inflammatory Responses in TECs

Since *Gdf15 -/-* mice showed an aggravated disruption of tubular morphology during I/R-induced CKD in-vivo (cf. Fig. 8 and 9), it seemed possible that GDF15 might act as

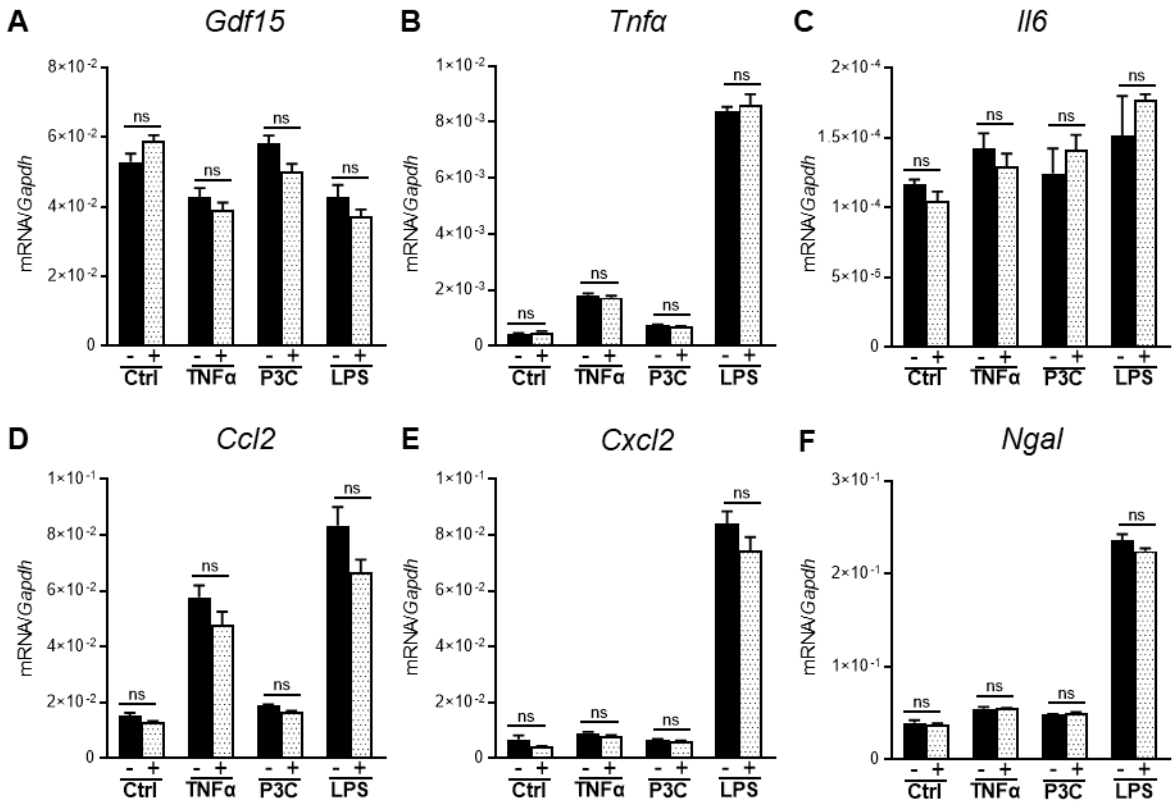

Fig. 18. Effect of reGDF15 pre-stimulation on gene expression in WT TECs exposed to ischemia-related, inflammatory stimuli. TECs were isolated from 4-week-old C57BL/6 WT mice and stimulated for 6 h with either medium (Ctrl), 100 ng/ml Tumor necrosis factor alpha (TNFα), 100 ng/ml Pam3Cys (P3C) or 100 ng/ml Lipopolysaccharide (LPS), after having been pre-stimulated for 2h with either 100 ng/ml reGDF15 (+) or medium control (-). Relative expression of *Gdf15* (A), *Tnfα* (B), *Il6* (C), *Ccl2* (D), *Cxcl2* (E) and *Ngal* (F) was assessed by RT-qPCR. Data are expressed as mean of the ratio of specific mRNA expression versus the respective *Gapdh* mRNA level ± SEM.

autocrine agent being not only released but also received by TECs, subsequently protecting them from injury caused by ischemia-related endogenous molecules. To examine this hypothesis, TECs were isolated from 4-week-old C57BL/6 WT mice and cultivated as described previously. After pre-stimulation with either recombinant GDF15 (reGDF15) or medium control for 2 h, TECs were exposed to either medium, TNFα, TLR2 ligand Pam3Cys or TLR4 ligand LPS for 6 h. After mRNA isolation and reverse transcription, transcript levels of target genes were quantified by qRT-PCR. *Gapdh* was used as reference gene. As indicated in Figure 18, *Gdf15* expression remained unaffected by pre-stimulation with reGDF15 regardless of the subsequently applied stimulus (Fig. 18A). Also, pre-stimulation with reGDF15 before exposure to the above listed stimuli did not alter the expression of pro-inflammatory genes *Tnfα* and *Il6* (Fig. 18, B and C). Likewise, expression of chemokines *Ccl2* and *Cxcl2* (Fig. 18, D and E) and tubular injury marker *Ngal* (Fig. 18F) remained uninfluenced by pre-stimulation with reGDF15 regardless of the subsequently applied stimulus. Contrary to the hypothesis, pre-stimulating WT TECs with reGDF15 before exposing them to ischemia-related stimuli did not result in altered gene expression.

3.2.2 Effect of recombinant GDF15 on Macrophage Polarization

It is known that macrophages differentiate into distinct functional phenotypes in response to specific microenvironmental stimuli, with pro-inflammatory M1 and anti-inflammatory M2 macrophages constituting the two extremes of this phenotypical continuum (Han et al., 2019;

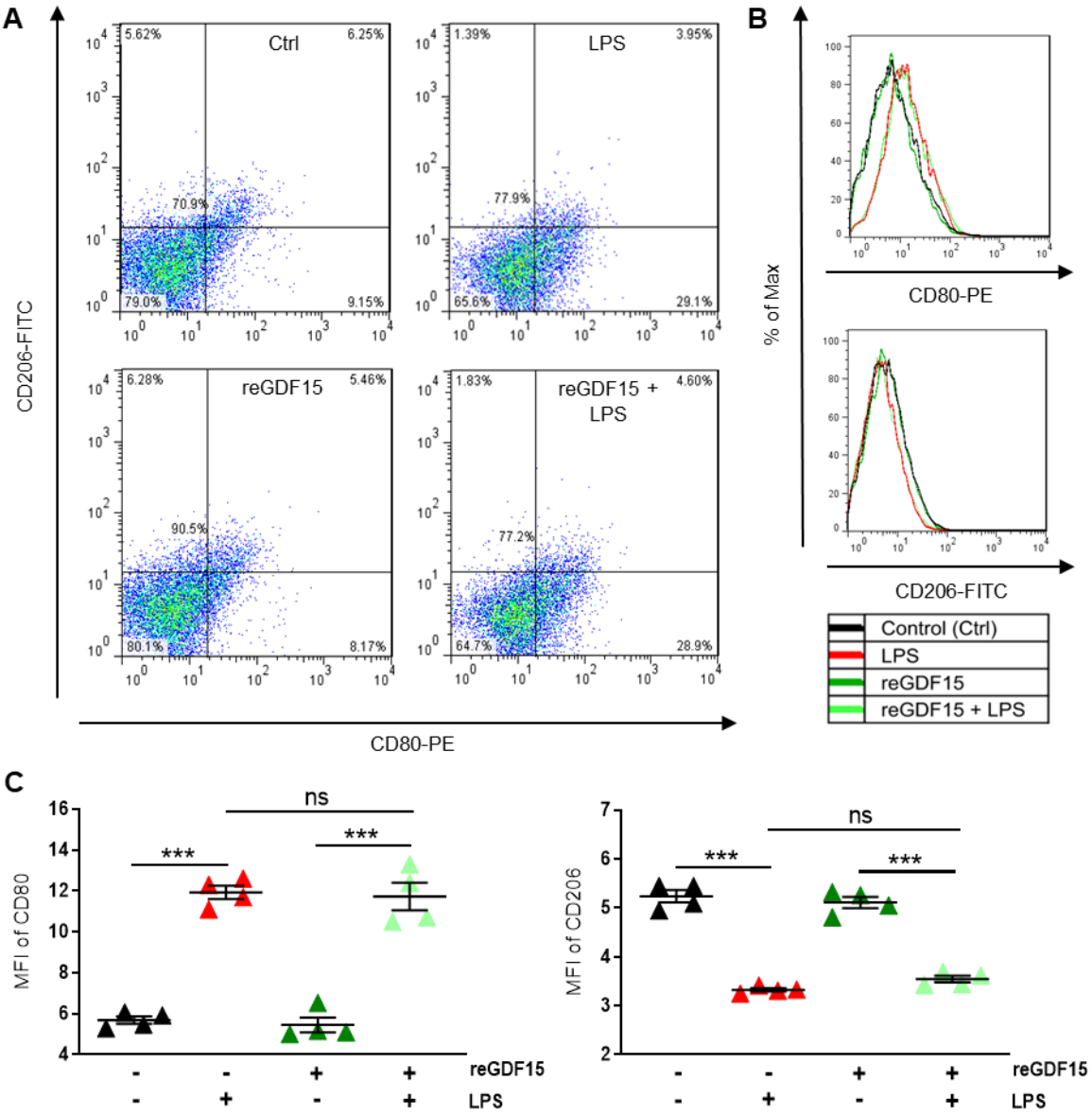

Fig. 19. Effect of reGDF15 on M1/M2 macrophage polarization. Bone marrow cells were isolated from 4-week-old C57BL/6 WT mice and differentiated for 10 days into bone marrow derived macrophages (BMDM) by supplementing standard cell culture medium with 10 ng/ml reMCSF. Mature BMDMs were stimulated for 24 h with 2 ng/ml LPS (+) or medium control (-), after having been pre-stimulated for 1 h with either 200 ng/ml reGDF15 (+) or medium control (-). Surface expression levels of prototypic M1 marker, CD80, and M2 marker, CD206, were evaluated by FACS analysis: BMDMs were first gated on SSC and FSC to remove cell debris and conjugates. Mature BMDMs were defined as CD11b+F4/80+ subpopulations to guarantee cell population purity. M1 macrophages were CD11b+F4/80+CD80+CD206-, whereas M2 macrophages were CD11b+F4/80+CD80-CD206+. (A) Pseudo-colour scatter dot plots showing CD80 surface expression (x-axis) in relation to CD206 surface expression (y-axis). (B) Overlay of histograms showing CD80-PE and CD206-FITC fluorescence as % of Max. (C) Comparison of mean fluorescence intensity (MFI) of CD80-PE and CD206-FITC between all experimental groups shown as scatter plot. Data expressed as MFI ± SEM.

Lee et al., 2011). *In-vivo* GDF15 was found to correlate with an overall less injured phenotype as well as the establishment of an anti-inflammatory environment in the kidney during I/R-induced CKD (c.f. Fig. 7 to 12). Therefore, it was hypothesized, that GDF15 secreted by TECs (c.f. Fig. 13B), might serve as a paracrine signal influencing macrophage polarization in favor of a more M2-dominant, anti-inflammatory phenotype. To examine this hypothesis, bone marrow cells were isolated from 4-week-old C57BL/6 WT mice and differentiated for 10 days into bone marrow derived macrophages (BMDMs) by supplementing standard cell culture medium with reMCSF. Mature BMDMs were pre-stimulated for 1 h with either reGDF15 or medium control and subsequently exposed to LPS or medium control for 24 h. Surface expression levels of prototypic M1 marker, CD80, and M2 marker, CD206, were evaluated by FACS analysis. The influence of reGDF15 on macrophage polarization is illustrated in Figure 19. Only pre-simulating BMDMs with reGDF15, did neither influence CD80 nor CD206 surface marker expression (Fig. 19). As expected, stimulation with LPS alone led both to a significant increase in CD80 and a significant decrease in CD206 surface marker expression of BMDMs, shifting macrophages towards a more M1-like phenotype (Fig. 19). Contrary to the hypothesis, pre-stimulating BMDMs with reGDF15 followed by subsequent exposure to LPS did not result in a more M2-like phenotype or did not prevent macrophages from shifting towards a more M1-like phenotype. Here, both CD80 and CD206 surface marker expression remained unaltered as compared to the group deprived of pre-stimulation with reGDF15 (Fig. 19). This indicates that extracellular GDF15 does not directly influence macrophage polarization.

3.2.3 Macrophage Polarization in Response to Stimulation with Supernatants of WT or *Gdf15 -/-* TECs

However, as shown previously (Fig. 12A), WT mice displayed significantly higher renal expression of *Il4*, *Il10* and *Il13* during I/R-induced CKD as compared to *Gdf15* -/- mice. These are all cytokines that are known to induce M2 polarization in resident tissue macrophages (Novak et al., 2013). Therefore, it was hypothesized that GDF15 activity in WT TECs might indirectly impact M1/M2 polarization by provoking a local microenvironment, that favors a more M2-dominant immune response. To investigate this hypothesis, TECs were isolated from 4-week-old C57BL/6 WT and *Gdf15 -/-* mice and cultivated as described previously. Bone marrow cells were isolated from 4-week-old C57BL/6 WT mice and differentiated for 10 days into BMDMs as described before. Subsequently, mature BMDMs were stimulated for 24 h with supernatant (SN) from either WT or *Gdf15 -/-* TECs, or with medium control. Surface expression levels of prototypic M1 marker, CD80, and M2 marker, CD206, were evaluated by FACS analysis. As shown in Figure 20, both BMDMs stimulated with SN from *Gdf15 -/-* TECs and those stimulated with SN from WT TECs displayed significantly increased CD80 surface marker expression compared to the medium control group (Fig. 20). Vice versa, both groups

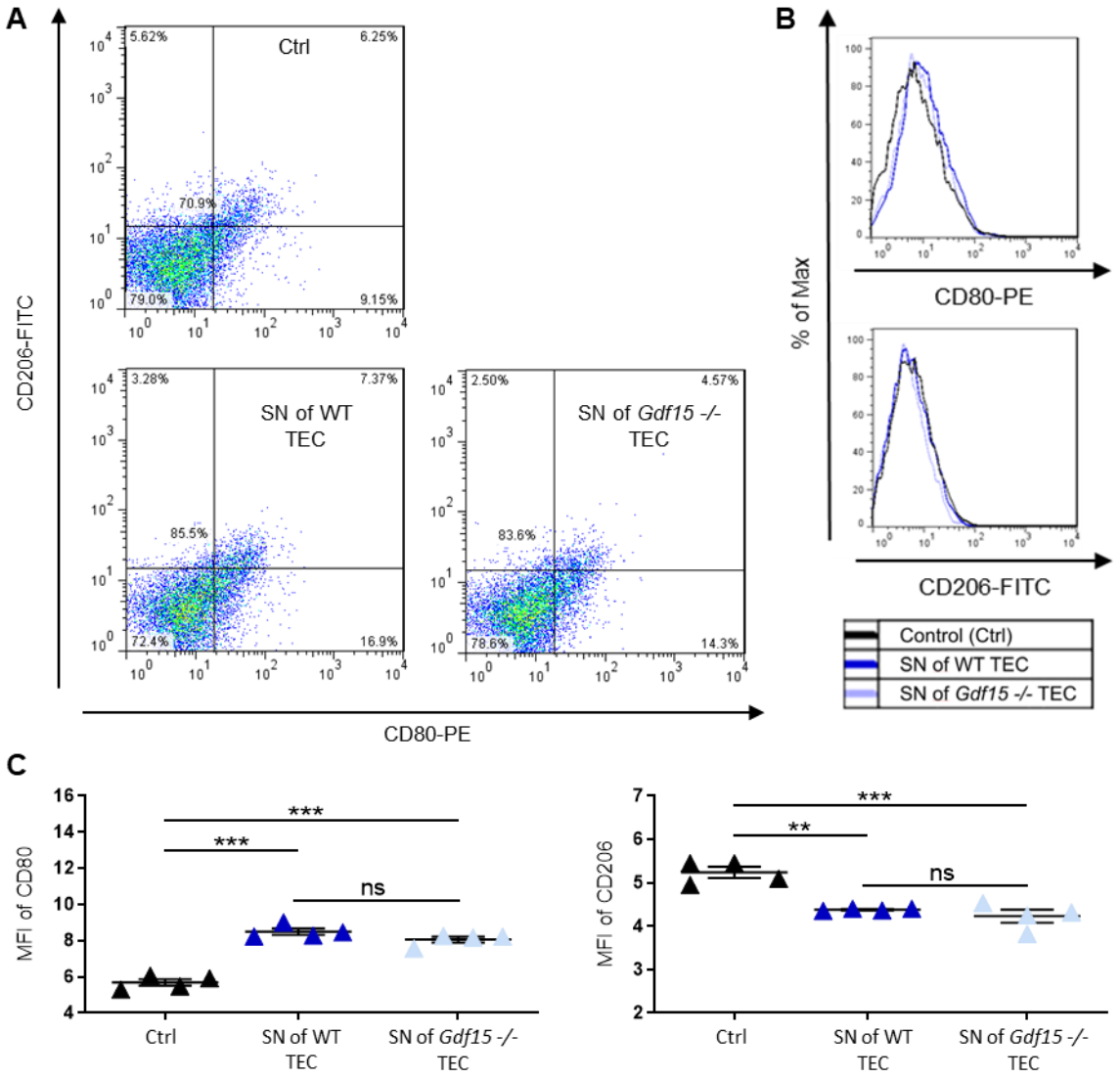

Fig. 20. M1/M2 macrophage polarization in response to stimulation with supernatants of WT or *Gdf15 -/-* TECs. In preparation, proximal tubular segments (PTS) were isolated from 4-week-old C57BL/6 WT and *Gdf15 -/-* mice. Mature TECs were obtained by culturing the isolated PTS in enriched K1 medium for 14 days. Bone marrow cells were isolated from 4-week-old C57BL/6 WT mice and differentiated into bone marrow derived macrophages (BMDM) by supplementing standard cell culture medium with 10 ng/ml reMCSF for 10 days. Mature BMDMs were stimulated for 24 h with supernatant (SN) of either WT or *Gdf15 -/-* TECs, or medium control (Ctrl). Surface expression levels of prototypic M1 marker, CD80, and M2 marker, CD206, were evaluated by FACS analysis: BMDMs were first gated on SSC and FSC to remove cell debris and conjugates. Mature BMDMs were defined as CD11b+F4/80+ subpopulations to guarantee cell population purity. M1 macrophages were CD11b+F4/80+CD80+CD206-, whereas M2 macrophages were CD11b+F4/80+CD80-CD206+. (A) Pseudo-colour scatter dot plots showing CD80 surface expression in relation to CD206 surface expression. (B) Overlay of histograms showing CD80-PE and CD206-FITC fluorescence as % of Max. (C) Comparison of mean fluorescence intensity (MFI) of CD80-PE and CD206-FITC between all experimental groups shown as scatter plot. Data expressed as MFI ± SEM.

also revealed significantly decreased expression of CD206 surface marker expression compared to the group stimulated with medium only (Fig. 20). Contrary to the expected, when comparing BMDMs exposed to SN from WT TECs and those exposed to SN from *Gdf15 -/-* TECs, no difference in CD80 and CD206 surface marker expression was detectable (Fig. 20). This indicates that intracellular GDF15 activity in TECs does not promote the

development of a local microenvironment, that favors a more M2-dominant macrophage polarization.

VI Discussion

1 The Role of GDF15 in Acute and Chronic Kidney Disease

To gain a deeper understanding of the complex pathophysiological processes as well as the intricate immune response in ischemia-related renal diseases and to shed light on potential molecular regulators of post-ischemic renal inflammation, *in-vivo* models of renal I/R represent valuable tools. The present work employed two setups of a murine I/R model to evaluate the role of GDF15 in both AKI and CKD.

1.1 The Impact of *Gdf15* Deficiency on I/R-Induced AKI

To investigate the influence of GDF15 on the development and severity of AKI, a murine I/R model was employed with paired groups of *Gdf15*-deficient and WT mice undergoing renal pedicel clamping for 30 minutes.

The analysis of post-ischemic renal tissues from WT mice revealed elevated *Gdf15* expression throughout all evaluated time points. This finding is confirmative of a previous study (Zimmers et al., 2005) and further supports - as another piece of the puzzle - the well-established hypothesis of GDF15 being a stress-inducible cytokine in numerous tissues and a myriad of pathophysiological conditions (Chung et al., 2017; Hsiao et al., 2000; Xu et al., 2006). Furthermore, this finding stands in good agreement with the reported GDF15 induction after myocardial ischemic injury in mice (Kempf et al., 2006), thus reinforcing the notion of GDF15 exerting a regulatory function after ischemic tissue damage. The degree of functional renal impairment after I/R was determined by quantification of serum creatinine (SCr), blood urea nitrogen (BUN) and proteinuria. Compared to the WT genotype, *Gdf15* deficiency correlated with significantly higher SCr and proteinuria levels at day 1 after I/R. Elevation of BUN levels appeared to be also more pronounced in the KO group. The significantly higher retention parameters are reflective of the comparatively more severe impairment of renal elimination capacity of *Gdf15*-deficient animals. Together with the marked increase of proteinuria in the KO group, this indicates a protective role for GDF15 during AKI. A comparable protective effect of GDF15 has been confirmed in the setting of a murine septic AKI model (Abulizi et al., 2017). However, to be able to review the impact of GDF15 on the gradual development of AKI over time more precisely, animal studies with repeated measurements of functional renal parameters would be beneficial. Examining gene expression profiles from post-ischemic kidney lysates, mice lacking *Gdf15* displayed mildly accentuated *Tnfα* and *Kim1* mRNA expression 1 and 5 days post-injury. This finding further supports a renoprotective, and eventually anti-inflammatory function for GDF15 and is in line with another murine *in-vivo* study, wherein administration of recombinant GDF15 attenuated the LPS-induced increase in hepatic expression of pro-inflammatory genes such as *Tnfα*, *Il6*, and *Il1β* (Li et al., 2018). In

consideration of the substantial proteinuria observed in *Gdf15*-deficient mice after I/R, impaired tubular reabsorption capacity as consequence of aggravated post-ischemic tubular damage seemed presumptive. Surprisingly, histopathological analysis of I/R-induced tubular damage revealed no significant differences between the WT and KO cohort. *Gdf15*-deficient and WT mice were found to score similarly high values on day 1 and day 5 post-injury not only in the overall tubular injury score but also in its individual subcategories – necrosis, tubular dilation, and intraluminal cast formation. This finding was not reflective of the observed significantly worse functional renal outcomes of mice lacking *Gdf15* and particularly surprising since other studies have previously reported a strong mitigating effect of GDF15 on the extent of tubular damage after renal injury (Abulizi et al., 2017; Mazagova et al., 2013; Moschovaki-Filippidou et al., 2020). However, as described before the post-ischemic expression of *Kim1*, a widely used marker of tubular injury (Han et al., 2002), appeared to be only slightly accentuated in renal tissues from *Gdf15*-deficient mice. Therefore, it remains conceivable that presumably existing subtle differences in tubular injury between the KO and WT group could statistically not be detected due to the small sample size of this study. Furthermore, despite the markedly aggravated impairment of renal function, neutrophil recruitment in *Gdf15*-deficient mice was found to be equivalent to reduced as compared to the WT control group.

In conclusion, although post-ischemic tubular injury did not appear to be affected by *Gdf15* deficiency, this work suggests that GDF15 serves a renoprotective function by ameliorating functional renal impairment after I/R injury. The protective role of GDF15 in transient organ ischemia has also been evidenced in experimental myocardial infarction (Kempf et al., 2006). In light of its beneficial effects on post-ischemic renal function, pharmacologically targeting the activity of GDF15 might present a novel tool to ameliorate ischemic AKI. This is particularly interesting since every renal transplantation inevitably involves transient renal ischemia.

1.2 The Impact of *Gdf15* Deficiency on I/R-Induced CKD

To investigate the influence of GDF15 on the development of CKD, a murine I/R model was used with paired groups of *Gdf15* KO and WT mice undergoing unilateral renal pedicel clamping for 30 minutes.

Renal atrophy is a common pathophysiological feature of advanced CKD. By measuring kidney weight in both WT and *Gdf15* KO mice before and 30 days after unilateral I/R, this study was able to demonstrate that genetic deletion of *Gdf15* in mice resulted in significantly aggravated renal atrophy. Although the extent of renal atrophy alone is not a reliable determinant of the degree of structural renal impairment, it still provides an easily obtainable first datapoint that can be indicative of the severity of chronic renal damage. Thus, the increased renal atrophy of *Gdf15*-deficient mice may be a sign of a particularly severe CKD manifestation. As the underlying pathomechanism of renal atrophy secondary to CKD commonly comprises a combination of mutually interfering compartmental processes, including renal tubular atrophy,

interstitial immune cell infiltration and tubulointerstitial fibrosis (Agarwal et al., 2020), histomorphological analysis was performed. Post-ischemic tissue sections from *Gdf15* KO mice featured a substantially aggravated disruption of tubular architecture relative to sections from their WT controls. Consistent with this finding, albeit not statistically significant, tubular atrophy appeared to be more accentuated in post-ischemic kidneys from *Gdf15*-deficient mice. Together with the significantly lower *Bcl-2* expression in post-ischemic kidney tissues of *Gdf15*-deficient animals, this might hint an anti-apoptotic, protective role for GDF15 within the setting of I/R-induced CKD. These findings are consistent with the observed anti-apoptotic effects of GDF15 during cardiac I/R (Kempf et al., 2006). Kempf et al. demonstrated that the anti-apoptotic effect of GDF15 in cultured cardiomyocytes exposed to experimental I/R was associated with activation of the serine-threonine kinase Akt as well as inactivation of its downstream effector Bad (Kempf et al., 2006). Bad is an important inhibitor of anti-apoptotic proteins of the Bcl-family, including Bcl2 (Singh et al., 2019). At the same time, the protective effect of GDF15 was reversible by PI3K inhibition (Kempf et al., 2006). These findings propose an involvement of the PI3K-Akt pathway in mediating the pro-survival effect of GDF15 after I/R. In view of the significantly aggravated tubular atrophy together with the strongly reduced Bcl2 expression in post-ischemic renal tissue of *Gdf15*-deficient mice, a similar mechanism during I/R-induced CKD could be discussed.

Although mice lacking *Gdf15* tended to display more severe macrophage infiltration 35 days after unilateral renal artery clamping than their WT controls, this study failed to detect statistically significant differences between both groups. However, it is known that not only the number of infiltrating macrophages but also their actual phenotype, being shaped by the local microenvironment, is contributing to the extent of renal injury. A recently published study, investigating a murine sepsis model, showed that treatment with reGDF15 served renoprotective due to an enhanced anti-inflammatory M2-like macrophage polarization (Zhang et al., 2022). In this study, gene expression analysis of post-ischemic renal tissues revealed that *Gdf15* deficiency correlated with reduced expression of anti-inflammatory and increased expression of pro-inflammatory genes, thus implicating that GDF15 might promote the establishment of an anti-inflammatory microenvironment in the kidney. Consequently, it could be speculated the renoprotective effects of GDF15 observed during ischemic renal injury to be also mediated by a potential regulatory impact on macrophage polarization. As GDF15 is a member of the TGFβ superfamily, it is reasonable to hypothesize that, like numerous other family members, it may participate in the regulation of ECM deposition and thus exert a regulatory influence on the development of fibrotic tissue remodelling. A previous *in-vivo* study investigating the influence of GDF15 on diabetic kidney disease hypothesized an anti-fibrotic effect for GDF15, as genetic deletion of *Gdf15* in diabetic mice correlated with enhanced fibrotic remodelling as witnessed by increased renal expression of profibrotic markers

(Mazagova et al., 2013). In light of the aforementioned, a particular striking observation of the present work was that genetic deletion of *Gdf15* significantly aggravated the development of post-ischemic tubulointerstitial fibrosis, indicating that GDF15 might provide potent protection against I/R-induced CKD by limiting the development of renal fibrosis. This finding may as well offer an explanation for the aggravated renal atrophy, observed in mice lacking *Gdf15*. Moreover, it aligns well with the histomorphological evidence of enhanced macrophage recruitment and exacerbated tubular atrophy as seen in the KO group. In addition, increased fibrotic burden in *Gdf15*-deficient animals was accompanied by markedly elevated renal expression of pro-fibrotic markers *Tgfβ* and *Vimentin*, further supporting an anti-fibrotic function for GDF15. All these findings are in line with a previous study showing that treatment with recombinant GDF15 markedly ameliorated renal fibrosis in mice subjected to UUO (Kim et al., 2018). The same study also suggested that this anti-fibrotic action may be mediated via indirect non-canonical TGFβ and *N*-Myc signaling (Kim et al., 2018).

In conclusion, the present work was the first study to evaluate the impact of *Gdf15* deficiency on the development of I/R-induced CKD *in-vivo*. Taken together, the previously discussed results suggest that GDF15 ameliorates I/R-induced CKD *in-vivo* by exerting anti-inflammatory as well as potent anti-fibrotic effects. Together with its renoprotective effects in I/R-induced AKI, GDF15 hence might represent a valuable target for new treatment strategies in both AKI and especially CKD.

2 Identification of the Main Source of Renal GDF15

Although injury-induced induction of *Gdf15* in the renal tissue has been evidenced by a previous study (Zimmers et al., 2005) and could be confirmed in the present work, the cellular origin of renal GDF15 has remained elusive.

By analysing basal cell type-specific *Gdf15* mRNA expression and GDF15 secretion of various renal-resident cell types using qRT-PCR and ELISA assays, this work was able to identify TECs as the primary GDF15 expressing and secreting cell type in the kidney. When assessing the physiological relevance of this finding, one must consider, that tubular epithelial cells compose the majority of renal parenchymal cells and that renal fibroblasts and tissue-resident macrophages, who were also found - although on much lower levels - to express *Gdf15*, only account for a comparatively small part of kidney cells (Balzer et al., 2022). Taking this numerical difference into the equation supports the conclusion, TECs to be the critically relevant source of GDF15 in the kidney. This finding is in good agreement with a recently published study, that, by using genome editing to directly visualize the distribution of renal *Gdf15* expression, was able to localize the majority of renal *Gdf15* expression in TECs of the S3 segment and the thin descending limb of the loop of Henle (Liu et al., 2020). At the same time, this finding is in accordance with the predicted allocation of *Gdf15* expression in the

"Kidney Cell Explorer" (https://cello.shinyapps.io/kidneycellexplorer/), an open-source single-cell RNA sequencing based anatomical atlas of the mammalian nephron and collecting system (Ransick et al., 2020). Of note, while TECs isolated from C57BL/6 WT mice displayed the highest *Gdf15* expression among all evaluated primary renal cell types, the corresponding immortalized murine tubular cell line did not show substantially higher *Gdf15* expression relative to other immortalized renal cell lines. This difference might be due to a variety of factors. However, a plausible cause may be the altered genomic content of immortalized cell lines compared to primary cells. Cell lines have often been in culture for many years and serial passaging is known to condition changes in the cellular geno- and phenotype often resulting in altered gene expression profiles (Masters et al., 2007). Hence, results obtained from cell lines must be viewed critically regarding their translatability to human physiology. To maximize the relevance of findings gained from experimental *in-vitro* studies for the human physiology, gene expression patterns of primary cells are preferably to be studied.

All in all, these results confirm that TECs are not only the main cells expressing renal *Gdf15*, but they are also capable of releasing the translated protein into their local microenvironment. Hence, GDF15 might not only act by impacting intracellular mechanisms of TECs but also by bridging intercellular crosstalk in the kidney. The identification of the primary site of GDF15 synthesis in the kidney represents a significant starting point for further research on the influence of GDF15 on both intra- and intercellular signaling pathways in the kidney.

3 Characterization of the Innate Immune Responses Affected by GDF15 Activity in the Kidney

The discussed *in-vivo* models of ischemic kidney injury strongly implicate a renoprotective function for GDF15 by mitigating both post-ischemic inflammatory and fibrotic responses. Subsequently, the question arises which mechanisms of the immune response may mediate the protective effects of GDF15 in the kidney. By suggesting that central metabolic adaptation via the hypothalamic GDF15-GFRAL axis is responsible for limiting inflammation-elicited tissue injury, a recent study provides an interesting, albeit limited, explanation for the observed anti-inflammatory effects of GDF15 (Luan et al., 2019). Considering the near ubiquitous stress-inducible expression of *Gdf15*, its pleiotropic functions, and the highly confined distribution of GFRAL, it appears more likely that other, yet unidentified, local mechanisms of action are also modulated by GDF15 activity. To illuminate these local ischemia-related mechanisms affected by GDF15, *in-vitro* experiments were performed on TECs, the primary source of renal GDF15. First, this study addressed the question of whether genetic abundance of *Gdf15* in TECs had an intracellular impact on gene expression upon exposure to ischemia-mimicking conditions. Apart from baseline differences in the expression of tubular injury markers, *Gdf15* deficiency did not impact transcript levels of various genes after hypoxic incubation in TECs. It is known

that deprivation of oxygen in TECs results in activation of HIF1α, the central sensor and regulator of hypoxic gene expression (Kimura et al., 2008). The absence of any differences in gene expression between WT and *Gdf15 -/-* TECs after hypoxic incubation, thus implicates that the protective effects of GDF15 might be conferred by a mechanism that is not directly dependent on hypoxic HIF1α activation.

Excessive activation of TLRs, resulting in aggravated and perpetuated renal injury, is known to be a pivotal maladaptive pathogenic mechanism in the context of post-ischemic renal inflammation (Anders, 2010). Several groups have reported both *Tlr2*- and *Tlr4*-deficiency protects mice from I/R injury as evidenced by attenuated histomorphological damage and reduced amounts of circulating pro-inflammatory cyto- and chemokines (Pulskens et al., 2008; Shigeoka et al., 2007). At the same time, consistent mRNA expression of *Tlr2* and *Tlr4* in TECs under physiological circumstances alongside significant upregulation after I/R injury was found, highlighting the central involvement of TECs in post-ischemic endogenous danger signaling (Leemans et al., 2005; Vries et al., 2002). As *Gdf15* deficiency correlated with increased expression of pro-inflammatory genes in murine models of both I/R-induced AKI and CKD, it was hypothesized that GDF15 might exert its immunomodulatory effects by attenuating TLR-mediated pro-inflammatory signaling in TECs. Indeed, when stimulated with TLR4-ligand LPS TECs isolated from WT mice were found to exhibit substantially lower expression of pro-inflammatory molecules, such as *Ccl2*, *Cxcl2*, *Il6* and *Tnfα*, compared to *Gdf15 -/-* TECs. This strongly supports the hypothesis that the renoprotective effects of GDF15 observed *in-vivo* might be the consequence of GDF15 attenuating the induction of pro-inflammatory cytokines in TECs upon TLR4 activation. This finding appears to be even more relevant since a pioneering *in-vivo* study pointed out that TLR4 activation on renal parenchymal cells dominates over TLR4 activation on infiltrating immune cells in conveying I/R-induced kidney damage (Wu et al., 2007). This work was able to uncover the regulatory impact of GDF15 on TLR4-mediated pro-inflammatory signaling in TECs. Yet, future studies are required to determine the precise molecular targets of intracellular GDF15 activity in TECs.

Moreover, *in-vitro* translated GDF15 was seen to be liberated by TECs into their local extracellular environment. Hence, an intercellular mode of action in the post-ischemic, inflamed kidney also seemed conceivable. As *Gdf15 -/-* mice revealed an aggravated disruption of tubular morphology during I/R-induced CKD, it was speculated whether GDF15 might act as autocrine agent being not only released but also received by TECs, subsequently protecting themselves from injury caused by ischemia-associated endogenous molecules. However, pre-stimulating TECs with reGDF15 before exposing them to ischemia-related stimuli - including TLR ligands - did not result in altered gene expression. Although relatively high levels of reGDF15 – based on previously published literature (Id et al., 2019; Kim et al., 2018; Li et al., 2023; Olsen et al., 2017) - were used in the present work it could be discussed whether its

concentration was high enough to obtain biologically relevant effects. It has been suggested by the manufacturer to use even higher concentrations of reGDF15 (cf. R&D Systems). However, several groups have previously reported that reGDF15, sold by prominent companies (including R&D Systems), was contaminated to varying degrees with relevant amounts of biologically active TGFβ (Olsen et al., 2017; Tsai et al., 2018; Wischhusen et al., 2020). Hence, an uncontrolled use of higher concentrations without extensive prior purity verification appears to be problematic since unwanted effects mediated by TGFβ also become more likely. Beyond some remaining uncertainty whether the concentration of reGDF15 used was high enough to reproduce physiological conditions, no clear evidence was found that TECs might be the primary recipient of extracellular GDF15.

Also, a paracrine effect of GDF15 bridging intercellular crosstalk with macrophages seemed conceivable. It is well known that the functional phenotype of these phagocytic cells depends on their environmental stimuli and ranges between two poles – pro-inflammatory M1- and anti-inflammatory M2-macrophages (Han et al., 2019; Lech et al., 2012). The finding, that GDF15 promoted *in-vivo* the establishment of an anti-inflammatory environment in the kidney during I/R-induced CKD, supported the speculation that the overall less injured phenotype of WT mice might be the result of a M2-dominant macrophage response, facilitated by GDF15. Yet, stimulation with recombinant GDF15 remained without direct effect on macrophage polarization. The issue of a potentially inadequate reGDF15 concentration has already been outlined previously. Moreover, stimulation with supernatants from *Gdf15* expressing WT TECs did not alter macrophage polarization. Thus, macrophages do also not appear to be a primary recipient of extracellular GDF15. Nevertheless, WT mice displayed high renal expression of *Il4*, *Il10* and *Il13* during I/R-induced CKD compared to *Gdf15 -/-* mice - cytokines that are known to induce M2 polarization in resident tissue macrophages (Mosser et al., 2008). GDF15 thus might amplify the accumulation of these interleukins in the extracellular environment. Although this study failed to show a direct impact of GDF15 on macrophage polarization, it still seems possible that GDF15 might indirectly impact M1/M2 polarization in the post-ischemic kidney by provoking a local microenvironment, that favors a more M2-dominant immune response. Therefore, more in depth research such as co-culturing *in-vitro* studies might be beneficial.

Taken together, these results imply that the renoprotective effects of GDF15 observed *in-vivo* might be the consequence of GDF15 mitigating TLR4-mediated pro-inflammatory signaling in TECs. Although this work did not depict the specific molecular targets of intracellular GDF15 activity, it highlights its important role as negative regulator of pro-inflammatory signaling in the kidney. Hereby, this work outlines the path for future research on the specific intracellular interactions of GDF15 in TECs.

4 Conclusion and Outlook

In this work, the impact of TGFβ-superfamily member GDF15 on both AKI and CKD was analysed. In addition, its intrarenal activity was further elucidated.

Analysis of the employed *in-vivo* model of I/R-induced AKI revealed that *Gdf15*-deficiency in mice correlated with increased post-ischemic renal dysfunction. The finding that WT mice displayed a substantially better-preserved renal function after I/R injury, demonstrates the renoprotective role of GDF15 and may indicate a potential pharmacological manipulation of its intrarenal activity in future clinical therapy of AKI. However, as growth factors commonly serve multiple functions during renal injury, directly targeting their activity might cause unexpected, potentially therapy-limiting adverse effects (Gao et al., 2020). Therefore, future studies should aim to identify and explore specific downstream effectors of GDF15.

Moreover, the present work was the first study to examine the impact of *Gdf15* deficiency on the development of I/R-induced CKD *in-vivo*. Given the conclusion that GDF15 ameliorates I/R-induced CKD due to its anti-inflammatory as well as anti-fibrotic effects, this work adds - as another piece of the puzzle - to the hypothesis that GDF15 exerts a protective effect on the development and severity of CKD. Along with the evidence from a recent *in-vivo* study (Kim et al., 2018) the findings of this work might also suggest a potential therapeutic use of reGDF15 as a novel treatment strategy in clinical CKD therapy. However, as CKD commonly comprises the ultimate consequence of a myriad of various underlying conditions, future studies are needed to investigate the impact of GDF15 on the development of CKD in relation to its particular etiology.

By identifying TECs as the primary site of renal GDF15 synthesis and secretion, the present work serves as a significant starting point for future research on the influence of GDF15 on both intra- and intercellular signaling pathways in the kidney. In addition, this study pointed out that the renoprotective effects of GDF15 observed *in-vivo* might be the result of GDF15 mitigating TLR4-mediated pro-inflammatory signaling in TECs. By suggesting a potential role as negative regulator of pro-inflammatory signaling in the kidney, this work has laid the foundation for future research on the molecular interactions of GDF15 in TECs. Following projects should aim to depict the precise targets of intracellular GDF15 activity in TECs to further facilitate the development of novel therapeutic approaches for both AKI and CKD.

VII Summary

There are currently no therapeutic strategies to successfully attenuate either AKI or CKD by directly targeting intrarenal molecular processes. Thus, there is a clear need to identify and explore new therapeutic targets to facilitate the development of novel treatment modalities. GDF15 is a stress-inducible cytokine of the TGFβ-superfamily. Although the literature indicates a clear link between GDF15 activity and renal homeostasis, its role in ischemic kidney disease has remained unclear. The aim of this thesis was to investigate the role of GDF15 in AKI and CKD. It also sought to elucidate the primary source of renal GDF15, and the molecular axes affected by GDF15 activity in the kidney.

In a first step, I/R injury-based models of both AKI and CKD were implemented in *Gdf15 -/-* and control WT mice. By performing kidney function measurements, comprehensive histopathological evaluation and gene expression analysis, the impact of *Gdf15* deficiency on the development and severity of AKI, or CKD, was assessed. In a second step, various primary renal cell types were isolated from WT mice and *Gdf15* expression as well as GDF15 secretion levels were determined. Thereafter, the influence of GDF15 on ischemia-related molecular mechanisms in TECs was studied in detail using quantitative gene expression analysis.

In this thesis, a renoprotective impact of GDF15 on both I/R-induced AKI and CKD could be uncovered. GDF15 was found to attenuate I/R-induced AKI, as WT mice were better protected from post-ischemic deterioration of kidney function than *Gdf15 -/-* mice. Moreover, GDF15 has been shown to exert anti-inflammatory as well as potent anti-fibrotic effects, ameliorating I/R-induced CKD. Subsequently, TECs could be identified as the primary site of *Gdf15* expression and GDF15 secretion in the kidney. By demonstrating that GDF15 attenuates TLR4-mediated pro-inflammatory signaling in TECs, the present work provides a potential mechanistic rationale for the protective effects of GDF15 observed *in-vivo*. In summary, this work discloses the renoprotective impact of GDF15 on the development and severity of AKI and CKD, potentially resulting from its mitigating influence on TLR4-mediated pro-inflammatory signaling in TECs.

The findings of this study might lead the way towards the development of innovative therapeutic approaches targeting renal GDF15 activity. More extensive research addressing the unique role of GDF15 in regulating pro-inflammatory signaling in TECs could help uncover its specific molecular targets and downstream effectors. This might further facilitate the development of novel targeted treatment strategies for both AKI and CKD.

Zusammenfassung (Übersetzung in das Deutsche)

Aktuell existieren keine therapeutischen Verfahren, um durch die gezielte Beeinflussung intrarenaler molekularer Prozesse das akute Nierenversagen (ANV) oder die chronische Niereninsuffizienz (CNI) erfolgreich zu behandeln. Daher ist es notwendig, neue therapeutische Zielstrukturen zu identifizieren und zu erforschen. GDF15 ist ein Stress-induzierbares Zytokin aus der TGFβ-Superfamilie. Obwohl die Literatur einen klaren Zusammenhang zwischen der Aktivität von GDF15 und der renalen Homöostase suggeriert, ist die Funktion von GDF15 in Bezug auf renale Erkrankungen bisher unklar geblieben. Ziel dieser Arbeit war, die Rolle von GDF15 im ANV und in der CNI zu untersuchen. Zudem sollten der primäre Ursprung von renalem GDF15 sowie die von GDF15 beeinflussten molekularen Achsen aufgedeckt werden.

Zunächst wurden I/R-basierte Modelle des ANV und der CNI in *Gdf15 -/-* und WT Mäusen implementiert. Durch Nierenfunktionsmessungen, histopathologische Untersuchungen und Genexpressionsanalysen wurde der Einfluss der *Gdf15* Defizienz auf die Entwicklung und den Schweregrad des ANV und der CNI untersucht. Anschließend wurden diverse primäre renale Zelltypen aus WT Mäusen isoliert und *Gdf15* Expressions- sowie GDF15 Sekretionsniveaus bestimmt. Weiterhin wurde der Effekt von GDF15 auf Ischämie-assoziierte molekulare Mechanismen in tubulären Epithelzellen mittels Genexpressionsanalysen untersucht.

Im Rahmen dieser Arbeit konnte ein renoprotektiver Effekt von GDF15 auf das I/R-induzierte ANV nachgewiesen werden, da WT Mäuse gegenüber *Gdf15 -/-* Mäusen besser vor einer post-ischämischen Reduktion der Nierenfunktion geschützt waren. Darüber hinaus wurde gezeigt, dass GDF15 durch seine anti-inflammatorischen und anti-fibrotischen Effekte auch das Ausmaß einer I/R-induzierten CNI *in-vivo* reduziert. Tubuläre Epithelzellen konnten als primäre Quelle renaler *Gdf15* Expression und GDF15 Sekretion identifiziert werden. Mit dem Nachweis, dass GDF15 die TLR4-vermittelte pro-inflammatorische Signalübertragung in tubulären Epithelzellen abschwächt, liefert die vorliegende Arbeit zudem eine mögliche mechanistische Erklärung für die *in-vivo* beobachteten protektiven Effekte von GDF15.

Zusammenfassend wurde in dieser Arbeit der renoprotektive Effekt von GDF15 auf die Entwicklung und den Schweregrad sowohl des ANV als auch der CNI dargelegt. Als potentiell zugrundeliegender Pathomechanismus wurde der mildernde Einfluss von GDF15 auf TLR4-vermittelte pro-inflammatorische Mechanismen in tubulären Epithelzellen identifiziert. Auf Basis dieser Arbeit sollten anknüpfende Projekte darauf abzielen, die spezifischen molekularen Zielstrukturen von GDF15 in tubulären Epithelzellen zu identifizieren. Langfristig könnte dies dazu beitragen, neue gezielte Therapieansätze für das ANV und die CNI zu entwickeln.

VIII Table Index

IX Figure Index

X References

Abulizi, P., Loganathan, N., Zhao, D., Mele, T., Zhang, Y., Zwiep, T., Liu, K., & Zheng, X. (2017). Growth Differentiation Factor-15 Deficiency Augments Inflammatory Response and Exacerbates Septic Heart and Renal Injury Induced by Lipopolysaccharide /631/80/82/23 /631/326/421 /13/31 /13/2 /13 /38 /64 /64/60 article. *Scientific Reports*, *7*(1), 1–10. https://doi.org/10.1038/s41598-017-00902-5

Adachi, T., & Sugiyama, N. (2014). Renal atrophy after ischemia – reperfusion injury depends on massive tubular apoptosis induced by TNF a in the later phase. *Medical Molecular Morphology*, *47*(4), 213–223. https://doi.org/10.1007/s00795-013-0067-3

Agarwal, A., & Nath, K. A. (2020). Pathophysiology of Chronic Kidney Disease Progression: Organ and Cellular Considerations. In *Chronic Renal Disease*. Elsevier Inc. https://doi.org/10.1016/B978-0-12-815876-0.00018-8

Agati, V. D. D. (2017). Podocyte Growing Pains in Adaptive FSGS. *Journal of the American Society of Nephrology*, *28*(10), 2825–2827. https://doi.org/10.1681/ASN.2017060612

Akcay, A., & Lee, D. (2010). Update on the diagnosis and management of acute kidney injury. *International Journal of Nephrology and Renovascular Disease*, *3*, 129–140. https://doi.org/10.2147/IJNRD.S8641

Al-lamki, R. S., & Mayadas, T. N. (2014). TNF receptors : signaling pathways and contribution to renal dysfunction. *Kidney International*, *87*(2), 281–296. https://doi.org/10.1038/ki.2014.285

Anders, H. (2010). Toll-Like Receptors and Danger Signaling in Kidney Injury. *Journal of the American Society of Nephrology*, *21*(8), 1270–1274. https://doi.org/10.1681/ASN.2010030233

Anders, H., Vielhauer, V., & Schlöndorf, D. (2003). Chemokines and chemokine receptors are involved in the resolution or progression of renal disease. *Kidney International*, *63*(2), 401–415. https://doi.org/10.1046/j.1523-1755.2003.00750.x

Asea, A., Rehli, M., Kabingu, E., Boch, J. A., Bare, O., Auron, P. E., Ann, M., & Calderwood, S. K. (2002). Novel signal transduction pathway utilized by extracellular HSP70: role of toll-like receptor (TLR) 2 and TLR4. *The Journal of Biological Chemistry*, *277*(17), 15028–15034. https://doi.org/10.1074/jbc.M200497200

Assadi, A., Zahabi, A., & Hart, R. A. (2020). GDF15, an update of the physiological and pathological roles it plays: a review. *Pflugers Archiv European Journal of Physiology*, *472*(11), 1535–1546. https://doi.org/10.1007/s00424-020-02459-1

Bagshaw, S. M., George, C., & Bellomo, R. (2007). Changes in the incidence and outcome for early acute kidney injury in a cohort of Australian intensive care units. *Critical Care*, *11*(3), 1–9. https://doi.org/10.1186/cc5949

Balzer, M. S., Rohacs, T., & Susztak, K. (2022). How Many Cell Types Are in the Kidney and What Do They Do? *Annual Review of Physiology*, *84*, 507–531. https://doi.org/10.1146/annurev-physiol-052521-121841.How

Basile, D. P., Bonventre, J. V, Mehta, R., Nangaku, M., Unwin, R., Rosner, M. H., Kellum, J. A., Ronco, C., & Work, X. (2016). Progression after AKI: Understanding Maladaptive Repair Processes to Predict and Identify Therapeutic Treatments. *Journal of the American Society of Nephrology*, *27*(3), 687–697. https://doi.org/10.1681/ASN.2015030309

Bauskin, A. R., Jiang, L., Luo, X. W., Wu, L., Brown, D. A., & Breit, S. N. (2010). The TGF-β Superfamily Cytokine MIC-1/GDF15: Secretory Mechanisms Facilitate Creation of Latent Stromal Stores. *Journal of Interferon & Cytokine Research*, *30*(6), 389–397. https://doi.org/10.1089/jir.2009.0052

Bauskin, A. R., Zhang, H., Fairlie, W. D., He, X. Y., Russell, P. K., Moore, A. G., Brown, D. A., Stanley, K. K., & Breit, S. N. (2000). The propeptide of macrophage inhibitory cytokine (MIC-1), a TGF-beta superfamily member, acts as a quality control determinant for correctly folded MIC-1. *The EMBO Journal*, *19*(10), 2212–2220. https://doi.org/10.1093/emboj/19.10.2212

Bidadkosh, A., Lambooy, S. P. H., Heerspink, H. J., Pena, M. J., Henning, R. H., Buikema, H., & Deelman, L. E. (2017). Predictive properties of biomarkers GDF-15, NTproBNP, and hs-TnT for morbidity and mortality in patients with type 2 diabetes with nephropathy. *Diabetes Care*, *40*(6), 784–792. https://doi.org/10.2337/dc16-2175

Biragyn, A., Ruffini, P. A., Leifer, C. A., Klyushnenkova, E., Shakhov, A., Chertov, O., Shirakawa, A. K., Farber, J. M., Segal, D. M., Oppenheim, J. J., & Kwak, L. W. (2002). Toll-like receptor 4-dependent activation of dendritic cells by beta-defensin 2. *Science*, *298*(5595), 1025–1029. https://doi.org/10.1126/science.1075565

Bonventre, J. V, & Yang, L. (2011). Cellular pathophysiology of ischemic acute kidney injury. *The Journal of Clinical Investigation*, *121*(11), 4210–4221. https://doi.org/10.1172/JCI45161.4210

Bootcov, M. R., Bauskin, A. R., Valenzuela, S. M., Moore, A. G., Bansal, M., He, X. Y., Zhang, H. P., Donnellan, M., Mahler, S., Pryor, K., Walsh, B. J., Nicholson, R. C., Fairlie, W. D., Por, S. B., Robbins, J. M., & Breit, S. N. (1997). MIC-1, a novel macrophage inhibitory cytokine, is a divergent member of the TGF-beta superfamily. *PNAS*, *94*(21), 11514–11519. https://doi.org/10.1073/pnas.94.21.11514

Böttner, M., Laaff, M., Schechinger, B., Rappold, G., Unsicker, K., & Suter-Crazzolara, C. (1999). Characterization of the rat, mouse, and human genes of growth/differentiation factor-15/ macrophage inhibiting cytokine-1 (GDF-15/MIC-1). *Gene*, *237*(1), 105–111. https://doi.org/10.1016/s0378-1119(99)00309-1

Breit, S. N., Brown, D. A., & Tsai, V. W. W. (2021). The GDF15-GFRAL Pathway in Health and Metabolic Disease: Friend or Foe? *Annual Review of Physiology*, *83*, 127–151. https://doi.org/10.1146/annurev-physiol-022020-045449

Breit, S. N., Carrero, J. J., Tsai, V. W. W., Yagoutifam, N., Luo, W., Kuffner, T., Bauskin, A. R., Wu, L., Jiang, L., Barany, P., Heimburger, O., Murikami, M. A., Apple, F. S., Marquis, C. P., MacIa, L., Lin, S., Sainsbury, A., Herzog, H., Law, M., … Brown, D. A. (2012). Macrophage inhibitory cytokine-1 (MIC-1/GDF15) and mortality in end-stage renal disease. *Nephrology Dialysis Transplantation*, *27*(1), 70–75. https://doi.org/10.1093/ndt/gfr575

Brezis, M., Rosen, S., Silva, P., & Epstein, F. H. (1984). Renal ischemia: A new

perspective. *Kidney International*, *26*(4), 375–383. https://doi.org/10.1038/ki.1984.185

Brezis, M., Rosen, S. (1995). Hypoxia of the renal medulla--its implications for disease. *The New England Journal of Medicine*, *332*(10), 647–655. https://doi.org/10.1056/NEJM199503093321006

Chamboredon, S., Ciais, D., Desroches-Castan, A., Savid, P., Bono, F., Feige, J. J., & Cherradi, N. (2011). Hypoxia-inducible factor-1α mRNA: A new target for destabilization by tristetraprolin in endothelial cells. *Molecular Biology of the Cell*, *22*(18), 3366–3378. https://doi.org/10.1091/mbc.E10-07-0617

Chatauret, N., Badet, L., Barrou, B., & Hauet, T. (2014). Ischemia-reperfusion: From cell biology to acute kidney injury. *Progres En Urologie*, *24*(SUPPL.1), S4–S12. https://doi.org/10.1016/S1166-7087(14)70057-0

Chawla, L. S., Amdur, R. L., Amodeo, S., Kimmel, P. L., & Palant, C. E. (2011). The severity of acute kidney injury predicts progression to chronic kidney disease. *Kidney International*, *79*(12), 1361–1369. https://doi.org/10.1038/ki.2011.42

Chawla, L. S., & Kimmel, P. L. (2012). Acute kidney injury and chronic kidney disease : an integrated clinical syndrome. *Kidney International*, *82*(5), 516–524. https://doi.org/10.1038/ki.2012.208

Chertow, G. M., Burdick, E., Honour, M., Bonventre, J. V., & Bates, D. W. (2005). Acute kidney injury, mortality, length of stay, and costs in hospitalized patients. *Journal of the American Society of Nephrology*, *16*(11), 3365–3370. https://doi.org/10.1681/ASN.2004090740

Cheval, L., Viollet, B., Klein, C., Figueres, L., Devevre, E., Zadigue, G., Crambert, G., Vogt, B., & Doucet, A. (2021). Acidosis-induced activation of distal nephron principal cells triggers Gdf15 secretion and adaptive proliferation of intercalated cells. *Acta Physiologica*, *232*(3), 1–17. https://doi.org/10.1111/apha.13661

Choi, D. E., Jeong, J. Y., Lim, B. J., Na, K. R., Shin, Y. T., & Lee, K. W. (2009). Pretreatment With the Tumor Nerosis Factor-α Blocker Etanercept Attenuated Ischemia-Reperfusion Renal Injury. *Transplantation Proceedings*, *41*(9), 3590–3596. https://doi.org/10.1016/j.transproceed.2009.05.042

Chung, H. K., Kim, J. T., Kim, H. W., Kwon, M., Kim, S. Y., Shong, M., Kim, K. S., & Yi, H. S. (2017). GDF15 deficiency exacerbates chronic alcohol- and carbon tetrachloride-induced liver injury. *Scientific Reports*, *7*(1), 1–13. https://doi.org/10.1038/s41598-017-17574-w

Coll, A. P., Chen, M., Taskar, P., Rimmington, D., Patel, S., Tadross, J. A., Cimino, I., Yang, M., Welsh, P., Virtue, S., Goldspink, D. A., Miedzybrodzka, E. L., Konopka, A. R., Esponda, R. R., Huang, J. T. J., Tung, Y. C. L., Rodriguez-Cuenca, S., Tomaz, R. A., Harding, H. P., … O'Rahilly, S. (2020). GDF15 mediates the effects of metformin on body weight and energy balance. *Nature*, *578*(7795), 444–448. https://doi.org/10.1038/s41586-019-1911-y

Day, E. A., Ford, R. J., Smith, B. K., Mohammadi-Shemirani, P., Morrow, M. R., Gutgesell, R. M., Lu, R., Raphenya, A. R., Kabiri, M., McArthur, A. G., McInnes, N., Hess, S., Paré, G., Gerstein, H. C., & Steinberg, G. R. (2019). Metformin-induced increases in GDF15 are important for suppressing appetite and promoting weight loss. *Nature Metabolism*, *1*(12), 1202–1208. https://doi.org/10.1038/s42255-019-0146-4

Dong, Y., Zhang, Q., Wen, J., Chen, T., He, L., Wang, Y., & Yin, J. (2019). Ischemic Duration and Frequency Determines AKI-to-CKD Progression Monitored by Dynamic Changes of Tubular Biomarkers in IRI Mice. *Frontiers in Physiology*, *10*(February), 1–15. https://doi.org/10.3389/fphys.2019.00153

Drożdżal, S., Lechowicz, K., Szostak, B., Rosik, J., Kotfis, K., Machoy-Mokrzyńska, A., Białecka, M., Ciechanowski, K., & Gawrońska-Szklarz, B. (2021). Kidney damage from nonsteroidal anti-inflammatory drugs—Myth or truth? Review of selected literature. *Pharmacology Research and Perspectives*, *9*(4), 1–7. https://doi.org/10.1002/prp2.817

Edeling, M., Ragi, G., Huang, S., Pavenstädt, H., & Susztak, K. (2016). Developmental signalling pathways in renal fibrosis: the roles of Notch, Wnt and Hedgehog. *Nature Reviews Nephrology*, *12*, 426–439. https://doi.org/10.1038/nrneph.2016.54

Emmerson, P. J., Wang, F., Du, Y., Liu, Q., Pickard, R. T., Gonciarz, M. D., Coskun, T., Hamang, M. J., Sindelar, D. K., Ballman, K. K., Foltz, L. A., Muppidi, A., Alsina-Fernandez, J., Barnard, G. C., Tang, J. X., Liu, X., Mao, X., Siegel, R., Sloan, J. H., … Wu, X. (2017). The metabolic effects of GDF15 are mediated by the orphan receptor GFRAL. *Nature Medicine*, *23*(10), 1215–1219. https://doi.org/10.1038/nm.4393

Fiorentino, M. (2018). Acute Kidney Injury to Chronic Kidney Disease Transition. *Basic Research and Clinical Practice*, *193*, 45–54. https://doi.org/10.1159/000484962

Gailit, J., Colflesh, D., Rabiner, I., Simone, J., & Goligorsky, M. S. (1993). Redistribution and dysfunction of integrins in cultured renal epithelial cells exposed to oxidative stress. *American Journal of Physiology - Renal Fluid and Electrolyte Physiology*, *264*(1), F149-57. https://doi.org/10.1152/ajprenal.1993.264.1.f149

Gameiro, J., Marques, F., & Lopes, J. A. (2021). Long-term consequences of acute kidney injury: a narrative review. *Clinical Kidney Journal*, *14*(3), 789–804. https://doi.org/10.1093/ckj/sfaa177

Gao, L., Zhong, X., Jin, J., Li, J., & Meng, X. ming. (2020). Potential targeted therapy and diagnosis based on novel insight into growth factors, receptors, and downstream effectors in acute kidney injury and acute kidney injury-chronic kidney disease progression. *Signal Transduction and Targeted Therapy*, *5*(1), 1–11. https://doi.org/10.1038/s41392-020-0106-1

Gaut, J. P., & Liapis, H. (2021). Acute kidney injury pathology and pathophysiology: A retrospective review. *Clinical Kidney Journal*, *14*(2), 526–536. https://doi.org/10.1093/ckj/sfaa142

Gerstein, H. C., Pare, G., Hess, S., Ford, R. J., Sjaarda, J., Raman, K., McQueen, M., Lee, S. F., Haenel, H., & Steinberg, G. R. (2017). Growth differentiation factor 15 as a novel biomarker for metformin. *Diabetes Care*, *40*(2), 280–283. https://doi.org/10.2337/dc16-1682

Gewin, L., Zent, R., & Pozzi, A. (2017). Progression of chronic kidney disease: too much cellular talk causes damage. *Kidney International*, *91*(3), 552–560. https://doi.org/10.1016/j.kint.2016.08.025

Gluba, A., Banach, M., Hannam, S., Mikhailidis, D. P., Sakowicz, A., & Rysz, J. (2010). The role of Toll-like receptors in renal diseases. *Nature Publishing Group*, *6*(APRIL), 224–235. https://doi.org/10.1038/nrneph.2010.16

Guenancia, C., Kahli, A., Laurent, G., Hachet, O., Malapert, G., Grosjean, S., Girard, C., Vergely, C., & Bouchot, O. (2015). Pre-operative growth differentiation factor 15 as a novel biomarker of acute kidney injury after cardiac bypass surgery. *International Journal of Cardiology*, *197*, 66–71. https://doi.org/10.1016/j.ijcard.2015.06.012

Guzzi, F., Cirillo, L., Roperto, R. M., Romagnani, P., & Lazzeri, E. (2019). Molecular Mechanisms of the Acute Kidney Injury to Chronic Kidney Disease Transition : An Updated View. *International Journal of Molecular Sciences*, *20(19)*(4941). https://doi.org/https://doi.org/10.3390/ijms20194941

Habib, R. (2021). Multifaceted roles of Toll-like receptors in acute kidney injury. *Heliyon*, *7*(3), e06441. https://doi.org/10.1016/j.heliyon.2021.e06441

Han, H. I., Skvarca, L. B., Espiritu, E. B., Davidson, A. J., & Hukriede, N. A. (2019). The role of macrophages during acute kidney injury: destruction and repair. *Pediatric Nephrology*, *34*(4), 561–569. https://doi.org/10.1007/s00467-017-3883-1

Han, S. J., Li, H., Kim, M., Shlomchik, M. J., & Lee, H. T. (2019). Kidney proximal tubular TLR9 exacerbates ischemic acute kidney injury. *Journal of Immunology*, *201*(3), 1073–1085. https://doi.org/10.4049/jimmunol.1800211.Kidney

Han, W. K., Bailly, V., Abichandani, R., Thadhani, R., & Bonventre, J. V. (2002). Kidney Injury Molecule-1 (KIM-1): A novel biomarker for human renal proximal tubule injury. *Kidney International*, *62*(1), 237–244. https://doi.org/10.1046/j.1523-1755.2002.00433.x

Hanindita, M. H., Prasetyo, R. V., Soemyarso, N. A., Utamayasa, I. K. A., & Tahalele, P. (2016). Neutrophil gelatinase-associated lipocalin as a biomarker for acute kidney injury in children after cardiac surgery. *Paediatrica Indonesiana*, *56*(4), 230. https://doi.org/10.14238/pi56.4.2016.230-7

Heringlake, M., Charitos, E. I., Erber, K., Berggreen, A. E., Heinze, H., & Paarmann, H. (2016). Preoperative plasma growth-differentiation factor-15 for prediction of acute kidney injury in patients undergoing cardiac surgery. *Critical Care*, *20*(1), 1–10. https://doi.org/10.1186/s13054-016-1482-3

Hill, N. R., Fatoba, S. T., Oke, J. L., Hirst, J. A., Callaghan, A. O., Lasserson, D. S., & Hobbs, F. D. R. (2016). Global Prevalence of Chronic Kidney Disease – A Systematic Review and Meta-Analysis. *PLoS One*, *11*(7). https://doi.org/https://doi.org/10.1371/journal.pone.0158765

Ho, J. E., Hwang, S., Wollert, K. C., Larson, M. G., Cheng, S., Kempf, T., Vasan, R. S., Januzzi, J. L., Wang, T. J., & Fox, C. S. (2013). Biomarkers of Cardiovascular Stress and Incident Chronic Kidney Disease. *Clinical Cheminstry*, *59*(11), 1613–1620. https://doi.org/10.1373/clinchem.2013.205716

Hoste, E. A. J., Kellum, J. A., Selby, N. M., Zarbock, A., Palevsky, P. M., Bagshaw, S. M., Goldstein, S. L., Cerdá, J., & Chawla, L. S. (2018). Global epidemiology and outcomes of acute kidney injury. *Nature Reviews Nephrology*, *14*(10), 607–625. https://doi.org/10.1038/s41581-018-0052-0

Hostetter, T. H., Olson, J. L., Rennke, H. G., Venkatachalam, M. A., & Brenner, B. M. (1981). Hyperfiltration in remnant nephrons: a potentially adverse response to renal ablation. *The American Journal of Physiology*, *241*(1), F85-93. https://doi.org/10.1152/ajprenal.1981.241.1.F85

Hsiao, E. C., Koniaris, L. G., Zimmers-Koniaris, T., Sebald, S. M., Huynh, T. V., & Lee,

S.-J. (2000). Characterization of Growth-Differentiation Factor 15, a Transforming Growth Factor β Superfamily Member Induced following Liver Injury. *Molecular and Cellular Biology*, *20*(10), 3742–3751. https://doi.org/10.1128/mcb.20.10.3742-3751.2000

Hsu, C. Y., Chinchilli, V. M., Coca, S., Devarajan, P., Ghahramani, N., Go, A. S., Hsu, R. K., Ikizler, T. A., Kaufman, J., Liu, K. D., Parikh, C. R., Reeves, W. B., Wurfel, M., Zappitelli, M., Kimmel, P. L., & Siew, E. D. (2020). Post-Acute Kidney Injury Proteinuria and Subsequent Kidney Disease Progression: The Assessment, Serial Evaluation, and Subsequent Sequelae in Acute Kidney Injury (ASSESS-AKI) Study. *JAMA Internal Medicine*, *180*(3), 402–410. https://doi.org/10.1001/jamainternmed.2019.6390

Hsu, J. Y., Crawley, S., Chen, M., Ayupova, D. A., Lindhout, D. A., Higbee, J., Kutach, A., Joo, W., Gao, Z., Fu, D., To, C., Mondal, K., Li, B., Kekatpure, A., Wang, M., Laird, T., Horner, G., Chan, J., Mcentee, M., … Allan, B. B. (2017). Non-homeostatic body weight regulation through a brainstem-restricted receptor for GDF15. *Nature*, *550*(7675), 255–259. https://doi.org/10.1038/nature24042

Huang, Y., Zhou, F., Xiao, Y., Shen, C., Liu, K., & Zhao, B. (2019). TLR7 mediates increased vulnerability to ischemic acute kidney injury in diabetes. *Rev. Assoc. Med. Bras.*, *65*(8), 1067–1073. https://doi.org/http://dx.doi.org/10.1590/1806-9282.65.8.1067 SUMMARY

Huen, S. C., Huynh, L., Marlier, A., Lee, Y., Moeckel, G. W., & Cantley, L. G. (2015). GM-CSF Promotes Macrophage Alternative Activation after Renal Ischemia/Reperfusion Injury. *Journal of the American Society of Nephrology*, *26*(6), 1334–1345. https://doi.org/10.1681/ASN.2014060612

Hutchison, N., Fligny, C., & Duf, J. S. (2013). Resident mesenchymal cells and fibrosis. *Biochimica et Biophysica Acta*, *1832*(7), 962–971. https://doi.org/10.1016/j.bbadis.2012.11.015

Ichimura, T., Bonventre, J. V., Bailly, V., Wei, H., Hession, C. A., Cate, R. L., & Sanicola, M. (1998). Kidney injury molecule-1 (KIM-1), a putative epithelial cell adhesion molecule containing a novel immunoglobulin domain, is up-regulated in renal cells after injury. *Journal of Biological Chemistry*, *273*(7), 4135–4142. https://doi.org/10.1074/jbc.273.7.4135

Id, G. H., Torres, F. De, Arouche, N., Benzoubir, N., Hatem, E., Anginot, A., & Uzan, G. (2019). GDF15 secreted by senescent endothelial cells improves vascular progenitor cell functions. *PLoS ONE*, *14*(5), 1–17. https://doi.org/https://doi.org/10.1371/journal.pone.0216602

Ishani, A. et al. (2011). The Magnitude of Acute Serum Creatinine Increase After Cardiac Surgery and the Risk of Chronic Kidney Disease, Progression of Kidney Disease, and Death. *JAMA Internal Medicine*, *171*(3), 226–233. https://doi.org/10.1001/archinternmed.2010.514

Iwano, M., Okada, H., Neilson, E. G., Iwano, M., Plieth, D., Danoff, T. M., Xue, C., Okada, H., & Neilson, E. G. (2002). Evidence that fibroblasts derive from epithelium during tissue fibrosis. *Journal of Clinical Investigation*, *110*(3), 341–350. https://doi.org/10.1172/JCI200215518.Introduction

Jang, H., In, J., Jung, K., Kim, J., Han, K., & Moo, K. (2013). Bone marrow-derived cells play a major role in kidney fibrosis via proliferation and differentiation in the

infiltrated site. *Biochimica et Biophysica Acta*, *1832*(6), 817–825. https://doi.org/10.1016/j.bbadis.2013.02.016

Jang, H. R., Ko, G. J., Wasowska, B. A., & Rabb, H. (2009). The interaction between ischemia – reperfusion and immune responses in the kidney. *Molecular Medicine*, *87*(9), 859–864. https://doi.org/10.1007/s00109-009-0491-y

Jang, H. R., & Rabb, H. (2009). The innate immune response in ischemic acute kidney injury. *Clinical Immunology*, *130*(1), 41–50. https://doi.org/10.1016/j.clim.2008.08.016

Joannidis, M., & Hoste, E. (2018). Angiotensin inhibition in patients with acute kidney injury: Dr. Jekyll or Mr. Hyde? *Intensive Care Medicine*, *44*(7), 1159–1161. https://doi.org/10.1007/s00134-018-5223-8

Johnen, H., Lin, S., Kuffner, T., Brown, D. A., Tsai, V. W. W., Bauskin, A. R., Wu, L., Pankhurst, G., Jiang, L., Junankar, S., Hunter, M., Fairlie, W. D., Lee, N. J., Enriquez, R. F., Baldock, P. A., Corey, E., Apple, F. S., Murakami, M. M., Lin, E. J., … Breit, S. N. (2007). Tumor-induced anorexia and weight loss are mediated by the TGF-β superfamily cytokine MIC-1. *Nature Medicine*, *13*(11), 1333–1340. https://doi.org/10.1038/nm1677

Johnson, G. B., Brunn, G. J., Kodaira, Y., & Platt, J. L. (2002). Receptor-Mediated Monitoring of Tissue Well-Being Via Detection of Soluble Heparan Sulfate by Toll-Like Receptor 4. *The Journal of Immunology*, *168*(10), 5233–5239. https://doi.org/10.4049/jimmunol.168.10.5233

Kalantar-zadeh, K., Jafar, T. H., Nitsch, D., Neuen, B. L., & Perkovic, V. (2021). Chronic kidney disease. *The Lancet*, *398*(10302), P786-802. https://doi.org/10.1016/S0140-6736(21)00519-5

Kastritis, E., Papassotiriou, I., Merlini, G., Milani, P., Terpos, E., Basset, M., Akalestos, A., Russo, F., Psimenou, E., Apostolakou, F., Roussou, M., Gavriatopoulou, M., Eleutherakis-Papaiakovou, E., Fotiou, D., Ziogas, D. C., Papadopoulou, E., Pamboucas, C., Dimopoulos, M. A., & Palladini, G. (2018). Growth differentiation factor-15 is a new biomarker for survival and renal outcomes in light chain amyloidosis. *Blood*, *131*(14), 1568–1575. https://doi.org/10.1182/blood-2017-12-819904

Kellum, J. A., Romagnani, P., Ashuntantang, G., Ronco, C., Zarbock, A., & Anders, J. (2021). Acute kidney injury. *Nature Reviews Disease Primers*. https://doi.org/10.1038/s41572-021-00284-z

Kempf, T., Eden, M., Strelau, J., Naguib, M., Willenbockel, C., Tongers, J., Heineke, J., Kotlarz, D., Xu, J., Molkentin, J. D., Niessen, H. W., Drexler, H., & Wollert, K. C. (2006). The transforming growth factor-β superfamily member growth-differentiation factor-15 protects the heart from ischemia/reperfusion injury. *Circulation Research*, *98*(3), 351–360. https://doi.org/10.1161/01.RES.0000202805.73038.48

Kempf, T., Zarbock, A., Widera, C., Butz, S., Stadtmann, A., Rossaint, J., Bolomini-Vittori, M., Korf-Klingebiel, M., Napp, L. C., Hansen, B., Kanwischer, A., Bavendiek, U., Beutel, G., Hapke, M., Sauer, M. G., Laudanna, C., Hogg, N., Vestweber, D., & Wollert, K. C. (2011). GDF-15 is an inhibitor of leukocyte integrin activation required for survival after myocardial infarction in mice. *Nature Medicine*, *17*(5), 581–588. https://doi.org/10.1038/nm.2354

Kers, J., Leemans, J. C., & Linkermann, A. (2016). An Overview of Pathways of

Regulated Necrosis in Acute Kidney Injury. *Seminars in Nephrology*, *36*(3), 139–152. https://doi.org/10.1016/j.semnephrol.2016.03.002

Kezi, A., Stajic, N., & Thaiss, F. (2017). Review Article Innate Immune Response in Kidney Ischemia / Reperfusion Injury : Potential Target for Therapy. *Journal of Immunology Research*. https://doi.org/https://doi.org/10.1155/2017/6305439

Kim, Y., Shin, H., Chun, Y., & Park, J. (2018). CST3 and GDF15 ameliorate renal fibrosis by inhibiting fibroblast growth and activation. *Biochemical and Biophysical Research Communications*, *500*(2), 288–295. https://doi.org/10.1016/j.bbrc.2018.04.061

Kimura, K., Iwano, M., Higgins, D. F., Yamaguchi, Y., Nakatani, K., Harada, K., Kubo, A., Akai, Y., Rankin, E. B., Neilson, E. G., Haase, V. H., Saito, Y., Kimura, K., Iwano, M., Df, H., Yamaguchi, Y., Harada, K., Kubo, A., Akai, Y., … Eg, N. (2008). Stable expression of HIF-1 in tubular epithelial cells promotes interstitial fibrosis. *American Journal of Physiology - Renal Physiology*, *295*(4), 1023–1029. https://doi.org/10.1152/ajprenal.90209.2008.

Kriz, W., Kaissling, B., Hir, M. Le, Kriz, W., Kaissling, B., & Hir, M. Le. (2011). Epithelial-mesenchymal transition (EMT) in kidney fibrosis: fact or fantasy ? *Journal of Clinical Investigation*, *121*(2), 468–474. https://doi.org/10.1172/JCI44595.468

Kriz, W., & Lemley, K. V. (2015). A Potential Role for Mechanical Forces in the Detachment of Podocytes and the Progression of CKD. *Journal of the American Society of Nephrology*, *26*(2), 258–269. https://doi.org/10.1681/ASN.2014030278

Lajer, M., Jorsal, A., Tarnow, L., Parving, H. H., & Rossing, P. (2010). Plasma growth differentiation factor-15 independently predicts all-cause and cardiovascular mortality as well as deterioration of kidney function in type 1 diabetic patients with nephropathy. *Diabetes Care*, *33*(7), 1567–1572. https://doi.org/10.2337/dc09-2174

Lameire, N., Van Biesen, W., & Vanholder, R. (2006). The changing epidemiology of acute renal failure. *Nature Clinical Practice Nephrology*, *2*(7), 364–377. https://doi.org/10.1038/ncpneph0218

Lebleu, V. S., Taduri, G., Connell, J. O., Teng, Y., Cooke, V. G., Woda, C., Sugimoto, H., & Kalluri, R. (2013). Origin and function of myofibroblasts in kidney fibrosis. *Nature Medicine*, *19*(8), 1047–1053. https://doi.org/10.1038/nm.3218

Lech, M., & Anders, H. (2013). Macrophages and fibrosis: How resident and infiltrating mononuclear phagocytes orchestrate all phases of tissue injury and repair. *BBA - Molecular Basis of Disease*, *1832*(7), 989–997. https://doi.org/10.1016/j.bbadis.2012.12.001

Lech, M., Gr, R., Weidenbusch, M., & Anders, H. (2012). Tissues Use Resident Dendritic Cells and Macrophages to Maintain Homeostasis and to Regain Homeostasis upon Tissue Injury: The Immunoregulatory Role of Changing Tissue Environments. *Mediators of Inflammation*. https://doi.org/10.1155/2012/951390

Lech, M., Gröbmayr, R., Ryu, M., Lorenz, G., Hartter, I., Mulay, S. R., Susanti, H. E., Kobayashi, K. S., Flavell, R. A., & Anders, H. (2014). Macrophage Phenotype Controls Long-Term AKI Outcomes — Kidney Regeneration versus Atrophy. *Journal of the American Society of Nephrology*, *25*(2), 292–304. https://doi.org/10.1681/ASN.2013020152

Lee, S., Huen, S., Nishio, H., Nishio, S., Lee, H. K., Choi, B., Ruhrberg, C., & Cantley, L.

G. (2011). Distinct Macrophage Phenotypes Contribute to Kidney Injury and Repair. *Journal of the American Society of Nephrology*, *22*(2), 317–326. https://doi.org/10.1681/ASN.2009060615

Leemans, J. C., Kors, L., Anders, H., & Florquin, S. (2014). Pattern recognition receptors and the inflammasome in kidney disease. *Nature Publishing Group*, *10*(July), 398–414. https://doi.org/10.1038/nrneph.2014.91

Leemans, J. C., Weening, J. J., Florquin, S., Leemans, J. C., Stokman, G., Claessen, N., Rouschop, K. M., Teske, G. J. D., Kirschning, C. J., Akira, S., & Poll, T. Van Der. (2005). Renal-associated TLR2 mediates ischemia/reperfusion injury in the kidney. *Journal of Clinical Investigation*, *115*(10), 2894–2903. https://doi.org/10.1172/JCI22832

Levey, A. S., Eckardt, K., Dorman, N. M., Christiansen, S. L., Hoorn, E. J., Ingelfinger, J. R., Inker, L. A., Levin, A., Mehrotra, R., & Palevsky, P. M. (2020). Nomenclature for kidney function and disease: report of a Kidney Disease: Improving Global Outcomes (KDIGO) Consensus Conference. *Kidney International*, *97*(6), 1117–1129. https://doi.org/10.1016/j.kint.2020.02.010

Li, J. J., Liu, J., Lupino, K., Liu, X., Zhang, L., & Pei, L. (2018). Growth Differentiation Factor 15 Maturation Requires Proteolytic Cleavage by PCSK3, -5, and -6. *Molecular and Cellular Biology*, *38*(21). https://doi.org/10.1128/MCB.00249-18

Li, J., Qu, X., & Bertram, J. F. (2009). Endothelial-Myofibroblast Transition Contributes to the Early Development of Diabetic Renal Interstitial Fibrosis in Streptozotocin-Induced Diabetic Mice. *The American Journal of Pathology*, *175*(4), 1380–1388. https://doi.org/10.2353/ajpath.2009.090096

Li, M., Song, K., Huang, X., Fu, S., & Zeng, Q. (2018). GDF-15 prevents LPS and D-galactosamine-induced inflammation and acute liver injury in mice. *International Journal of Molecular Medicine*, *42*(3), 1756–1764. https://doi.org/10.3892/ijmm.2018.3747

Li, X., Huai, Q., Zhu, C., Zhang, X., Xu, W., & Dai, H. (2023). GDF15 Ameliorates Liver Fibrosis by Metabolic Reprogramming of Macrophages to Acquire Anti-Inflammatory Properties. *Cellular and Molecular Gastroenterology and Hepatology*, *August*, 1–24. https://doi.org/10.1016/j.jcmgh.2023.07.009

Liu, J., Kumar, S., Heinzel, A., Gao, M., Guo, J., Alvarado, G. F., Reindl-schwaighofer, R., Krautzberger, A. M., Cippà, P. E., Mcmahon, J., Oberbauer, R., & Mcmahon, A. P. (2020). *Renoprotective and Immunomodulatory Effects of GDF15 following AKI Invoked by Ischemia-Reperfusion Injury*. *31*(4), 701–715. https://doi.org/10.1681/ASN.2019090876

Luan, H. H., Wang, A., Hilliard, B. K., Ring, A. M., Young, L. H., Medzhitov, R., Luan, H. H., Wang, A., Hilliard, B. K., Carvalho, F., Rosen, C. E., & Ahasic, A. M. (2019). GDF15 Is an Inflammation-Induced Central Mediator of Tissue Tolerance Article GDF15 Is an Inflammation-Induced Central Mediator of Tissue Tolerance. *Cell*, *178*(5), 1231–1244. https://doi.org/10.1016/j.cell.2019.07.033

Luo, X., Jiang, L., Du, B., Wen, Y., Wang, M., & Xi, X. (2014). A comparison of different diagnostic criteria of acute kidney injury in critically ill patients. *Critical Care*, *18*(4), 1–8. https://doi.org/10.1186/cc13977

Lyu, Z., Mao, Z., Li, Q., Xia, Y., Liu, Y., He, Q., Wang, Y., Zhao, H., Lu, Z., & Zhou, Q. (2018). PPARγ maintains the metabolic heterogeneity and homeostasis of renal

tubules. *EBioMedicine*, *38*, 178–190. https://doi.org/10.1016/j.ebiom.2018.10.072

Macia, L., Tsai, V. W. W., Nguyen, A. D., Johnen, H., Kuffner, T., Shi, Y. C., Lin, S., Herzog, H., Brown, D. A., Breit, S. N., & Sainsbury, A. (2012). Macrophage inhibitory cytokine 1 (MIC-1/GDF15) decreases food intake, body weight and improves glucose tolerance in mice on normal & obesogenic diets. *PLoS ONE*, *7*(4), 1–8. https://doi.org/10.1371/journal.pone.0034868

Magna, M., & Pisetsky, D. S. (2014). The role of HMGB1 in the pathogenesis of inflammatory and autoimmune diseases. *Molecular Medicine*, *20*(1), 138–146. https://doi.org/10.2119/molmed.2013.00164

Mansour, A. S. (2023). Autoregulation: mediators and renin–angiotensin system in diseases and treatments. *Future Journal of Pharmaceutical Sciences*, *9*(1). https://doi.org/10.1186/s43094-023-00482-4

Masters, J. R., & Stacey, G. N. (2007). Changing medium and passaging cell lines. *Nature Protocols*, *2*(9), 2276–2284. https://doi.org/10.1038/nprot.2007.319

Mazagova, M., Buikema, H., Buiten, A. Van, Duin, M., Goris, M., Sandovici, M., Henning, R. H., & Deelman, L. E. (2013). Genetic deletion of growth differentiation factor 15 augments renal damage in both type 1 and type 2 models of diabetes. *American Journal of Physiology - Renal Physiology*, *305*(9), F1249–F1264. https://doi.org/10.1152/ajprenal.00387.2013

Mehta, R. L., Kellum, J. A., Shah, S. V., Molitoris, B. A., Ronco, C., Warnock, D. G., Levin, A., Bagga, A., Bakkaloglu, A., Bonventre, J. V., Burdmann, E. A., Chen, Y., Devarajan, P., D'Intini, V., Dobb, G., Durbin, C. G., Eckardt, K. U., Guerin, C., Herget-Rosenthal, S., … Webb, S. (2007). Acute kidney injury network: Report of an initiative to improve outcomes in acute kidney injury. *Critical Care*, *11*(2), 1–8. https://doi.org/10.1186/cc5713

Mehta, S., Chauhan, K., Patel, A., Patel, S., Pinotti, R., Nadkarni, G. N., Parikh, C. R., & Coca, S. G. (2018). The prognostic importance of duration of AKI : a systematic review and meta-analysis. *BMC Nephrology*, *19*(91), 1–10. https://doi.org/10.1186/s12882-018-0876-7.

Meng, X., Nikolic-paterson, D. J., & Lan, H. Y. (2016). TGF-β: the master regulator of fibrosis. *Nature Reviews Nephrology*, *12*(6), 325–338. https://doi.org/10.1038/nrneph.2016.48

Mishra, J., Qing, M. A., Prada, A., Mitsnefes, M., Zahedi, K., Yang, J., Barasch, J., & Devarajan, P. (2003). Identification of neutrophil gelatinase-associated lipocalin as a novel early urinary biomarker for ischemic renal injury. *Journal of the American Society of Nephrology*, *14*(10), 2534–2543. https://doi.org/10.1097/01.ASN.0000088027.54400.C6

Miyazawa, S., Watanabe, H., Miyaji, C., Hotta, O., & Abo, T. (2002). Leukocyte accumulation and changes in extra-renal organs during renal ischemia reperfusion in mice. *Journal of Laboratory and Clinical Medicine*, *139*(5), 269–278. https://doi.org/10.1067/mlc.2002.122832

Moghazi, S., Jones, E., Schroepple, J., Arya, K., McClellan, W., Hennigar, R. A., & O'Neill, W. C. (2005). Correlation of renal histopathology with sonographic findings. Kidney International, 67, 1515–1520. https://doi.org/10.1111/j.1523-1755.2005.00230.xMolitoris, B. A., Dahl, R., & Geerdes, A. (1992). Cytoskeleton disruption and apical redistribution of proximal tubule Na(+)-K(+)-ATPase during

ischemia. *American Journal of Physiology - Renal Fluid and Electrolyte Physiology*, *263*(3), F488-95. https://doi.org/10.1152/ajprenal.1992.263.3.f488

Molitoris, Bruce A., & Wagner, M. C. (1996). Surface membrane polarity of proximal tubular cells: Alterations as a basis for malfunction. *Kidney International*, *49*(6), 1592–1597. https://doi.org/10.1038/ki.1996.231

Moore, P. K., Hsu, R. K., & Liu, K. D. (2018). Management of Acute Kidney Injury : Core Curriculum 2018. *American Journal of Kidney Diseases*, *72*(1), 136–148. https://doi.org/10.1053/j.ajkd.2017.11.021

Moschovaki-Filippidou, F., Steiger, S., Lorenz, G., Schmaderer, C., Ribeiro, A., Rauchhaupt, E. Von, Cohen, C. D., Anders, H., Lindenmeyer, M., & Lech, M. (2020). Growth Differentiation Factor 15 Ameliorates Anti-Glomerular Basement Membrane Glomerulonephritis in Mice. *International Journal of Molecular Sciences*, *21*(19). https://doi.org/10.3390/ijms21196978

Mosser, D. M., & Edwards, J. P. (2008). Exploring the full spectrum of macrophage activation. *Nature Publishing Group*, *8*(12), 958–969. https://doi.org/10.1038/nri2448

Mullican, S. E., Lin-Schmidt, X., Chin, C. N., Chavez, J. A., Furman, J. L., Armstrong, A. A., Beck, S. C., South, V. J., Dinh, T. Q., Cash-Mason, T. D., Cavanaugh, C. R., Nelson, S., Huang, C., Hunter, M. J., & Rangwala, S. M. (2017). GFRAL is the receptor for GDF15 and the ligand promotes weight loss in mice and nonhuman primates. *Nature Medicine*, *23*(10), 1150–1157. https://doi.org/10.1038/nm.4392

Nair, V., Robinson-cohen, C., Smith, M. R., Bellovich, K. A., Bhat, Z. Y., Bobadilla, M., Brosius, F., Boer, I. H. De, Essioux, L., Formentini, I., Gadegbeku, C. A., Gipson, D., Hawkins, J., Himmelfarb, J., Kestenbaum, B., Kretzler, M., Magnone, M. C., Perumal, K., Steigerwalt, S., … Bansal, N. (2017). Growth Differentiation Factor – 15 and Risk of CKD Progression. *Journal of the American Society of Nephrology*, *28*(7), 2233–2240. https://doi.org/10.1681/ASN.2016080919

Nakano, D. (2020). Septic acute kidney injury: a review of basic research. *Clinical and Experimental Nephrology*, *24*(12), 1091–1102. https://doi.org/10.1007/s10157-020-01951-3

Nelson, D. A., Marks, E. S., Deuster, P. A., O'Connor, F. G., & Kurina, L. M. (2019). Association of Nonsteroidal Anti-inflammatory Drug Prescriptions with Kidney Disease among Active Young and Middle-aged Adults. *JAMA Network Open*, *2*(2). https://doi.org/10.1001/jamanetworkopen.2018.7896

Novak, M. L., & Koh, T. J. (2013). Macrophage phenotypes during tissue repair. *Journal of Leucocyte Biology*, *93*(June), 875–881. https://doi.org/10.1189/jlb.1012512

Olsen, O. E., Skjærvik, A., Fladvad, B., Sundan, A., & Holien, T. (2017). TGF- β contamination of purified recombinant GDF15. *PLoS ONE*, *12*(11), 1–10. https://doi.org/https://doi.org/10.1371/journal.pone.0187349

Palmisano, A., Gandolfini, I., Delsante, M., Cantarelli, C., Fiaccadori, E., Cravedi, P., & Maggiore, U. (2021). Acute Kidney Injury (AKI) before and after Kidney Transplantation: Causes, Medical Approach, and Implications for the Long-Term Outcomes. *Journal of Clinical Medicine*, *10*(7), 1484. https://doi.org/10.3390/jcm10071484

Papadimitraki, E. D., Tzardi, M., Bertsias, G., Sotsiou, E., & Boumpas, D. T. (2009).

Glomerular expression of toll-like receptor-9 in lupus nephritis but not in normal kidneys: implications for the amplification of the inflammatory response. *Lupus*, *18*(9), 831–835. https://doi.org/10.1177/0961203309103054

Patra, M. C., Shah, M., & Choi, S. (2020). Toll-like receptor-induced cytokines as immunotherapeutic targets in cancers and autoimmune diseases. *Seminars in Cancer Biology*, *64*, 61–82. https://doi.org/10.1016/j.semcancer.2019.05.002

Paul, J., Huyen, D. Van, Cheval, L., Bloch-faure, M., Belair, M. F., Heudes, D., Bruneval, P., & Doucet, A. (2008). GDF15 Triggers Homeostatic Proliferation of Acid-Secreting Collecting Duct Cells. *Journal of the American Society of Nephrology*, *19*(10), 1965–1974. https://doi.org/10.1681/ASN.2007070781

Polichnowski, X. A. J., Griffin, K. A., Licea-vargas, H., Lan, R., Picken, M. M., Long, J., Williamson, G. A., Rosenberger, C., Mathia, S., Venkatachalam, M. A., & Bidani, X. A. K. (2020). Pathophysiology of unilateral ischemia-reperfusion injury: importance of renal counterbalance and implications for the AKI-CKD transition. *American Journal of Physiology - Renal Physiology*, *318*(5), F1086–F1099. https://doi.org/10.1152/ajprenal.00590.2019

Pulskens, W. P., Teske, G. J., Butter, L. M., Roelofs, J. J., & Poll, T. Van Der. (2008). Toll-like receptor-4 coordinates the innate immune response of the kidney to renal ischemia/reperfusion injury. *PLoS ONE*, *3*(10), 1–9. https://doi.org/10.1371/journal.pone.0003596

Radi, Z. A. (2018). Immunopathogenesis of Acute Kidney Injury. *Toxicologic Pathology*, *46*(8), 930–943. https://doi.org/10.1177/0192623318799976

Ransick, A., Lindström, N. O., Liu, J., Zhu, Q., Guo, J., Gregory, F., Kim, A. D., Black, H. G., Kim, J., & Mcmahon, A. P. (2020). Single-Cell Profiling Reveals Sex, Lineage, and Regional Diversity in the Mouse Kidney. *Developmental Cell*, *51*(3), 399–413. https://doi.org/10.1016/j.devcel.2019.10.005

Roh, J. S., & Sohn, D. H. (2018). Damage-Associated Molecular Patterns in Inflammatory Diseases. *Immune Network*, *18*(4), 1–14. https://doi.org/10.4110/in.2018.18.e27

Romagnani, P., Remuzzi, G., Glassock, R., Levin, A., Tonelli, M., Massy, Z., & Wanner, C. (2017). Chronic kidney disease. *Nature Reviews Disease Primers*, *3*. https://doi.org/10.1038/nrdp.2017.88

Ronco, C., Bellomo, R., & Kellum, J. A. (2019). Acute kidney injury. *The Lancet*, *394*(10212), 1949–1964. https://doi.org/10.1016/S0140-6736(19)32563-2

Saeed, A. S., Hossein, M., Taghadosi, M., Fatemeh, S. E., Bita, M., Mohammadi, A., Afshari, J. T., & Sahebkar, A. (2018). Macrophage plasticity, polarization, and function in health and disease. *Journal of Cellular Physiology*, *233*(9), 6425–6440. https://doi.org/10.1002/jcp.26429

Sato, Y., & Yanagita, M. (2023). Immune cells and inflammation in AKI to CKD progression. *Am J Physiol Renal Physiol*, *315*, F1501–F1512. https://doi.org/10.1152/ajprenal.00195.2018

Schaefer, L., Babelova, A., Kiss, E., Hausser, H., Baliova, M., Malle, E., Schaefer, R. M., & Gröne, H. (2005). The matrix component biglycan is proinflammatory and signals through Toll-like receptors 4 and 2 in macrophages. *The Journal of Clinical Investigation*, *115*(8), 2223–2233. https://doi.org/10.1172/JCI23755.There

Schiffer, T. A., Gustafsson, H., & Palm, F. (2018). Kidney outer medulla mitochondria are more efficient compared with cortex mitochondria as a strategy to sustain ATP production in a suboptimal environment. *American Journal of Physiology - Renal Physiology*, *315*(3), F677–F681. https://doi.org/10.1152/ajprenal.00207.2018

Schindelin, J., Arganda-Carreras, I., Frise, E., Kaynig, V., Longair, M., Pietzsch, T., Preibisch, S., Rueden, C., Saalfeld, S., Schmid, B., Tinevez, J. Y., White, D. J., Hartenstein, V., Eliceiri, K., Tomancak, P., & Cardona, A. (2012). Fiji: An open-source platform for biological-image analysis. *Nature Methods*, *9*(7), 676–682. https://doi.org/10.1038/nmeth.2019

Schindelin, J., Rueden, C. T., Hiner, M. C., & Eliceiri, K. W. (2015). The ImageJ ecosystem: An open platform for biomedical image analysis. *Molecular Reproduction and Development*, *82*(7–8), 518–529. https://doi.org/10.1002/mrd.22489

Schnaper, H. W. (2017). The tubulointerstitial pathophysiology of progressive kidney disease. *Advances in Chronic Kidney Disease*, *24*(2), 107–116. https://doi.org/10.1053/j.ackd.2016.11.011

Scholz, H., Boivin, F. J., Schmidt-Ott, K. M., Bachmann, S., Eckardt, K. U., Scholl, U. I., & Persson, P. B. (2021). Kidney physiology and susceptibility to acute kidney injury: implications for renoprotection. *Nature Reviews Nephrology*, *17*(5), 335–349. https://doi.org/10.1038/s41581-021-00394-7

Sharfuddin, A. A., & Molitoris, B. A. (2011). Pathophysiology of ischemic acute kidney injury. *Nature Publishing Group*, *7*(April), 189–200. https://doi.org/10.1038/nrneph.2011.16

Shigeoka, A. A., Holscher, T. D., King, A. J., Hall, F. W., Kiosses, W. B., Tobias, P. S., Mckay, D. B., Shigeoka, A. A., Holscher, T. D., King, A. J., Hall, F. W., Kiosses, W. B., Tobias, P. S., Mackman, N., & Mckay, D. B. (2007). TLR2 is constitutively expressed within the kidney and participates in ischemic renal injury through both MyD88-dependent and -independent pathways. *The Journal of Immunology*, *178*(10), 6252–6258. https://doi.org/10.4049/jimmunol.178.10.6252

Singh, R., Letai, A., & Sarosiek, K. (2019). Regulation of apoptosis in health and disease: the balancing act of BCL-2 family proteins. *Nature Reviews Molecular Cell Biology*, *20*, 175–193. https://doi.org/10.1038/s41580-018-0089-8

Smiley, S. T., King, J. A., & Hancock, W. W. (2022). Fibrinogen Stimulates Macrophage Chemokine Secretion Through Toll-Like Receptor 4. *The Journal of Immunology*, *167*(5), 2887–2894. https://doi.org/10.4049/jimmunol.167.5.2887

Staender, S., Davies, J., Helmreich, B., Sexton, B., & Kaufmann, M. (1997). The anaesthesia critical incident reporting system: An experience based database. *International Journal of Medical Informatics*, *47*(1–2), 87–90. https://doi.org/10.1016/S1386-5056(97)00087-7

Susantitaphong, P., Cruz, D. N., Cerda, J., Abulfaraj, M., Alqahtani, F., Koulouridis, I., & Jaber, B. L. (2013). World incidence of AKI: A meta-analysis. *Clinical Journal of the American Society of Nephrology*, *8*(9), 1482–1493. https://doi.org/10.2215/CJN.00710113

Tammaro, A., Kers, J., & Scantlebery, A. M. L. (2020). Metabolic Flexibility and Innate Immunity in Renal Ischemia Reperfusion Injury: The Fine Balance Between Adaptive Repair and Tissue Degeneration. *Frontiers in Immunology*, *11*(7), 1–17.

https://doi.org/10.3389/fimmu.2020.01346

Termeer, C., Benedix, F., Sleeman, J., Fieber, C., Voith, U., Ahrens, T., Miyake, K., Freudenberg, M., Galanos, C., & Simon, J. C. (2002). Oligosaccharides of Hyaluronan Activate Dendritic Cells via Toll-like Receptor 4. *Journal of Experimental Medicine*, *195*(1), 99–111. https://doi.org/10.1084/jem.20001858

Thakar, C. V, Christianson, A., Himmelfarb, J., & Leonard, A. C. (2011). Acute Kidney Injury Episodes and Chronic Kidney Disease Risk in Diabetes Mellitus. *Clinical Journal of the American Society of Nephrology*, *6*(11), 2567–2572. https://doi.org/10.2215/CJN.01120211

Thorsteinsdottir, H., Salvador, C. L., Mjøen, G., Lie, A., Sugulle, M., Tøndel, C., Brun, A., Almaas, R., & Bjerre, A. (2020). Growth Differentiation Factor 15 in Children with Chronic Kidney Disease and after Renal Transplantation. *Disease Markers*, *2020*(Cvd). https://doi.org/10.1155/2020/6162892

Tsai, V. W. W., Husaini, Y., Sainsbury, A., Brown, D. A., & Breit, S. N. (2018). The MIC-1/GDF15-GFRAL Pathway in Energy Homeostasis: Implications for Obesity, Cachexia, and Other Associated Diseases. *Cell Metabolism*, *28*(3), 353–368. https://doi.org/10.1016/j.cmet.2018.07.018

Tuegel, C., Katz, R., Alam, M., Bhat, Z., Bellovich, K., Boer, I. De, Brosius, F., Gadegbeku, C., Gipson, D., Hawkins, J., Himmelfarb, J., Ju, W., Kestenbaum, B., Kretzler, M., Robinson-cohen, C., Steigerwalt, S., & Bansal, N. (2018). GDF-15, Galectin 3, Soluble ST2, and Risk of Mortality and Cardiovascular Events in CKD. *American Journal of Kidney Diseases*, *72*(4), 519–528. https://doi.org/10.1053/j.ajkd.2018.03.025

Vaidya, V. S., Ferguson, M. A., & Bonventre, J. V. (2008). Biomarkers of acute kidney injury. *Annual Review of Pharmacology and Toxicology*, *48*, 463–493. https://doi.org/10.1146/annurev.pharmtox.48.113006.094615

Venkatachalam, M. A., Weinberg, J. M., Kriz, W., & Bidani, A. K. (2015). Failed Tubule Recovery, AKI-CKD Transition, and Kidney Disease Progression. *Journal of the American Society of Nephrology*, *26*(8), 1765–1776. https://doi.org/10.1681/ASN.2015010006

Villanueva, S., Céspedes, C., & Vio, C. P. (2006). Ischemic acute renal failure induces the expression of a wide range of nephrogenic proteins. *American Journal of Physiology - Regulatory Integrative and Comparative Physiology*, *290*(4), 861–870. https://doi.org/10.1152/ajpregu.00384.2005

Vries, B. De, Daemen, M. A. R. C., & Pieter, S. (2002). In vivo expression of Toll-like receptor 2 and 4 by renal epithelial cells: IFN-gamma and TNF-alpha mediated up-regulation during inflammation. *The Journal of Immunologye Journal of Immunology*, *168*(3), 1286–1293. https://doi.org/10.4049/jimmunol.168.3.1286

Vriese, A. S. De, Sethi, S., Nath, K. A., Fervenza, F. C., & Glassock, R. J. (2018). Differentiating Primary, Genetic, and Secondary FSGS in Adults: A Clinicopathologic Approach. *Journal of the American Society of Nephrology*, *29*, 759–774. https://doi.org/10.1681/ASN.2017090958

Wang, S., Song, R., Wang, Z., Jing, Z., & Wang, S. (2018). S100A8 / A9 in inflammation. *Frontiers in Immunology*, *9*(June). https://doi.org/10.3389/fimmu.2018.01298

Wischhusen, J., Melero, I., & Fridman, W. H. (2020). Growth/Differentiation Factor-15

(GDF-15): From Biomarker to Novel Targetable Immune Checkpoint. *Frontiers in Immunology*, *11*(May). https://doi.org/10.3389/fimmu.2020.00951

Wu, H., Chen, G., Wyburn, K. R., Yin, J., Bertolino, P., Eris, J. M., Alexander, S. I., Sharland, A. F., & Chadban, S. J. (2007). TLR4 activation mediates kidney ischemia/reperfusion injury. *Journal of Clinical Investigation*, *117*(10), 2847–2859. https://doi.org/10.1172/JCI31008

Xu, J., Kimball, T. R., Lorenz, J. N., Brown, D. A., Bauskin, A. R., Klevitsky, R., Hewett, T. E., Breit, S. N., & Molkentin, J. D. (2006). GDF15/MIC-1 functions as a protective and antihypertrophic factor released from the myocardium in association with SMAD protein activation. *Circulation Research*, *98*(3), 342–350. https://doi.org/10.1161/01.RES.0000202804.84885.d0

Yang, L., Chang, C. C., Sun, Z., Madsen, D., Zhu, H., Padkjær, S. B., Wu, X., Huang, T., Hultman, K., Paulsen, S. J., Wang, J., Bugge, A., Frantzen, J. B., Nørgaard, P., Jeppesen, J. F., Yang, Z., Secher, A., Chen, H., Li, X., … Jørgensen, S. B. (2017). GFRAL is the receptor for GDF15 and is required for the anti-obesity effects of the ligand. *Nature Medicine*, *23*(10), 1158–1166. https://doi.org/10.1038/nm.4394

You, A. S., Kalantar-zadeh, K., Lerner, L., Nakata, T., Lopez, N., Lou, L., Veliz, M., Soohoo, M., Jing, J., Zaldivar, F., Gyuris, J., Nguyen, D. V, & Rhee, C. M. (2017). Association of Growth Differentiation Factor 15 with Mortality in a Prospective Hemodialysis Cohort. *Cardiorenal Medicine*, *7*(2), 158–168. https://doi.org/10.1159/000455907

Ysebaert, D. K., Greef, K. E. De, Vercauteren, S. R., Ghielli, M., Verpooten, G. A., Eyskens, E. J., & Broe, M. E. De. (2000). Identification and kinetics of leukocytes after severe ischaemia / reperfusion renal injury. *Nephrology Dialysis Transplantation*, *15*(10), 1562–1574. https://doi.org/10.1093/ndt/15.10.1562

Zamami, R. (2021). The Association between Glomerular Diameter and Secondary Focal Segmental Glomerulosclerosis in Chronic Kidney Disease. *Kidney and Blood Pressure Research*, *46*(4), 433–440. https://doi.org/10.1159/000515528

Zhang, M., Singh, A., Harris, R. C., Zhang, M., Yao, B., Yang, S., Jiang, L., Wang, S., & Fan, X. (2012). CSF-1 signaling mediates recovery from acute kidney injury. *The Journal of Clinical Investigation*, *122*(12), 4519–4532. https://doi.org/10.1172/JCI60363.stem

Zhang, X., & Dong, S. (2022). Protective effect of growth differentiation factor 15 in sepsis by regulating macrophage polarization and its mechanism. *Bioengineered*, *13*(4), 9687–9707. https://doi.org/10.1080/21655979.2022.2059903

Zimmers, T. A., Jin, X., Hsiao, E. C., McGrath, S. A., Esquela, A. F., & Koniaris, L. G. (2005). Growth differentiation factor-15/macrophage inhibitory cytokine-1 induction after kidney and lung injury. *Shock*, *23*(6), 543–548. https://doi.org/10.1097/01.shk.0000163393.55350.70

Zoccali, C., Vanholder, R., Massy, Z. A., & Ortiz, A. (2017). The systemic nature of CKD. *Nature Reviews Nephrology*, *13*(6), 344–358. https://doi.org/10.1038/nrneph.2017.52

Zuk, A., Bonventre, J. V., Brown, D., & Matlin, K. S. (1998). Polarity, integrin, and extracellular matrix dynamics in the postischemic rat kidney. *American Journal of Physiology - Cell Physiology*, *275*(3), C711-31. https://doi.org/10.1152/ajpcell.1998.275.3.c711

Zuk, A., Bonventre, J. V., & Matlin, K. S. (2001). Expression of fibronectin splice variants in the postischemic rat kidney. *American Journal of Physiology - Renal Physiology*, *280*(6 49-6), 1037–1053. https://doi.org/10.1152/ajprenal.2001.280.6.f1037

XI Appendix

1 Acknowledgements

My heartfelt thanks go to Prof. Dr. Maciej Lech for the opportunity to carry out my medical doctorate thesis under his excellent supervision as well as his constant support, encouragement, and guidance during these last years. I would like to especially thank Dr. Mohsen Honarpisheh for his outstanding supervision of my work and his moral support far beyond that. Thank you for the great cooperation. Furthermore, I would like to thank all members of the Lech Lab for their help and support in the laboratory, for the pleasant working atmosphere and the social activities outside of work. Special thanks go to my colleagues Dr. Andrea Ribeiro, Vivian Würf, Sylke Rohrer and Prof. Dr. Stefanie Steiger for many encouraging conversations, valuable ideas, and their constant willingness to help. Finally, I would like to thank my family and friends for always having an open ear and for always being by my side. Your encouraging words, emotional support and constant presence carried me through this thesis. Above all, I would like to thank my parents for their great support and guidance in every situation.

2 Affidavit

Eidesstattliche Versicherung

Krill, Moritz Johannes

_____

Name, Vorname

Ich erkläre hiermit an Eides statt, dass ich die vorliegende Dissertation mit dem Titel:

Analysis of Growth Differentiation Factor 15 and Its Role in Acute and Chronic Kidney Injury

……

selbständig verfasst, mich außer der angegebenen keiner weiteren Hilfsmittel bedient und alle Erkenntnisse, die aus dem Schrifttum ganz oder annähernd übernommen sind, als solche kenntlich gemacht und nach ihrer Herkunft unter Bezeichnung der Fundstelle einzeln nachgewiesen habe.

Ich erkläre des Weiteren, dass die hier vorgelegte Dissertation nicht in gleicher oder in ähnlicher Form bei einer anderen Stelle zur Erlangung eines akademischen Grades eingereicht wurde.

München, 07.07.2024 Moritz Johannes Krill

_____ _____

Ort, Datum Unterschrift Doktorandin bzw. Doktorand

3 Declaration of Personal Contribution

This thesis was carried out at the Nephrological Center at the Department of Medicine IV of the Ludwig-Maximilians-University in Munich. The conception of the study and supervision of this dissertation was provided by Prof. Maciej Lech, PhD.

The planning, execution and analysis of the experiments was done independently under the guidance of Prof. Maciej Lech, PhD.
All histological evaluations, all *in-vitro* experiments, cell isolations and cultivation, RNA isolation, ELISA, and qRT-PCR experiments as well as their analyses were performed by me.

All experimental *in-vivo* procedures, i.e., animal handling and the experimental implementation of the I/R-based *in-vivo* models were performed by qualified members of the laboratory under the supervision of Prof. Maciej Lech, PhD. The assessment of kidney function was performed by Prof. Maciej Lech, PhD. FACS experiments and the analysis of the obtained FACS data were performed together with and under the guidance of Prof. Stefanie Steiger, PhD.

This dissertation was written independently.

4 Curriculum Vitae

5 List of Publications

5.1 Original Publications

Ribeiro A, Dobosz E, Krill M, Köhler P, Wadowska M, Steiger S, Schmaderer C, Koziel J, Lech M. Macrophage-Specific MCPIP1/Regnase-1 Attenuates Kidney Ischemia-Reperfusion Injury by Shaping the Local Inflammatory Response and Tissue Regeneration. Cells, 11(3), 397. https://doi.org/10.3390/cells11030397 (2022).

5.2 Oral and Posterpresentations

Krill M, Würf V, Honarpisheh M, Ribeiro A, Lech M. Growth Differentiation Factor 15 Deficiency Aggravates Acute and Chronic Kidney Injury Caused by Ischemia/Reperfusion, 56. ERA-EDTA Congress, European Renal Association, Budapest, Hungary, Posterpresentation (2019).

Krill M, Honarpisheh M, Ribeiro A, Lech M. The Role of Growth Differentiation Factor 15 in Acute and Chronic Kidney, “Junge Niere 2019”, Graz, Austria, Oral Presentation (2019).